Investigation of Impact of Generation Uncertainty on Optimal Power Flow Using New Hybrid Multi-Objective Evolutionary Algorithms

Thesis

Submitted in partial fulfillment of the requirements

for the award of the degree of

Doctor of Philosophy

in

Electrical Engineering

By

Avvari Ravi Kumar

(Roll No: 718122)

Supervisor

Dr. D. M. Vinod Kumar

Professor (HAG)

DEPARTMENT OF ELECTRICAL ENGINEERING

NATIONAL INSTITUTE OF TECHNOLOGY WARANGAL

(An Institution of National Importance, Ministry of Education, Govt. of India)

Hanumakonda-506004, Telangana State, India

December-2022

APPROVAL SHEET

This thesis entitled **"Investigation of Impact of Generation Uncertainty on Optimal Power Flow Using New Hybrid Multi-Objective Evolutionary Algorithms"** by **Mr. Avvari Ravi Kumar, Roll No: 718122** is approved for the degree of Doctor of Philosophy in Electrical Engineering.

Examiners

_____

_____

_____

Supervisor

Dr. D. M. Vinod Kumar

Professor (HAG)

EED, NIT Warangal

Chairman

Dr. S. Srinivasa Rao

Professor

EED, NIT Warangal

Date: _____

DEPARTMENT OF ELECTRICAL ENGINEERING

NATIONAL INSTITUTE OF TECHNOLOGY WARANGAL

HANUMAKONDA- 506004

DEPARTMENT OF ELECTRICAL ENGINEERING
NATIONAL INSTITUTE OF TECHNOLOGY WARANGAL

CERTIFICATE

This is to certify that the thesis entitled **"Investigation of Impact of Generation Uncertainty on Optimal Power Flow Using New Hybrid Multi-Objective Evolutionary Algorithms",** which is being submitted by **Mr. Avvari Ravi Kumar, Roll No: 718122**, is a bonafide work submitted to National Institute of Technology Warangal in partial fulfillment of the requirements for the award of the degree of **Doctor of Philosophy** in Electrical Engineering. To the best of my knowledge, the work incorporated in this thesis has not been submitted elsewhere for the award of any degree.

Date: 21 December, 2022
Place: Hanumakonda

Dr. D. M. Vinod Kumar
(Thesis Supervisor)
Professor (HAG)
Department of Electrical Engineering
National Institute of Technology Warangal
Hanumakonda –506004, India.

DECLARATION

This is to certify that the work presented in the thesis entitled "**Investigation of Impact of Generation Uncertainty on Optimal Power Flow Using New Hybrid Multi-Objective Evolutionary Algorithms**", is bonafide work done by me under the supervision of Dr. D.M.Vinod Kumar, Professor (HAG), Department of Electrical Engineering, National Institute of Technology Warangal, India and was not submitted elsewhere for the award of any degree.

I declare that this written submission represents my ideas in my own words and where others' ideas or words have been included; I have adequately cited and referenced the sources. I also declare that I have adhered to all principles of academic honesty and integrity and have not misrepresented or fabricated or falsified any idea/date/fact/source in my submission. I understand that any violation of the above will be a cause for disciplinary action by the institute and can also evoke penal action from the sources which have thus not been properly cited or from whom proper permission has not been taken when needed.

Date: 21 December, 2022
Place: Hanumakonda

Avvari Ravi Kumar
(Roll No: 718122)

I would like to dedicate my thesis to my parents:

Late ***Sri Avvari Ramanaiah***

Late ***Smt. Avvari Mahalakshmamma***

ACKNOWLEDGEMENTS

I am glad to express my deep sense of gratitude and thanks to my supervisor **Dr. D.M. Vinod Kumar**, Professor (HAG), Department of Electrical Engineering, National Institute of Technology Warangal, for his continuous support, guidance, and valuable suggestions. I am grateful to him for having faith in me throughout my Ph.D. His knowledge, expertise, and experience helped me to perform extensive research.

I am very much thankful to **Dr. S. Srinivasa Rao**, Chairman of the Doctoral Scrutiny Committee, and Professor, Department of Electrical Engineering for his continuous support, encouragement, and suggestions.

I am very thankful to **Dr. B. L. Narasimharaju**, Professor & Head, Department of Electrical Engineering for his continuous support, encouragement, and suggestions.

I take this privilege to thank my Doctoral Scrutiny Committee members, **Dr. Ch. Venkaiah,** Professor, Department of Electrical Engineering, **Dr. A.V.Giridhar**, Associate Professor, Department of Electrical Engineering, **Dr. P. Muthu**, Associate Professor, Department of Mathematics, for their detailed review, constructive suggestions, and excellent advice during the process of this research work. I would like to thank **Dr. M. Raja Vishwanathan**, Associate Professor, Department of Humanities and Social Science for his valuable suggestions, continuous support, and cooperation.

I would like to thank the teaching, and non-teaching members, and fraternity of the Department of Electrical Engineering of NIT Warangal for their support and encouragement.

I wish to express my sincere thanks to **Prof. N. V. Ramana Rao**, Director, NIT Warangal for his support and encouragement.

I would like to take this opportunity to thank my seniors Dr. S. Kayalvizhi, Dr. Kiran Teeparthi, Dr. C. Bhanu Prasad, and fellow scholar Mr. T. Vinod Kumar for their support and encouragement.

I would like to thank all my teachers, colleagues, and seniors at various places for their support and encouragement.

I would like to thank my wife **Mrs. Lavanya** for being a constant source of inspiration and support. I take this opportunity to thank all my family members and my well-wishers for their understanding, support, and encouragement during this research work. I would like to thank all those who helped me directly and indirectly at various stages of this work.

Avvari Ravi Kumar

ABSTRACT

In general, optimization promotes the economical and efficient operation of electrical systems. The majority of power system issues are often non-linear, non-convex, and involve the simultaneous optimization of multiple contrasting objective functions. Optimization approaches may be required to address a variety of continuous and discrete variables in the problems. In the past, classical/traditional/conventional optimization approaches were employed. Conventional techniques typically use gradient-based searches that converge to local optimal solutions, and it was known that they performed well for convex and continuous optimization problems. Later, a transformation in optimization methods initiated Evolutionary Algorithms (EAs) into the picture. The majority of these techniques can effectively circumvent the issue of premature convergence and explore the search area toward the global optimal solution. In addition, renewable energy sources (RESs) have become a vital part of the modern power system. Due to the uncertainty and unpredictability of RESs, the formulation of the power system problem has grown complex and dynamic. The main purpose of this research is to implement cutting-edge variations of decomposition-based MOEA (MOEA/D) for the OPF problems in power systems. Moreover, operational and security limitations are prevalent in electrical networks. The static penalty method was the simplest and most easy strategy for addressing power system limits. In this thesis, a new constraint handling method (CHM) referred to as the superiority of feasible solutions (SF) method in addition to the penalty method was introduced. In conjunction with MOEAs, CHM has been effectively used to previously known and freshly formulated constrained optimization issues in the power system, notably the OPF problem.

The following are the thesis contributions:

- A novel hybrid MOEA based on decomposition and local dominance was proposed for the OPF problem. The MOOPF aims to minimize total generation cost, emission, active power loss, and voltage magnitude deviation. To address the limitations of the MOOPF problem, a penalty function method was implemented. In addition, a fuzzy technique was used to determine the optimal values among Pareto-optimal alternatives. The proposed strategy combines the decomposition and local dominance strategies to promote convergence by enhancing diversity.
- A new hybrid decomposition and summation of normalized objectives with improved diversified selection-based MOEA including wind energy conversion system (WECS)

and solar photo-voltaic system (SPVS) uncertainty for OPF was carried out. This chapter recommends a novel CHM, that adaptively inserts penalty and avoids the parameter relying on penalty calculation. In the OPF cost study, the influence of RES such as WECS and SPVS integration was examined. To minimize the total generation cost, the cost of RESs is factored into the OPF issue to examine the influence of intermittent and unpredictable renewable sources on cost and operation. Weibull and Lognormal PDFs are applied to characterize the unpredictability of WECS and SPVS respectively.

- A new hybrid decomposition and summation of normalized objectives with improved diversified selection-based MOEA including WECS, SPVS, and plug-in electric vehicle system (PEVS) uncertainty for the OPF problem were done. The MOOPF problem was solved using a unique CHM that adaptively inserts the penalty and avoids the parameter relying on penalty calculation. In addition, a fuzzy technique was used to determine the optimal values among Pareto-optimal alternatives. The impact of intermittence of WECS, SPVS, and PEV integration was considered for optimal cost analysis.
- A new hybrid decomposition and invasive weed optimization (IWO) based MOEA including WECS, SPVS, and PEV uncertainty was presented for the OPF problem. The standard OPF problem was transformed into a stochastic OPF by incorporating the uncertainty of WECS, SPVS, and PEVSs. The MOOPF problem was solved using a unique CHM that adaptively inserts the penalty and avoids the parameter relying on penalty calculation. In addition, a fuzzy technique was used to determine the optimal values among Pareto-optimal alternatives. The impact of intermittence of WECS, SPVS, and PEV integration was considered for optimal cost analysis.

Contents

List of Figures

List of Tables

List of Abbreviations

BCS	Best-Compromised Solution
CHM	Constraint Handling Method
EA	Evolutionary Algorithm
IEEE	Institute of Electrical and Electronics Engineers
ISO	Independent System Operator
IWO	Invasive Weed Optimization
MOEA	Multi-Objective Evolutionary Algorithm
MOEA/D	MOEA based on Decomposition
MOP	Multi-Objective Optimization Problem
MW	Mega Watt
MVAR	Mega Volt Ampere Reactive
MOPSO	Multi-Objective Particle Swarm Optimization
MOOPF	Multi-Objective Optimal Power Flow
NDS	Non-Dominated Sorting
NSGA-II	Non-Dominated Sorting Genetic Algorithm-II
OPF	Optimal Power Flow
PBI	Penalty Based Intersection
PF	Pareto-Optimal Front
p.u.	Per Unit
PDF	Probability Density Function
PEV	Plug-in Electric Vehicle
RES	Renewable Energy Source
SF	Superiority of Feasible Solutions
SSA	Systematic Sampling Approach
SPVS	Solar Photo-Voltaic System
WECS	Wind Energy Conversion System

List of Symbols

J_1	Total generation cost ($/h)
J_2	Emission (ton/h)
J_3	Active power loss (MW)
J_4	Voltage magnitude deviation (p.u.)
$CV(x)$	Penalty function
$dis(x, y)$	Euclidean distance between solutions x and y.
D	Number of divisions along with each objective coordinate
M	Number of objective functions
N	Population size
$\mathcal{N}()$	Normal distribution
Pc	Crossover probability
Pm	Mutation probability
P_t	Old population
Q_t	New population
T	Neighborhood size
w	Weight vector

Chapter 1

Introduction

Chapter 1
Introduction

1.1 Optimal Power Flow Overview

The OPF has become a popular topic of discussion amongst power system academics all over the world due to the interesting variety of issues it raises. The OPF is presented as a single or multi-objective issue to minimize total generating cost, emission, active power loss, voltage magnitude deviation, etc., subject to restrictions on the generator's capability, the line's capacity, the bus voltage, and the balance of power flow. The OPF program provides the ideal values for the decision variables, resulting in the efficient and economic operation of the power system. Main control variables refer to the network's generator bus real power, reactive power, and bus voltages. The latter regulates the flow of reactive power, which is often balanced by connecting capacitors with the proper ratings to the network that supplies inductive loads. The bus voltages and complex powers in the lines obtained throughout the optimization indicate the optimum operating condition, which may result in the fulfillment of one or more network objectives. Therefore, OPF, which requires complex computations with various parameters and the identification of optimal solutions while simultaneously fulfilling all restrictions, remains the most challenging problem to solve.

In recent days, issues such as the rise in penetration of renewable sources and the rise in load demand are posing new challenges to the modern power system. The OPF is a technique for power system planning to find the best operating point in terms of real power generation, voltage magnitude, tap settings of transformers, and compensators to optimize the specific objective function(s). The OPF is a nonlinear optimization issue with continuous and discontinuous control variables. However, discrete control variables like transformer tap settings, shunt devices, and phase shifters make the OPF problem highly complicated.

In recent times, RESs penetration has increased drastically in power systems. The penetration of RESs has introduced many challenges to the power system. The intermittent nature of RESs makes the system highly complex in terms of operation and control. The uncertain nature of RESs is required to be modeled accurately to examine the dynamic functioning of the power system. Due to its unpredictable nature, protection schemes need to be updated for operating the power system in a secure region. In a power system, the main aim is to operate it with optimal cost and simultaneously satisfy the operating and security constraints. The OPF determines the optimal control settings satisfying system constraints and

security constraints to operate economically. OPF is an optimizing tool for power system operation analysis, scheduling, and energy management applications.

1.2 Mathematical Representation

The OPF is a non-linear, non-convex optimization problem that aims to minimize a given objective function under a variety of equality and inequality restrictions. The OPF model is formulated as follows:

$$Minimize:\ f(x,u) \tag{1.1}$$

$$subject\ to: \begin{cases} g(x,u) = 0 \\ h(x,u) \leq 0 \end{cases}$$

Where $f(x,u)$ is the objective function, *x* and *u* are the vector of state and control variables respectively, $g(x,u)$ and $h(x,u)$ are the collection of equality and inequality restrictions respectively.

a) State variables

The state variables for the power system can be written as follows in the vector *x*:

$$x = [P_{G1}, V_{L1}, \dots V_{LNL}, Q_{G1}, \dots Q_{GNG}, S_{l1}, \dots S_{lnl}\ ] \tag{1.2}$$

Where, NL and nl denote the number of load buses and lines respectively. $P_{G1}$is the slack bus real power, Q_{Gi} is the *i*-th generator bus reactive power, V_{Li} denotes *i*-th load bus voltage and S_{li} is the *i*-th line loading.

b) Control variables

The decision variables for the power system can be written as follows in the vector *u*:

$$u = [P_{G2}, \dots P_{GNG}, V_{G1}, \dots V_{GNG}, T_1, \dots T_{NT}, Q_{C1}, \dots Q_{CNC}] \tag{1.3}$$

Where NG, NT and NC are the number of generators, transformers and shunt compensators respectively. P_{Gi} is the *i*-th generator bus real power (except slack bus). V_{Gi} is the *i*-th generator bus voltage magnitude, T_i is the *i*-th transformer tap ratio, Q_{Ci} is the *i*-th bus shunt compensator.

In general, a problem having more than one objective is treated as a multi-objective optimization problem (MOP). While formulating the MOP, the objective functions are chosen such that they conflict with each other. The conflict between objectives depends on the correlation among the objectives. Different objectives will have different degrees of correlation among a combination of objectives. To formulate the combination of objectives, four different objectives are considered in this thesis, which are minimization of (a) total generation cost (J_1), (b) emission (J_2), (c) active power loss (J_3), and (d) voltage magnitude deviation (J_4). To show the change in trade-off solutions with an increase in objectives, the multi-objective problems were designed with two objectives, three objectives, and four objectives. These multi-objectives was formulated from the combination of four objectives. The combination of

objectives were taken into account to test the MOP with different degrees of correlation among the objectives.

1.3 Best-Compromised Solution (BCS)

The fuzzy method [12] was employed to obtain the BCS from a set of non-dominated solutions of the Pareto optimal front. The membership value (μ_m^k) of every objective is computed as follows:

$$\mu_m^k = \begin{cases} 1;\ for\ F_m^k \le F_m^{min} \\ \frac{F_m^{max} - F_m^k}{F_m^{max} - F_m^{min}} \quad ;for \quad F_m^{min} \le F_m^k \le F_m^{max} \\ 0;\ for\ F_m^k \ge F_m^{max} \end{cases} \tag{1.4}$$

where $F_m^{min}, and\ F_m^{max}$ are the limits on fitness values for the objective m out of all the non-dominated solutions; F_m^k is the fitness value of objective m for non-dominated solution k. The normalized membership value (μ^k) for every non-dominant solution is determined as follows:

$$\mu^k = \frac{\sum_{m=1}^{M} \mu_m^k}{\sum_{k=1}^{N_d} \sum_{m=1}^{M} \mu_m^k} \tag{1.5}$$

where N_d and M indicate the number of non-dominated solutions and objective functions respectively. The optimal trade-off is represented as the solution with the highest μ^k value.

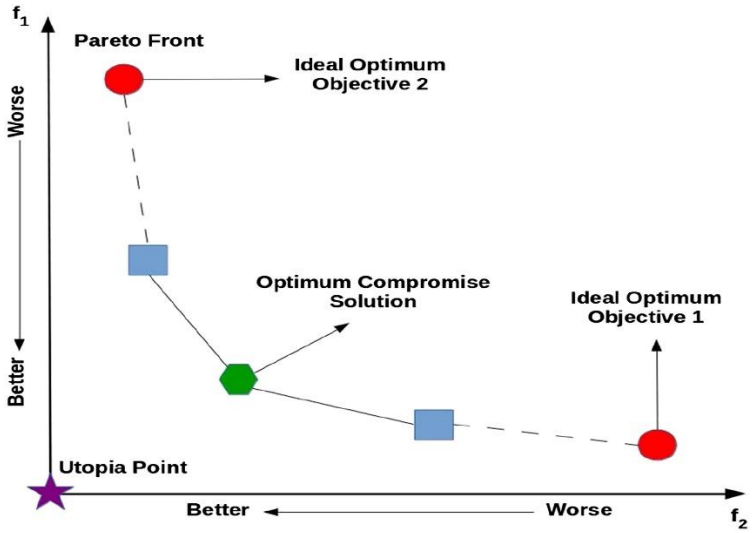

Fig.1.1. Pictorial representation of Pareto-optimal solutions.

1.4 Evolutionary Optimization Algorithms

The limitation of conventional optimization methods can be overcome with alternative optimization techniques such as evolutionary optimization techniques, which can handle nonlinear, non-differentiable, real-world complex problems, highly constrained, high dimensionality problems, and discrete optimization problems. Evolutionary optimization algorithms are one of the branches of meta-heuristic optimization methods, which are inspired

by the biological evolutionary theory to solve optimization problems. The evolutionary algorithms can be classified into two categories: i) population-based and ii) trajectory-based algorithms. Population-based algorithms are inspired by the biology and swarms of different species. In population-based algorithms, multiple solutions are propagated to find the optimal solution in the decision space. genetic algorithm (GA), particle swarm optimization (PSO), etc., are examples of population-based algorithms. Trajectory-based algorithms are adapted from physics, in which a single solution is propagated to find the optimal solution. Tabu search, simulated annealing, etc., are examples of trajectory-based algorithms. Evolutionary optimization algorithms are best suited to resolve the OPF issue. The OPF can be structured as both single-objective and multiple-objective issues. In practical applications of power systems, one needs to consider multiple objectives rather than a single objective. The multi-objective formulation gives the trade-off solutions which are useful in making the decision of power system planning studies.

1.5 Multi-Objective Evolutionary Algorithms (MOEAs)

The OPF problem can be solved using MOEA. The optimization process provides the best feasible value which is the maximum or minimum value of a given objective. In general, multi-objective optimization is expressed as follows:

$$minimize \;\; F(x) = (f_1(x), f_2(x), \dots\dots, f_m(x))^T \qquad (1.6)$$
$$subjected\ to\ constraints$$

Where $F(x)$ is the multi-objective function formulated from 'm' individual objectives $f(x)$. When $m \geq 2$, the optimization is referred to as multi-objective optimization problem (MOP).

The MOEAs are divided into four categories: i) Pareto dominance based, ii) Decomposition based, iii) Indicator based, and iv) Model-based.

i. **Pareto dominance-based MOEA:** The individuals are ordered based on their Pareto dominance using the non-dominated sorting method, which increases the convergence of MOEA, and the crowding distance is used to increase the diversity of solutions on the Pareto front.

ii. **Decomposition-based MOEA:** The MOP is transformed into several single objective optimization problems. The algorithm divides the problem into subproblems using scalarization methods based on weights. Based on the distance between aggregation weights, neighborhoods are generated. The subproblem is simultaneously solved by exchanging information among the neighboring solutions. This improves the efficiency of searching the objective space for optimal solutions.

iii. **Indicator-based MOEA:** These methods use performance indicators to guide the search process and the solutions are selected based on performance indicator value. Several types of indicator metrics are available in the literature such as hypervolume indicator, R2 indicator, inverted generational distance (IGD), and so on.

iv. **Model-based MOEA:** The model-based MOEAs add the ability to learn from the environment in evolutionary algorithms. Traditional MOEAs such as Pareto, decomposition, and indicator-based are intended to operate on fixed heuristic strategies such as reproduction, selection, and variation. In the process of searching for a feasible solution, traditional MOEAs may not interact with the rapidly changing environment due to the complex properties of the problem to be solved. The model-based MOEAs uses machine learning techniques to adapt to environmental changes in the evolutionary process. The model-based MOEA replaces the traditional heuristic operators such as selection, reproduction, and fitness evaluation with a machine learning model. The models use the candidate solutions as sample training data from the current generation to generate the best solutions by learning the changes in the environment.

In all evolutionary algorithms, maintaining a proper balance between exploitation and exploration is necessary to get the global optimum solution. Exploration is the process of searching broadly in objective space, whereas exploitation is the local searching done in the vicinity of an optimal or nearly ideal solution. Excessive exploitation results in the algorithm being stopped at a local optimum point rather than getting close to the global optimum solution, whereas exhaustive exploration lengthens the convergence time. Therefore, while building evolutionary algorithms, striking the right balance between exploitation (local search) and exploration (global search) is crucial.

The MOEAs are normally modeled to handle different conflicting goals, such as maximizing the spread of solutions along the Pareto front (i.e., diversity) and minimizing the distance between the solutions along the Pareto front (i.e., convergence) [23]. The trade-off between convergence and diversity is important to choose the best solution among the solutions obtained. Therefore, to attain a balance between exploration and exploitation in this thesis, a new hybrid MOEAs were proposed.

Chapter 2

Literature Review

Chapter 2

Literature Review

2.1 Overview

In recent years, the penetration of RESs has increased rapidly in the power system, which in turn has led to many challenges to monitor and operate the modern power system. The OPF is a technique in power system planning to find the best operating point in terms of real power generation, voltage magnitude, off-nominal transformer tap positions, and shunt compensator to optimize the specific objective function(s) [1]. The OPF is a non-linear, and non-convex optimization problem that includes both continuous and discrete control variables. A discrete control variable like transformer tap setting, shunt device, and phase shifter makes the OPF problem complex. Moreover, the uncertainty and unpredictability of renewable energy sources make the system highly complex to operate and control [1]. The uncertain nature of RESs is required to be modeled accurately to monitor and control the dynamic behavior of the power system network more reliably and operate more efficiently. The OPF determines the optimal control variables by meeting the system constraints. A significant amount of research has been carried out in the OPF using both deterministic and stochastic methods.

Several deterministic methods have been offered in the literature to resolve PF problems. It includes linear programming (LP), non-linear programming (NLP), etc. Lobato *et. al.* [2] presented LP-based OPF for power loss reduction and reactive power margin minimization of generators. Yan *et. al.* [3] proposed the predictor-corrector interior-point method for the OPF problem in the form of a rectangle. During optimization, the Hessian matrices were computed only once and treated as constant. In [4], the authors proposed a quadratic programming method to minimize power loss in the OPF problem. The gradient method was proposed in [5] to develop the dynamic OPF to include wind farms without considering the cost of wind power. For solving the OPF model including wind plant, authors [6] used the Newton method and interior-point methods. However, conventional or deterministic optimization method may not handle mixed variable optimization problems; it requires mathematically well-defined objective functions and constraints, are sensitive to initial values of the problem, are problem-specific, exhibits poor convergence characteristics, and the theoretical assumptions related to problems that lead to solutions stuck at local optima points. Moreover, these methods are unable to solve real-world optimization issues. Likewise, several authors have attempted the OPF as a single-objective optimization approach with conventional optimization methods [7, 8]. To overcome the limitations of classical or deterministic

techniques, various population-based EAs were developed, which can handle nonlinear, non-differentiable, real-world complex problems, highly constrained, and high dimensionality problems, and discrete optimization problems.

The stochastic search approach adopted by EAs may explore the search area for global optimality effectively. Genetic algorithm [9], Evolutionary programming [10], and others were among the initial attempts to apply stochastic population-based techniques for OPF. Duman *et. al.* [11], the symbiotic organisms search (SOS) algorithm was proposed to solve security-constrained AC-DC OPF including wind, PV, and PEV sources. Sarda *et. al.* [12], proposed a robust CE-CMAES for solving the dynamic OPF problems. In this work, the dynamic OPF problem was modeled by including the wind, PV, and PEV uncertainties. In [13], the authors proposed an SOS method for resolving the AC OPF problem with thermal-wind-solar-tidal systems. The uncertainties associated with wind, PV, and tidal energy systems were modeled with Weibull, Lognormal, and Gumbel PDFs respectively. In [14], the authors developed and solved different constrained OPF problems for power systems containing RESs like wind and solar power using an HMICA-SQP. Biswas *et. al.* [15], used the SHADE algorithm with the SF method for arriving at the solution to OPF with RESs. Similarly, in [16, 17] the authors proposed several meta-heuristic optimization methods for solving OPF with RESs. However, these were formulated as single-objective optimization problems. In the real world, the OPF problem is multi-objective and the tradeoff between multiple objects gives better optimal conditions for operation. In most practical optimization problems, the objective functions conflict mutually. According to the no free lunch (NFL) theorem [18], no single solution is available which can optimize all the objectives. To overcome this problem, MOPs have been developed and widely exist in all applications, such as cloud computing, path planning, design, and scheduling [19]. These problems consist of more than one conflicting objective.

In contrast to the majority of single-objective examples addressed in the aforementioned OPF literature, the weighted sum method was provided utilizing a backtracking search optimization [20], the moth swarm algorithm [21], etc. In this optimization problem, weights are assigned to the objectives, and the weighted sum of the objectives is minimized. The OPF problem is solved using linear scalarization or weighted-sum-based multi-objective optimization [22-25], in which every objective is given a weight and the summation of weights must be one. In [26], the authors proposed a weighted sum-based differential evolution (DE) algorithm for the MOOPF problem. In the weighted sum-based method, multiple objectives are transformed into a single objective problem by multiplying each objective by weight such that the sum of all weights is one. The authors considered

different objective functions in both normal and contingency conditions. Roy and Paul [27], proposed a krill herd algorithm (KHA) for solving MOOPF problems using the weighted sum-based method. The crossover and mutation operator of the DE algorithm was merged with KHA to enhance the reliability of the solution and also to select a high-quality solution. Ozan [28], proposed an improved Archimedes optimization method for multi/single-objective OPF problems. Many authors used [29, 30] weighted sum-based MOOPF problems with different objectives. The weighted sum-based methods are simple in combining multi-objectives into a single objective with suitable weights. A weighted sum-based method is the basic type of a decomposition-based MOEA method. However, the fundamental disadvantage of this method is that it must be executed multiple times to produce the approximation set. Moreover, the weighted sum-based method fails to obtain the compromised solutions, and in concave optimization problems, the weighted sum-based method produces optimal solutions for one of the objective functions. This approach heavily depends on weights that are assigned to each objective value, and these, in turn, affect the optimal solution. A series of solutions using multi-objective approaches is preferable to a single solution employing a weighted sum strategy for various reasons.

Abido *et. al.* [31] introduced SPEA to address the active and reactive power dispatch problem. SPEA's main drawback is that the beginning population has only one set of non-dominated solutions and the external population is filled with the same ones. This will lead to Pareto optimal front being suboptimal, leading to a non-uniformly distributed Pareto front. Jeyadevi *et. al.* [32], Pareto dominance-based method was adduced as modified NSGA-II to solve the multi-objective optimization of the reactive power dispatch problem, and the controlled elitism method was deployed to preserve the diversity in Pareto-front; to obtain high uniformity, dynamic crowding distance (DCD) based strategy was proposed. Several authors [33-39] proposed Pareto dominance-based multi-objective optimization for OPF. However, Pareto-based methods suffer from limitations. The selection pressure reduces with an increase in the number of objectives and as a result, the effectiveness of the solution deteriorates proportionately to such an extent that a loss of diversity occurs in the population.

While the aforementioned articles focused exclusively on thermal units, a system that combines thermal and wind powers was explored in the literature to achieve the lowest possible generation cost. To specify the boundaries of reactive power generation ability, Panda *et. al.* [40] suggested a modified bacteria foraging algorithm (MBFA) and built the DFIG model within the OPF architecture. Static synchronous compensation an external reactive power assisting was utilized in [41] to examine a network having wind and thermal sources, and the

OPF issue was handled using the ant colony algorithm and MBFA. In an OPF dispatching program, a stochastic model of wind generation was described in [42]. Included in [43] was the DFIG wind turbine model. [44] presents the OPF model for a hybrid model with PV, a diesel generator, and a battery that operates in isolated mode. In [45], pumped hydro was presented as an alternative method of storage for an autonomous hybrid system composed of PV, wind, and diesel generation. In conclusion, the OPF including thermal, wind, PV, and PEV powers requires additional investigation.

In the literature, numerous single-objective problems of OPF have been resolved. In the current socio-economic environment, it becomes vital to evaluate multiple objectives for OPF. In the past, the typical formulation of OPF consisted of a single target, which was primarily the minimization of generation cost. In several countries, legislation and the installation of a carbon tax have heightened the significance of decreasing greenhouse gas emission. Maintaining power quality necessitates low voltage fluctuations from the desired voltage, and any improvement in power loss provides utilities a financial advantage. Therefore, the MOOPF problem must take into account emission, voltage variation, and power loss in addition to the cost. Since this MOOPF problem is highly non-linear and aims are frequently contradictory, it necessitates the application of effective techniques. An appropriate MOEA can yield a Pareto front (PF) with multiple non-dominated optimal values for balancing multiple objectives.

Several researchers expanded their work on OPF utilizing hybrid heuristic-based multi-objective optimization algorithms[46, 47]. Nonetheless, as the number of objective functions increases, so does the size of the objective space. Therefore, nearly all solutions became non-dominant with each other. This worsens the selection pressure on the PF, a collection of all Pareto-optimal solutions, and leads to a population diversity loss during the evolution as well as a slower pace of convergence for MOPs [48, 49].

The MOEAs are normally modeled to tackle different conflicting objectives, such as maximizing the spread of solutions along the Pareto front (i.e., diversity) and minimizing the distance between the solutions along the Pareto front (i.e., convergence) [50, 51]. The trade-off between convergence and diversity is important to choose a good quality solution among the solutions obtained. Therefore, to attain a balance between exploration and exploitation, several hybrid MOEAs are proposed in this thesis for solving the OPF problem.

2.2 Motivation

In addition to the benefits cited in the existing literature for various optimization strategies, there are also certain drawbacks. The limitations are as follows:

- In the literature, the OPF problem is typically written as a single objective optimization problem [9–17], however, the practical OPF problem has several objectives, and trade-off solutions play a crucial part in power system decision-making.
- The weighted-sum-based technique [20-30] is easy to construct and apply to multi-objective problems. This strategy turns a MOP into a single-objective problem by combining weighted objectives. Apart from the merits, the demerits are: (i) It is incapable of dealing with non-convex Pareto fronts (PF) or the method yields solutions that are optimal in one of the objective functions for non-concave PF and (ii) The weights assigned to the objectives have a substantial effect on the optimal solutions.
- The Pareto-oriented MOEAs [31-39] are gaining importance because they outperform the constraints of weighted-sum-based MOEAs. The solutions are prioritized according to Pareto rather than weighted objectives, which enhances MOEA convergence. Then, the crowding distance method is applied to ensure the diversity of the solutions in the PF. In addition to their benefits, Pareto-based MOEAs have the following disadvantages: (i) In dominance-based approaches, it may be impossible to ensure a level of convergence, and it is difficult to obtain a particularly regular spacing of solutions along the PF. (ii) As objective space expands, nearly all solutions inside a population become non-dominant with one another [48]. (iii) Because dominance resistance solutions exist [49], selection pressure degrades and it may lead to the loss of population diversity during the evolutionary process, and it degrades the effectiveness of MOEA [50], and (iv) Pareto dominance may not give any assurance that the solution provided is an optimal one, as there is no indicator of performance during the evolution.
- In a power system, integrating RESs like WECS and SPVS with conventional OPF is necessary to consider the impact of uncertainty of these sources. The uncertain nature of WECS and SPVS are modeled using PDFs and their uncertainty cost is calculated using Monte-Carlo simulations.
- In addition to RESs, integrating the PEVs with conventional OPF to consider the impact of uncertainty of these sources becomes necessary. The uncertain nature of PEVs is modeled using PDFs and their uncertainty cost is calculated using Monte-Carlo simulations.
- The OPF problem is a constrained optimization problem, which requires an efficient CHM in combination with an evolutionary algorithm to obtain feasible optimal solutions. The commonly used one is the static penalty approach here a penalty is applied to the fitness of an infeasible individual for breaching limitations.

- However, the drawback with the static penalty-based method is that the accuracy of OPF suffers due to the huge error associated with penalty factors. The penalty factors of each objective that are needed to be added to the objective function are fine-tuned by trial and error.

2.3 Objectives of the Research

The objective of the research work is to design a multi-objective framework to handle issues with OPF problems in power systems.

The research contributions are as follows:

- A new hybrid decomposition and local-dominance based MOEA was proposed for the OPF problem. Combining decomposition and dominance approaches produced qualitatively and quantitatively distinct compromised solutions along the Pareto optimal front. In this approach, the static penalty-based CHM is proposed to handle equality and inequality restrictions of the OPF problem. In addition, a fuzzy technique is applied to Pareto-optimal solutions to determine the optimal trade-off solution.
- A new hybrid decomposition and summation of normalized objectives with an improved diversified selection-based MOEA including WECS and SPVS uncertainty were proposed for the OPF problem. This chapter suggests a novel CHM that adds the penalty adaptively and avoids parameter dependence on penalty calculation. The summation-based sorting and enhanced diverse selection were applied to increase the diversity of MOEA. On OPF cost analysis, the impact of RES like WECS and SPVS on integration is evaluated. To reduce the total generation cost, the OPF problem takes into account the cost of RESs to study the influence of intermittent and unpredictable renewable sources on operation cost. Weibull and Lognormal PDFs were used, respectively, to describe the uncertainty of WECS and SPVS sources.
- A new hybrid decomposition and summation of normalized objectives with improved diversified selection-based MOEA including WECS, SPVS, and PEVs uncertainty were proposed for the OPF problem. The MOOPF problem was solved using a unique CHM that adaptively adds the penalty and avoids the parameter relying on the penalty calculation. The summation-based sorting and enhanced diverse selection were applied to increase the diversity of MOEA. In addition, a fuzzy technique is applied to Pareto-optimal solutions to determine the optimal trade-off solution. The impact of intermittence of WECS, SPVS, and PEVs integration was considered for optimal cost analysis. The uncertainty associated with WECS, SPVS, and PEV systems was

represented using PDFs and its uncertainty cost was calculated using Monte-Carlo simulations (MCSs).

- A novel hybrid decomposition and invasive weed optimization (IWO) based MOEA was proposed for the OPF problem. The standard OPF problem was transformed into a stochastic OPF by incorporating the uncertainty of WECS, SPVS, and PEV systems. The MOOPF problem was solved using a unique CHM that adaptively inserts the penalty and avoids the parameter relying on penalty calculation. The IWO technique's selection qualities were utilized to boost the diversity of the proposed method. Monte Carlo simulations were used to assess the generation cost of WECS, SPVS, and PEVS in an effort to lower the total generation cost. Weibull, Lognormal, and Normal PDFs were used to characterize the unpredictability of WECS, SPVS, and PEV sources, respectively.

2.4 Thesis Organization

The thesis is organized as follows:

Chapter 1 introduces the OPF problem and its importance in monitoring and operation of the network. It describes briefly the necessities of the OPF problem and the impact of WECS, SPVS, and PEVS penetrations on the power system.

Chapter 2 presents a comprehensive literature overview of the OPF issue in a power system and discusses the existing methods and their strengths and weaknesses. It provides details of methods used to formulate the optimal power flow problem such as single objective and multi-objective frameworks and discusses different optimization techniques to handle the problem.

Following an extensive literature review on the topic, the motivation for the proposed research work is presented, followed by the objectives of the research, contributions, and organization of the thesis.

Chapter 3 proposes a new hybrid decomposition and local-dominance based MOEA for the OPF problem. The four objectives considered are minimizing the total generation cost, emission, active power loss, and voltage magnitude deviation. As the OPF problem is a constrained optimization problem, the static penalty-based constrained handling method was used to handle several equal and inequality constraints, which aims to obtain the feasible global optimal solution. The outcomes of the proposed algorithm were compared with NSGA-II and MOPSO methods and demonstrated on IEEE 57-bus and IEEE 118-bus systems.

Chapter 4 proposes a new hybrid decomposition and summation of normalized objectives with improved diverse selection-based MOEA, including WECS and SPVS generation uncertainty for the OPF problem. This work recommends a novel CHM, that adaptively inserts the penalty and avoids the parameter relying on penalty calculation. The summation-based sorting and enhanced diverse selection were applied to increase the diversity of MOEA. The MOOPF problem was modeled with four objectives: minimizing total generation cost, including WECS and SPVS generation cost, emission, active power loss, and voltage magnitude deviation. In the OPF cost analysis, the influence of RESs such as WECS and SPVS on integration was examined. To minimize the overall cost, the cost of RESs was factored into the OPF to study the influence of intermittent and unpredictable renewable sources on cost and operation. The uncertainty of WECS and SPVS was described using Weibull and Lognormal PDFs respectively. The versatility of the proposed method was demonstrated on IEEE 57-bus and IEEE 118-bus systems and the results obtained were compared with NSGA-II, and MOPSO algorithms to demonstrate the superiority of the proposed method.

Chapter 5 proposes a new hybrid decomposition and summation of normalized objectives with improved diversified selection-based MOEA including WECS, SPVS, and PEVs uncertainty for the OPF problem. The MOOPF problem includes minimization of the total generation cost, emission, active power loss, and voltage magnitude deviation as objectives, and a novel CHM, that adaptively inserts the penalty and avoids the parameter relying on penalty calculation. The summation-based sorting and enhanced diverse selection were applied to increase the diversity of MOEA. In addition, a fuzzy technique is applied to Pareto-optimal solutions to determine the optimal trade-off solution. The impact of intermittence of WECS, SPVS, and PEVs integration was considered for optimal cost analysis. The uncertainty associated with WECS, SPVS, and PEV systems was represented using PDFs and the uncertainty cost was calculated using Monte-Carlo simulation. The superiority of the proposed method was validated by comparing it with NSGA-II, and MOPSO algorithms and tested on IEEE 57-bus and IEEE 118-bus systems.

Chapter 6 proposes a new hybrid decomposition and invasive weed optimization (IWO) based MOEA for the OPF problem. The standard OPF problem was transformed into a stochastic OPF by incorporating the uncertainty of WECS, SPVS, and PEV systems. This chapter presents a new CHM that adaptively inserts the penalty and avoids the parameter relying on penalty calculation. The IWO technique's selection qualities were utilized to increase the diversity of MOEA. The MOOPF problem includes minimization of the total generation cost,

emission, active power loss, and voltage magnitude deviation as objectives. The generation cost of WECS, SPVS, and PEV sources was examined using Monte Carlo simulations to reduce the total generation cost. Weibull, Lognormal, and Normal PDFs were used to characterize the unpredictability of WECS, SPVS, and PEV sources, respectively. The impact of WECS, SPVS, and PEV uncertainties, was taken into account to validate the proposed method. The superiority of the proposed method was validated by comparing it with NSGA-II, and MOPSO algorithms and tested using IEEE 57-bus and IEEE 118-bus systems.

Chapter 7 summarizes the research contribution, findings, and observations on the proposed research work. Then it presents the scope for future work on the topic.

2.5 Summary

This chapter provides a summary of existing literature on OPF in power systems. With the penetration of renewable energy sources, power system operation becomes more challenging. This chapter discusses different OPF solutions in literature, constraint handling methods, and literature on the integration of uncertain sources like WECS, SPVS, and PEVs. This chapter also deals with MOOPF problem-related research and presents a discussion of various types of multi-objective evolutionary algorithms. Furthermore, motivation, contributions of the study, and organization of the thesis are presented in this chapter.

Chapter 3

A Novel Hybrid Multi-Objective Evolutionary Algorithm Based on Decomposition and Local Dominance for the Optimal Power Flow

This work is published in:

Ravi Kumar Avvari and Vinod Kumar D. M. “Multi-Objective Optimal Power Flow with efficient Constraint Handling using Hybrid Decomposition and Local Dominance Method.” **Journal of The Institution of Engineers (India): Series B,** Springer, Vol. 103, No. 5, pp. 1643-1658, Oct 2022. **(Scopus)**.

Chapter 3

A Novel Hybrid Multi-Objective Evolutionary Algorithm Based on Decomposition and Local Dominance for the Optimal Power Flow

3.1 Introduction

In this chapter, a novel hybrid decomposition and local dominance-based MOEA was proposed for the OPF problem with four conflicting objectives including minimization of total generation cost, emission, active power loss, and voltage magnitude deviation. A penalty method was used to address multiple MOOPF problem restrictions. In addition, a fuzzy technique was employed to identify the best compromise solution among Pareto-optimal solutions. The decomposition and local dominance methods were employed to get a uniformly distributed Pareto front and improved convergence characteristics. The suggested method combines decomposition and local dominance strategies to enhance effectiveness, (i.e., the exploring and exploitation) of MOEA. To evaluate the suggested method IEEE 57-bus, and IEEE 118-bus systems were studied, and the obtained results were evaluated using the NSGA-II and MOPSO algorithms. The contributions of this chapter are as follows:

i. Proposed a new hybrid decomposition and local dominance-based MOEA for the OPF problem.
ii. The trade-off between convergence and diversity in the solutions was obtained using hybrid decomposition and dominance methods.
iii. Using a fuzzy technique, the optimal trade-off solution among Pareto-optimal solutions was determined.
iv. An efficient CHM to tackle constraints in the MOOPF problem was used.

3.2 Problem Formulation

The MOOPF seeks to optimize objective functions while adhering to limitations by identifying the optimal decision variables. Accordingly, the MOOPF problem is stated as follows:

$$Min\ F(x,u) = [F_1(x,u), F_2(x,u), \ldots . F_m(x,u)] \tag{3.1}$$

Subject to:

$$g(x,u) = 0 \tag{3.2}$$

$$h(x,u) \leq 0 \tag{3.3}$$

where $F_m(x,u)$ denotes m^{th} objective; $g(x,u)$ and $h(x,u)$ indicates equality and inequality constraints respectively.

3.2.1 Objectives

The MOOPF problem considered the minimization of four objectives: a) total generation cost (J_1), b) emission (J_2), c) active power loss (J_3), and d) voltage magnitude deviation (J_4).

a) Total generation cost ($/h):

The quadratic connection approximates the relationship between the cost of generation and power output. The following expression describes the total generation cost from thermal generators:

$$Min\ J_1 = \sum_{i=1}^{N_G}(a_i + b_i P_{Gi} + c_i P_{Gi}^2) \tag{3.4}$$

where N_G is the number of generators; P_{Gi} is the i^{th} generator output active power; a_i, b_i, c_i is the i^{th} generator cost coefficients;

b) Emission (ton/h):

The generation of electric power from traditional fossil fuels would result in the emission of hazardous gases into the atmosphere. The following expression describes the total emission from thermal generators:

$$MinJ_2 = \sum_{i=1}^{N_G}(\alpha_i + \beta_i P_{Gi} + \gamma_i P_{Gi}^2 + \delta_i e^{\varepsilon_i P_{Gi}}) \tag{3.5}$$

where $\alpha_i, \beta_i, \gamma_i, \delta_i, \varepsilon_i$ are the i^{th} generator emission coefficients;

c) Active power loss (MW):

The following equation can be used to express active power loss:

$$Min\ J_3 = \sum_{k=1}^{N_L}\left(G_k\left(V_i^2 + V_j^2 - 2V_iV_j\cos\theta_{ij}\right)\right) \tag{3.6}$$

where N_L is the number of lines; θ_{ij} is the voltage angles between buses i and j; G_k indicates conductance of the k^{th} branch; V_i, V_j is the voltage magnitudes at i^{th} and j^{th} bus respectively.

d) Voltage magnitude deviation (p.u.):

The voltage variation is the sum of all voltage variations at load buses in the network relative to the reference voltage. The mathematical expression is as follows:

$$Min\ J_4 = \sum_{i=1}^{N_{PQ}}\left|\left(V_i - V_{ref}\right)\right| \tag{3.7}$$

where N_{PQ} is the number of PQ buses; V_{ref} is the reference voltage set to 1 p.u.; V_i is the i^{th} load bus voltage.

3.2.2 Constraints

The MOOPF objectives are subjected to the following equality and inequality constraints.

a) Equality constraints:

The equality constraints are power-balancing equations in which the sum of the generations of the real and reactive powers is equal to their corresponding demands and losses.

- Power flow constraints

$$P_{Gi} - P_{Di} - V_i \sum_{j=1}^{N_B} V_j \left(G_{ij} \cos\theta_{ij} + B_{ij} \sin\theta_{ij}\right) = 0; i = 1,2, \dots N_B \quad (3.8)$$

$$Q_{Gi} - Q_{Di} - V_i \sum_{j=1}^{N_B} V_j \left(G_{ij} \sin\theta_{ij} - B_{ij} \cos\theta_{ij}\right) = 0; i = 1,2, \dots N_B \quad (3.9)$$

where N_B is the number of buses; P_{Gi}, Q_{Gi}, and P_{Di}, Q_{Di} represent the real, reactive power generations and demands at the i^{th} bus, respectively; G_{ij}, B_{ij} is the conductance, susceptance of lines between buses i and j respectively;

b) Inequality constraints:

The operational limitations on generators, transformers, and shunt devices, as well as the security requirements on lines and load buses, constitute inequality constraints.

- Generator constraints: The boundary limits of real and reactive powers and voltage magnitude of the generator buses are expressed as follows:

$$P_{Gi}^{min} \le P_{Gi} \le P_{Gi}^{max}; i = 1,2, \dots N_G \quad (3.10)$$

$$Q_{Gi}^{min} \le Q_{Gi} \le Q_{Gi}^{max}; i = 1,2, \dots N_G \quad (3.11)$$

$$V_{Gi}^{min} \le V_{Gi} \le V_{Gi}^{max}; i = 1,2, \dots N_G \quad (3.12)$$

- Shunt VAR compensator constraints: The following are the boundary values for shunt compensators:

$$Q_{Ci}^{min} \le Q_{Ci} \le Q_{Ci}^{max}; i = 1,2, \dots N_C \quad (3.13)$$

- Transformer constraints: The ideal operating limits for tap settings on a transformer are given as follows:

$$T_i^{min} \le T_i \le T_i^{max}; i = 1,2, \dots N_T \quad (3.14)$$

- Security constraints: The voltage limits of the load buses and the apparent power value of each transmission line, which can be restricted by its maximum capacity, are given as follows:

$$V_{Li}^{min} \le V_{Li} \le V_{Li}^{max}; i = 1,2, \dots N_{PQ} \quad (3.15)$$

$$|S_{li}| \le S_{li}^{max}; i = 1,2, \dots N_L \quad (3.16)$$

where N_C, N_T is the number of shunt compensators and transformers respectively; S_{li} and S_{li}^{max} are the apparent power flow and its max. limit of i^{th} line; P_{Gi}^{min},P_{Gi}^{max} are the limits on real power generation; Q_{Gi}^{min},Q_{Gi}^{max} are the limits on reactive power generation; V_{Gi}^{min},V_{Gi}^{max} are the limits on generator bus voltages; T_i^{min},T_i^{max} are the limits on transformer taps; Q_{Ci}^{min},Q_{Ci}^{max} are the limits on shunt compensator; V_{Li}^{min}, V_{Li}^{max} are the limits on load bus voltages;

3.3 Constraint Handling Method

To address the MOOPF problem restrictions, a constraint-handling process was deployed. Boundary limits of the decision variables are self-constrained and can be reset using Eq. (3.18) during simulation. In addition, changes to the equality restrictions of real and reactive power flows can be done during load flow calculation using Newton-Raphson (Polar) method. The remaining constraints (inequality) are handled using the penalty factor approach. In the penalty factor approach, the violated restrictions are multiplied by the punishment factor and added to the corresponding objective value. This can be formulated as shown in Eq. (3.17).

It should be mentioned that the decision variables are self-constrained. The inequality constraints of P_{G1},V_L,Q_G, and S_l can be included in the objective function as quadratic penalty terms. Thus, the augmented objective function will be as:

$$J_{MOOPF}(x,u) = \begin{bmatrix} J_{OPF1}(x,u) \\ . \\ . \\ . \\ . \\ . \\ J_{OPFM}(x,u) \end{bmatrix} = \begin{bmatrix} F_{OPF1} + \lambda_P\left(P_{G1} - P_{G1}^{lim}\right)^2 + \lambda_V \sum_{i=1}^{N_{PQ}} \left(V_{Li} - V_{Li}^{lim}\right)^2 \\ +\lambda_Q \sum_{i=1}^{N_G} \left(Q_{Gi} - Q_{Gi}^{lim}\right)^2 + \lambda_S \sum_{i=1}^{N_L} \left(S_{li} - S_{li}^{lim}\right)^2 \\ . \\ . \\ . \\ . \\ . \\ F_{OPFM} + \lambda_P\left(P_{G1} - P_{G1}^{lim}\right)^2 + \lambda_V \sum_{i=1}^{N_{PQ}} \left(V_{Li} - V_{Li}^{lim}\right)^2 \\ +\lambda_Q \sum_{i=1}^{N_G} \left(Q_{Gi} - Q_{Gi}^{lim}\right)^2 + \lambda_S \sum_{i=1}^{N_L} \left(S_{li} - S_{li}^{lim}\right)^2 \end{bmatrix} \tag{3.17}$$

where λ_P, λ_V, λ_Q and λ_S are the penalty factors; M is the number of objective functions; x^{lim} is the limit value of the independent variable x and is given as:

$$x^{lim} = \begin{cases} x_{min};\ if & x < x_{min} \\ x;\quad if & x_{min} \le x \le x_{max} \\ x_{max};\ if & x > x_{max} \end{cases} \tag{3.18}$$

3.4 Proposed Method

The proposed MOEA is obtained by combining the Pareto-dominance and decomposition techniques to exploit the advantages in both methods and to maintain the balance between exploration and exploitation. The Pareto-dominance and decomposition techniques were incorporated from the NSGA-II [57] and MOEA/D [53] methods.

In Pareto dominance method, the feasible solutions are selected using non-dominated sorting technique to rank the solutions and crowding distance method is employed to improve

the population diversity. However, with increase in objective size dominance methods may not maintain the diversity of the population. On the other hand, Decomposition methods decompose the MOP into multiple sub-problems using weight vectors. The sub-problems are then simultaneously optimized. The neighborhoods are created based on the distance between weights. In each population evolution, neighborhood information is used to choose which solutions to select. The penalty-based intersection (PBI) is utilized to assign relative fitness values to each solution [53]. The PBI is stated below:

$$PBI(X|w, z^*) = d_1 + \theta d_2$$

$$where\ d_1 = \frac{\|(z^* - F(X)^T.w)\|}{\|w\|} \text{ and } d_2 = \|F(X) - (z^* - d_1.w)\|$$

$$\text{where } F(X) = [J_1, J_2, J_3, J_4] \tag{3.19}$$

where z* is the ideal point, w is the weight vector, and θ be the penalty value.

Randomly generate a population of size 'N', which is equal to the number of weight vectors. The weight vectors with a uniform distribution are created using SSA [54]. Each member of the population is given a weight vector and is associated with a neighborhood. The mating parents are then selected from the nearby region using the minimum angle requirement and a probability of 'δ'. The typical value set to selection probability 'δ' is 0.8. The angle criteria are used to identify weight vectors' nearest neighbors. The vectors with the least angles are chosen to be the neighbors. Based on the angle, a neighborhood is allotted to each weight vector. For every vector, a set of parents is chosen from the neighbors depending on selection probability. If there are no individuals in the given region, the mating parent is selected from the entire population. The angle between the two vectors is given by the formulae [55] as given below:

$$\tan\varphi = \frac{d_2}{d_1}$$

$$where\ d_1 = \frac{\|w_i^T.w_j\|}{\|w_j\|}\ and\ d_2 = \left\|w_i - d_1 \frac{w_j}{\|w\|}\right\|$$

$$where\ i, j = 1, 2, \dots, N\ and\ i \neq j \tag{3.20}$$

$$where\ \varphi = \text{angle between } d_1 \text{ and } d_2.$$

The new offspring population is reproduced via crossover and mutation. The old and new populations are partitioned into 'N' sub-populations. The partition is done by comparing the two individuals. For comparing the individuals, the dominance method and PBI are used Eq. (3.19). To choose competent individuals from 'N' subpopulations, the elitist selection procedure is then employed. This procedure is repeated until the termination criterion has been

satisfied. The maximum number of iterations served as the termination criterion for this approach. Using a fuzzy technique, the optimal solution is determined [56].

The steps in the proposed method are as follows:

Initialization: Randomly generate initial population (P_t) of size 'N' and weight vectors with a uniform distribution using SSA [54] as follows:

$$N(D, M) = \binom{D + M - 1}{M - 1} \; for \; D > 0 \tag{3.21}$$

Here *D* and *M* represent the number of divisions for each objective coordinate and objective function respectively.

Run the load flow to determine the fitness value of the chosen objective function and compute the constraint violations. If any constraint violation occurs, it is penalized using Eq. (3.17), and Eq. (3.18).

Find the neighboring solutions, the vectors with the least angles are chosen to be the neighbors. The angle between two vectors is given by Eq. (3.20).

Find the minimum values for all the objectives to form the current ideal point.

Reproduction: Select N mating pairings based on angle requirements. With the probability of δ, a pair of mated parents is chosen for each weight vector. To generate new population (Qt) use crossover and mutation.

Population-partition: The old (P_t) and new (Q_t) populations are partitioned into N subpopulations. Based on the partition, every sub-population has Ni individual populations. The partition is done by comparing the two individuals.

For Comparing the individuals, the dominance and PBI methods are used. Firstly the dominance between individuals x and y is compared. If solution x is seen as better compared to y, return true; otherwise, their respective PBI values are compared. The lower the PBI value the better the solution.

Elitist selection: Here, all individuals are partitioned into multiple levels. During elitist selection, the individuals for the next-level Pt+1 are chosen. Choose the individual from each population subset till 'N' is not exceeded. Otherwise, a random sample is selected from the partitioned population.

Use the fuzzy approach [59] on the final Pareto front to choose the best-compromised solution.

3.5 Results and Discussions

The proposed method was executed on MATLAB R2016a and the simulation was carried out on i3-Processor with 4GB RAM. To validate the efficacy of the proposed method, it was compared to NSGA-II [57] and MOPSO [58] algorithms. The control parameters of the proposed method, NSGA-II, and MOPSO are given in Table 3.1, these values are selected in accordance with the global optimal solution. A total of five cases were considered on IEEE 57-bus, and IEEE 118-bus systems to test the efficiency of the proposed method for the MOOPF problem. The various cases considered are given in Table 3.2. The description of the test systems was given in Table 3.3. Appendices A and B contain system data for the IEEE 57-bus, and 118-bus, respectively.

Table 3.1: Control parameters of the proposed method, NSGA-II, and MOPSO.

S. No.	Method	Control parameters
1.	**Proposed method**	**Population size (*N*) = 100, number of divisions made along the every objective (*D*) = 12, neighborhood size (*T*) = 20, crossover probability (*Pc*) = 1.0, mutation probability (*Pm*) = 0.05, and maximum iterations= 100.**
2.	NSGA-II [57]	N = 100, Pc = 0.8, Pm = 0.01, and max. iterations = 100.
3.	MOPSO [58]	N = 100, $C_1 = C_2 = 2$, W = 0.5, and max. iterations = 100.

Table 3.2: Various cases considered.

S. No.	Test Systems	Case #	J_1	J_2	J_3	J_4
1.	IEEE 57-bus system	Case-1	✓	✓	--	--
		Case-2	✓	--	✓	✓
		Case-3	✓	✓	✓	✓
2.	IEEE 118-bus system	Case-4	✓	--	✓	--
		Case-5	✓	--	✓	✓

Table 3.3: Test systems description.

Specifications	IEEE 57-bus system		IEEE 118-bus system	
Buses	57	[59]	118	[59]
Lines	80		186	
Thermal units	7	Buses:1,2,3,6,8,9 and 12	54	Buses: [59]
Slack bus	1	Bus:1	69	Bus: 69
Transformer tap positions	17	Lines:19,20,31,35,36,37,41,46, 54,58,59,65,66,71,73,76, and 80	9	Lines: 8,32,36, 51, 93,95,102,107 and 127
Shunt capacitors	3	Buses:18, 25, and 53	12	Buses:34,44,45,46,48,74,79,82, 83, 105, 107 and 110
Control variables	33	Generator bus real powers (6) + voltages (7) + transformer tap settings (17) + shunt capacitor (3).	128	Generator bus real powers (53) + voltages (54) + transformer tap settings (9) + shunt capacitor (12).
Load	-	1250.80MW, 336.40MVAR	-	4242.00MW, 1439.00MVAR

3.5.1 IEEE 57-bus system

The proposed method was tested on an IEEE 57-bus system [59], which has 7 thermal generators (#1 bus as a slack bus), 80 lines, 17 off-nominal transformers, 3 shunt VAR compensators, the real and reactive power demand of 1250.80 MW and 336.40 MVAR, respectively.

a) Case-1: Minimize J_1, and J_2 simultaneously

In this case, the proposed method was simulated by considering two objectives J_1 and J_2. The Pareto-optimal fronts (PFs) observed in this case, are depicted in Figure 3.1. The optimal decision variables obtained by the proposed method are presented in Table 3.4. The proposed method obtains a total generation cost of **42082.05$/h** and emission of **1.2233ton/h**. NSGA-II [57] gives 42091.76$/h, 1.2971ton/h and MOPSO [58] gives 42576.62$/h, 1.4976ton/h respectively as shown in Table 3.5.

b) Case-2: Minimize J_1, J_3, and J_4 simultaneously

In this case, the proposed method was simulated by considering three objectives J_1, J_3, and J_4. The Pareto-optimal fronts (PFs) observed in this case are depicted in Figure 3.1. The optimal decision variables obtained by the proposed method are presented in Table 3.4. The proposed method obtains a total generation cost of **41919.00$/h,** active power loss of **12.2322MW**, and voltage magnitude deviation of **0.8198p.u**. NSGA-II [57] gives 42001.15$/h, 12.2673MW, 0.8312p.u and MOPSO [58] gives 42770.65$/h, 16.7486MW, 1.2838p.u respectively as shown in Table 3.5.

c) Case-3: Minimize J_1, J_2, J_3, and J_4 simultaneously

In this case, the proposed method was simulated by considering four objectives J_1, J_2, J_3, and J_4. The optimal decision variables obtained by the proposed method are presented in Table 3.4. The proposed method obtains a total generation cost of **42419.00$/h**, emission of **1.3065ton/h**, active power loss of **12.3121MW**, and voltage magnitude deviation of **0.8918p.u**. NSGA-II [57] gives 42601.15$/h, 1.4190ton/h, 12.3673MW, 1.0315p.u and MOPSO [58] gives 42970.14 $/h, 1.4998ton/h, 15.7126MW, 1.3638p.u respectively as shown in Table 3.5.

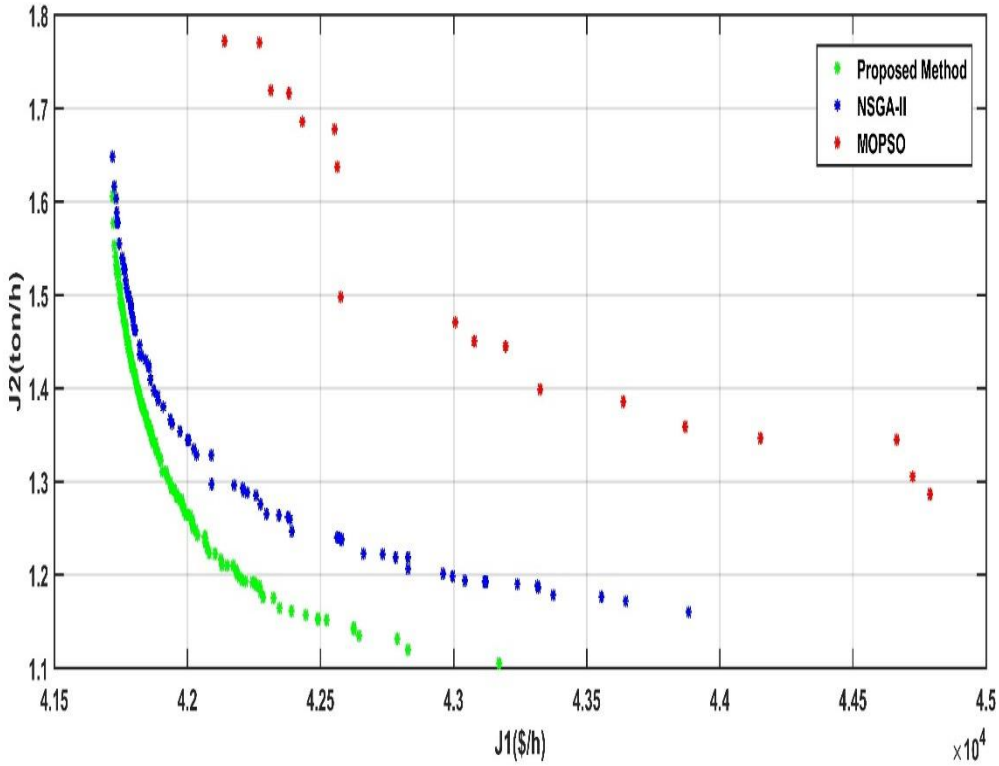

(a)

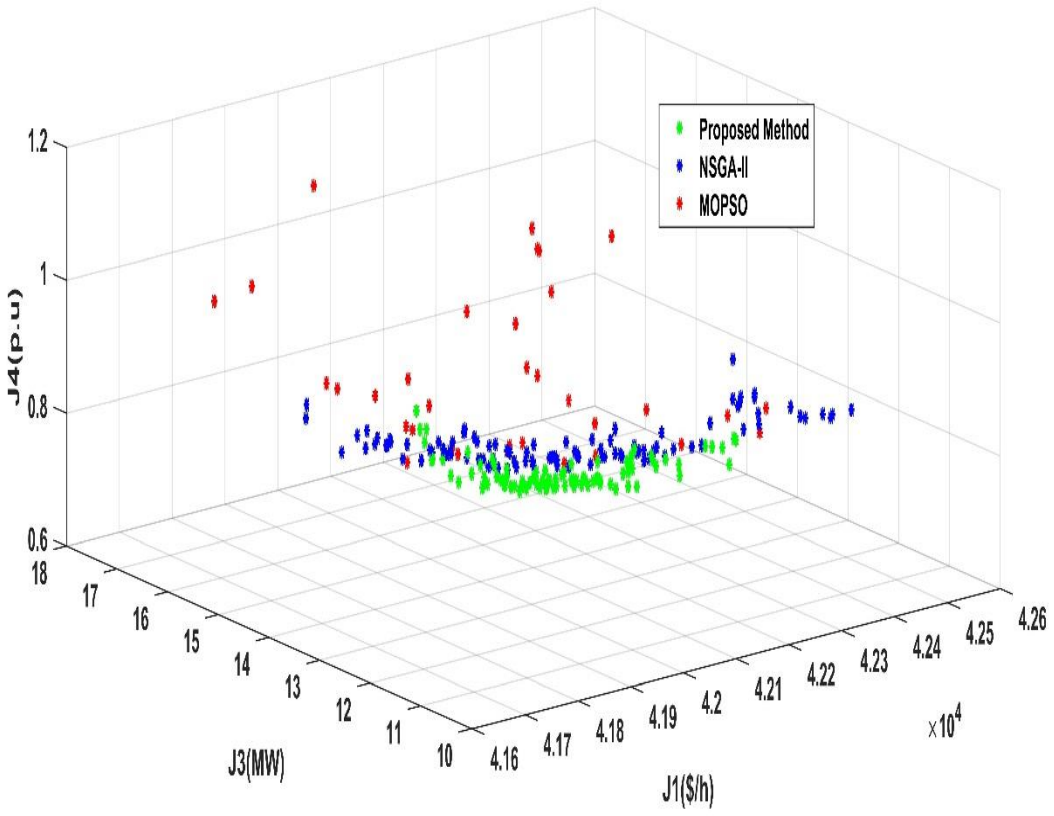

(b)

Fig. 3.1: IEEE 57-bus system: Pareto-optimal fronts. a) Case-1, and b) Case-2.

Table 3.4: IEEE 57-bus system: Optimal control variables obtained by the proposed method.

S. No.	Control variables	Limits		Case-1	Case-2	Case-3
		min	max			
1.	P2	0	100	99.8169	99.2934	69.0674
2.	P3		140	69.7015	65.0581	63.5966
3.	P6		100	98.4023	98.3741	77.8914
4.	P8		550	405.9038	391.7069	414.1483
5.	P9		100	99.7592	99.9813	85.0678
6.	P12		410	354.3541	349.8846	408.3763
7.	V1	0.95	1.1	1.0469	1.0304	1.0273
8.	V2			1.0474	1.0371	1.0300
9.	V3			1.0370	1.0328	1.0200
10.	V6			1.0519	1.0062	1.0094
11.	V8			1.0491	1.0173	1.0359
12.	V9			1.0325	1.0337	1.0315
13.	V12			1.0215	1.0230	1.0233
14.	T19	0.9	1.1	0.9887	1.0067	0.9858
15.	T20			1.0476	1.0132	0.9979
16.	T31			1.0129	1.0035	1.0175
17.	T35			1.0297	0.9925	1.0093
18.	T36			0.9765	1.0075	1.0280
19.	T37			0.9898	1.0215	1.0226
20.	T41			1.0232	1.0041	1.0057
21.	T46			0.9654	0.9629	0.9614
22.	T54			0.9773	0.9266	0.9417
23.	T58			1.0087	0.9709	0.9680
24.	T59			1.0011	0.9692	0.9679
25.	T65			0.9711	0.9972	0.9813
26.	T66			0.9804	0.9548	0.9499
27.	T71			1.0055	0.9879	0.9435
28.	T73			1.0286	1.0202	1.0036
29.	T76			0.9956	1.0042	0.9911
30.	T80			1.0116	1.0298	1.0285
31.	QC18	0	20	9.9675	9.3891	12.6199
32.	QC25			8.4505	12.2131	11.0358
33.	QC53			4.4013	7.0793	5.0682
1.	**J_1($/h)**	**-**	**-**	**42082.05**	**41919.00**	**42419.00**
2.	**J_2(ton/h)**	**-**	**-**	**1.2233**	**-**	**1.3065**
3.	**J_3(MW)**	**-**	**-**	**-**	**12.2322**	**12.3121**
4.	**J_4(p.u.)**	**-**	**-**	**-**	**0.8198**	**0.8918**

Table 3.5: IEEE 57-bus system: Comparison of the proposed method.

Case #	Objective functions	**Proposed method**	NSGA-II [57]	MOPSO [58]
Case-1	J_1($/h)	**42082.05**	42091.76	42576.62
	J_2(ton/h)	**1.2233**	1.2971	1.4976
Case-2	J_1($/h)	**41919.00**	42001.15	42770.65
	J_3(MW)	**12.2322**	12.2673	16.7486
	J_4(p.u.)	**0.8198**	0.8312	1.2838
Case-3	J_1($/h)	**42419.00**	42601.15	42970.14
	J_2(ton/h)	**1.3065**	1.4190	1.4998
	J_3(MW)	**12.3121**	12.3673	15.7126
	J_4(p.u.)	**0.8918**	1.0315	1.3638

3.5.2 IEEE 118-bus system

The proposed technique has also been investigated for the IEEE 118-bus system [59], which has 54 thermal generator buses (# 69 bus as a slack bus), 186 lines, 9 off-nominal transformers, 12 shunt VAR compensators, the real and reactive power demand of 4242.00MW and 1439.00MVAR, respectively.

a) Case-4: Minimize J_1 and J_3 simultaneously

In this case, the proposed method was simulated by considering two objectives J_1 and J_3. The Pareto-optimal fronts (PFs) observed in this case are shown in Figure 3.2. The optimal decision variables obtained by the proposed method are presented in Table 3.6. The proposed method obtains a total generation cost of **135716.72$/**h, and active power loss of **34.5983MW**. NSGA-II [57] gives 135948.25$/h, 35.6852MW and MOPSO [58] gives 136865.18$/h, 57.6587MW respectively as shown in Table 3.7.

b) Case-5: Minimize J_1, J_3, and J_4 simultaneously

In this case, the proposed method was simulated by considering three objectives J_1, J_3, and J_4. The Pareto-optimal fronts (PFs) observed in this case are shown in Figure 3.2. The optimal decision variables obtained by the proposed method are presented in Table 3.6. The proposed method obtains a total generation cost of **137715.17$/h**, active power loss of **33.3462MW**, and voltage magnitude deviation of **0.4779p.u**. NSGA-II [57] gives 138441.48$/h, 37.8479MW, 0.5067p.u and MOPSO [58] gives 138501.58$/h, 51.5057MW, 0.5750p.u respectively as shown in Table 3.7.

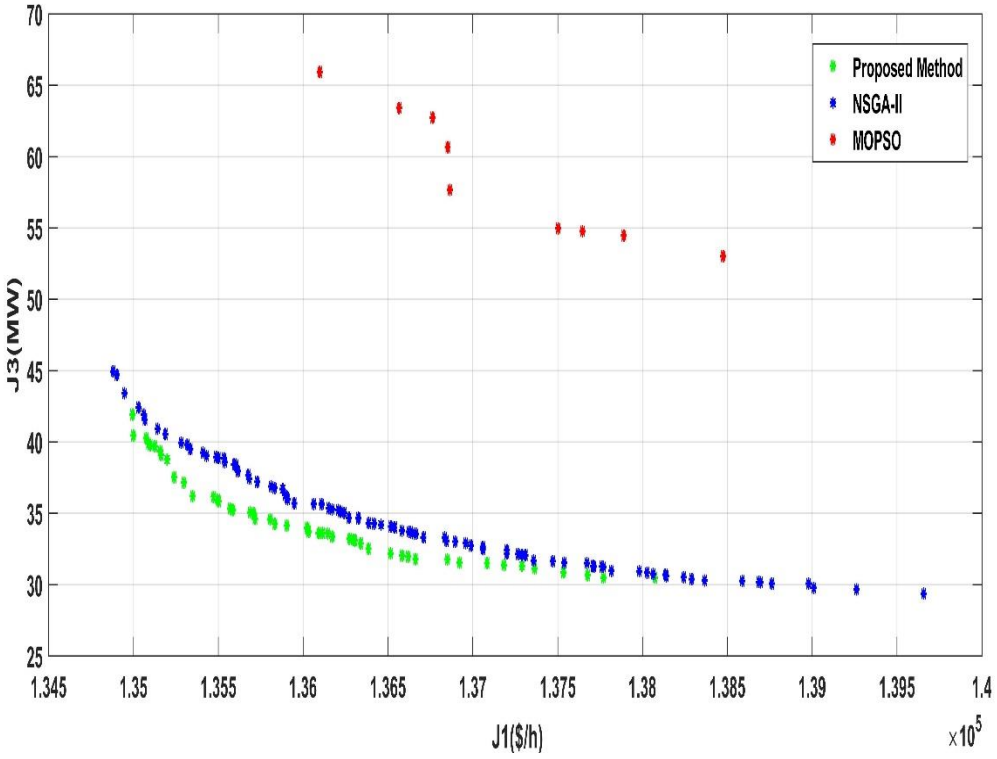

(a)

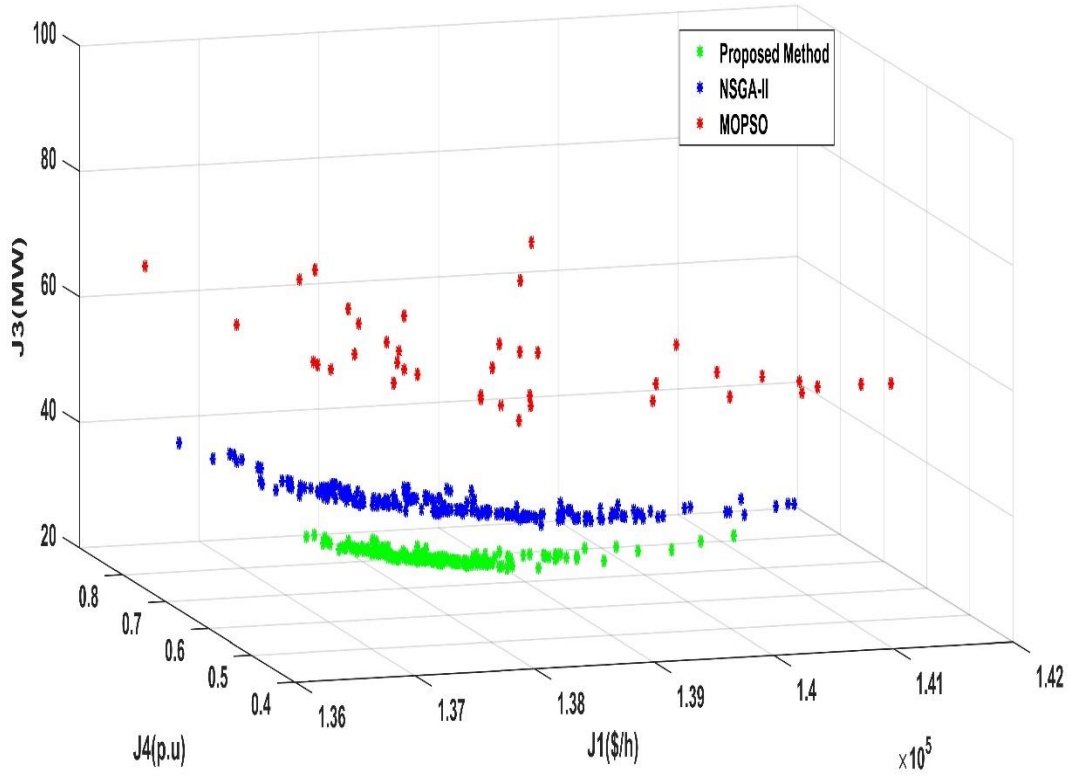

(b)

Fig. 3.2: IEEE 118-bus system: Pareto-optimal fronts. a) Case-4, and b) Case-5.

Table 3.6: IEEE 118-bus system: Optimal control variables obtained by the proposed method.

S. No.	Control variables	Limits		Case-4	Case-5	S. No.	Control variables	Limits		Case-4	Case-5
		min	max					min	max		
1.	P1	0	100	54.5475	49.8078	67.	V31	0.95	1.1	1.0280	1.0087
2.	P4		100	45.7797	52.5061	68.	V32			1.0239	1.0059
3.	P6		100	37.6966	37.9561	69.	V34			1.0264	1.0117
4.	P8		100	27.8767	40.4637	70.	V36			1.0215	1.0063
5.	P10		550	239.410	208.349	71.	V40			1.0248	1.0177
6.	P12		185	82.4114	96.2351	72.	V42			1.0251	1.0118
7.	P15		100	49.3221	59.9765	73.	V46			1.0226	1.0197
8.	P18		100	45.0909	44.6825	74.	V49			1.0347	0.9980
9.	P19		100	56.6271	46.3333	75.	V54			1.0211	1.0128
10.	P24		100	12.7429	23.7604	76.	V55			1.0234	1.0182
11.	P25		320	125.497	117.692	77.	V56			1.0241	1.0187
12.	P26		414	150.881	154.555	78.	V59			1.0225	1.0141
13.	P27		100	47.2764	44.1010	79.	V61			1.0253	1.0143
14.	P31		107	13.9278	19.6902	80.	V62			1.0227	1.0226
15.	P32		100	42.2914	31.9930	81.	V65			1.0278	1.0260
16.	P34		100	40.2518	51.7709	82.	V66			1.0251	0.9859
17.	P36		100	48.8938	56.1834	83.	V69			1.0137	1.0281
18.	P40		100	72.1668	87.8627	84.	V70			1.0334	1.0192
19.	P42		100	67.5902	75.2689	85.	V72			1.0311	1.0316
20.	P46		119	35.6793	35.1325	86.	V73			1.0405	1.0333
21.	P49		304	187.765	159.304	87.	V74			1.0130	1.0048
22.	P54		148	69.1268	81.8220	88.	V76			1.0322	1.0080
23.	P55		100	76.0840	80.5026	89.	V77			1.0195	1.0037
24.	P56		100	87.1884	70.8324	90.	V80			1.0270	1.0135
25.	P59		255	146.100	145.991	91.	V85			1.0330	1.0100
26.	P61		260	116.626	127.139	92.	V87			1.0260	1.0091
27.	P62		100	46.2975	49.8338	93.	V89			1.0293	1.0412
28.	P65		491	221.758	229.532	94.	V90			1.0253	1.0141
29.	P66		492	264.060	231.120	95.	V91			1.0293	1.0157
30.	P70		100	47.4251	45.4400	96.	V92			1.0149	1.0235
31.	P72		100	14.0937	20.0243	97.	V99			1.0257	1.0199
32.	P73		100	36.3494	23.8761	98.	V100			1.0171	1.0172
33.	P74		100	41.4494	50.1527	99.	V103			1.0125	1.0196
34.	P76		100	54.4665	44.8794	100	V104			1.0244	1.0173
35.	P77		100	47.1822	38.0621	101	V105			1.0176	1.0104
36.	P80		577	303.266	297.003	102	V107			1.0128	1.0184
37.	P85		100	32.3521	42.5265	103	V110			1.0274	1.0193
38.	P87		104	7.4605	10.9515	104	V111			1.0270	1.0205
39.	P89		707	268.214	229.933	105	V112			1.0164	1.0275
40.	P90		100	38.1081	50.8835	106	V113			1.0354	1.0091
41.	P91		100	42.9526	48.0809	107	V116			1.0329	1.0113
42.	P92		100	34.9052	49.2068	108	T8	0.9	1.1	0.9967	1.0108
43.	P99		100	23.6065	35.9029	109	T32			0.9954	0.9910
44.	P100		352	143.338	141.629	110	T36			0.9782	0.9937
45.	P103		140	44.2004	43.1302	111	T51			0.9767	0.9670
46.	P104		100	39.6433	42.4401	112	T93			0.9821	0.9810
47.	P105		100	46.5554	50.3917	113	T95			1.0022	1.0004
48.	P107		100	48.2829	35.5470	114	T102			0.9967	0.9954
49.	P110		100	31.1740	40.3137	115	T107			1.0132	1.0100
50.	P111		136	36.4716	35.5358	116	T127			1.0088	0.9757
51.	P112		100	42.5151	45.4344	117	QC34			14.7568	12.5994
52.	P113		100	25.4710	46.0275	118	QC44			12.0512	12.4520

53.	P116		100	5.4126	39.6684	119	QC45	0	25	11.3411	13.4924
54.	V1			1.0311	1.0116	120	QC46			10.8431	11.5359
55.	V4			1.0239	1.0034	121	QC48			9.5642	10.4103
56.	V6			1.0381	1.0186	122	QC74			11.2007	13.0703
57.	V8			1.0233	1.0130	123	QC79			13.6252	9.8725
58.	V10			1.0350	0.9954	124	QC82			13.2053	12.7137
59.	V12			1.0367	1.0202	125	QC83			11.8160	11.7299
60.	V15	0.95	1.1	1.0151	1.0114	126	QC105			11.9498	9.9882
61.	V18			1.0270	1.0142	127	QC107			13.1417	13.0359
62.	V19			1.0265	1.0155	128	QC110			11.9534	13.6171
63.	V24			1.0290	1.0165						
64.	V25			1.0295	1.0118	**1.**	**J_1($/h)**	-	-	**135716.7**	**137715.1**
65.	V26			1.0309	1.0076	**2.**	**J_3(MW)**	-	-	**34.5983**	**33.3462**
66.	V27			1.0260	1.0123	**3.**	**J_4(p.u)**	-	-	-	**0.4779**

Table 3.7: IEEE 118-bus system: Comparison of the proposed method.

Case #	Objective functions	**Proposed method**	NSGA-II [57]	MOPSO [58]
Case-4	J_1($/h)	**135716.72**	135948.25	136865.18
	J_3(MW)	**34.5983**	35.6852	57.6587
Case-5	J_1($/h)	**137715.17**	138441.48	138501.48
	J_3(MW)	**33.3462**	37.8479	51.5057
	J_4(p.u)	**0.4779**	0.5067	0.5750

3.6 Summary

In this work, a new hybrid decomposition and local dominance-based MOEA was proposed for solving the OPF problem. Minimizing the total generation cost, emission, active power loss, and voltage magnitude deviation are the four objectives that were considered. The hybridization of decomposition and dominance approaches increases the convergence and diversity of Pareto optimum front solutions. The static penalty-based method was deployed to tackle both equality and inequality constraints. In addition, a fuzzy technique was used to obtain the best-compromised solutions from the Pareto-optimal set. The proposed method was tested on IEEE 57-bus and IEEE 118-bus systems using different cases to validate its efficiency and the obtained results were compared with NSGA-II and MOPSO methods. This work is restricted to conventional MOOPF with only thermal units, to assess the impact of wind, and solar integration on the MOOPF problem next work is proposed.

Chapter 4

A New Hybrid Decomposition and Summation of Normalized Objectives with Improved Diversified Selection Based Multi-Objective Evolutionary Algorithm Including Wind, and Solar Uncertainty for the Optimal Power Flow

This work is published in:

Ravi Kumar Avvari and Vinod Kumar D. M. "Multi-Objective Optimal Power Flow including Wind and Solar Generation Uncertainty Using New Hybrid Evolutionary Algorithm with Efficient Constraint Handling Method." **International Transactions on Electrical Energy Systems,** Wiley, Vol. 2022, 7091937, Jul 2022. **(SCIE, IF:2.639)**.

Chapter 4

A New Hybrid Decomposition and Summation of Normalized Objectives with Improved Diversified Selection Based Multi-Objective Evolutionary Algorithm Including Wind, and Solar Uncertainty for the Optimal Power Flow

4.1 Introduction

This chapter proposes a new hybrid decomposition, and summation of normalized objectives with improved diversified selection-based MOEA for the OPF including WECS and SPVS uncertainty. This work recommends a novel CHM, that adaptively inserts penalty and avoids the parameter relying on penalty calculation. The summation-based sorting and enhanced diverse selection techniques are employed to increase the diversity of MOEA. The MOOPF is defined using four objectives: minimizing total generating cost, comprising WECS and SPVS generation cost, emission, active power loss, and voltage magnitude deviation. In the OPF cost study, the influence of RES such as WECS and SPVS on integration is taken into account. To reduce the total generation cost, the cost of RESs is factored into the OPF issue to study the impact of intermittent and unpredictable renewable sources on cost and operational viability. The uncertainty of WECS and SPVS sources was described using Weibull and Lognormal PDFs respectively. The efficacy of the proposed method was tested on IEEE 57-bus, and 118-bus systems under all possible RES situations using Monte Carlo simulations. The work makes the following contributions:

i. Proposing a novel MOEA based on decomposition and summation of normalized objectives with improved diversified selection for the MOOPF problem.
ii. Integrating RESs like WECS and SPVS with conventional OPF to consider the impact of the uncertain nature of these sources.
iii. Modeling the uncertain nature of WECS and SPVS using PDFs and calculating the uncertain cost using Monte-Carlo simulations.
iv. Using a new CHM called superiority of feasible solution (SF) to tackle constraints in the MOOPF problem.

4.2 Problem Formulation

The MOOPF problem's objective functions and constraints are stated as follows:

4.2.1 Objectives

The MOOPF problem was formulated using four objectives: minimizing a) total generation cost including the cost of WECS and SPVS generation (J_1), b) emission (J_2), c) active power loss (J_3), and d) voltage magnitude deviation (J_4).

a) Total generation cost ($/h):

The overall generating cost is the sum of the generation cost of thermal, WECS, and SPVS and is expressed by the following equation:

$$\begin{aligned} Min\, J_1 = & \sum_{i=1}^{N_{TG}} (a_i + b_i P_{TGi} + c_i P_{TGi}^2) \\ & + \sum_{j=1}^{N_{WG}} \left[C_{w,j}(P_{ws,j}) + C_{Rw,j}(P_{ws,j} - P_{wav,j}) + C_{Pw,j}(P_{wav,j} - P_{ws,j}) \right] \\ & + \sum_{k=1}^{N_{SG}} \left[C_{s,j}(P_{ss,k}) + C_{Rs,k}(P_{ss,k} - P_{sav,k}) + C_{Ps,k}(P_{sav,k} - P_{ss,k}) \right] \end{aligned} \tag{4.1}$$

where N_{TG}, N_{WG}, and N_{SG} are the number of thermal, WECS, and SPVS respectively; $P_{ws,j}$, and $P_{ss,k}$ is the scheduled powers of j^{th} WECS and k^{th} SPVS respectively; $P_{wav,j}$, and $P_{sav,k}$ are the actual powers of j^{th} WECS and k^{th} SPVS respectively; P_{TGi} is the i^{th} thermal generator output power; a_i, b_i, c_i is the i^{th} thermal generator cost coefficients;

b) Emission (ton/h):

The generation of electric power from traditional fossil fuels would result in the emission of hazardous gases into the atmosphere. The following expression describes the total emission from thermal generators:

$$MinJ_2 = \sum_{i=1}^{N_{TG}} (\alpha_i + \beta_i P_{TGi} + \gamma_i P_{TGi}^2 + \delta_i e^{\varepsilon_i P_{TGi}}) \tag{4.2}$$

where $\alpha_i, \beta_i, \gamma_i, \delta_i, \varepsilon_i$ are the i^{th} thermal generator emission coefficients;

c) Active power loss (MW):

The following equation can be used to express active power loss:

$$Min\, J_3 = \sum_{k=1}^{N_L} \left(G_k \left(V_i^2 + V_j^2 - 2V_i V_j \cos\theta_{ij} \right) \right) \tag{4.3}$$

where N_L is the number of lines; θ_{ij} represents the voltage angle between buses i and j; G_k shows the conductance of branch k; V_i, V_j is the voltage magnitudes at i^{th} and j^{th} buses respectively.

d) Voltage magnitude deviation (p.u.):

The voltage variation is the sum of all voltage variances at load buses in the network relative to the reference voltage. The mathematical expression is as follows:

$$Min\, J_4 = \sum_{i=1}^{N_{PQ}} \left|\left(V_i - V_{ref}\right)\right| \tag{4.4}$$

where N_{PQ} is the number of PQ buses; V_{ref} is the reference voltage set to 1 p.u.; V_i is the i^{th} load bus voltage.

4.2.2 Constraints

The MOOPF objectives are subjected to the following equality and inequality constraints.

a) Equality constraints:

The equality constraints are power-balancing equations in which the sum of the generations of the real and reactive powers is equal to their corresponding demands and losses.

- Power flow constraints

The overall demand and losses throughout the system are equal to the total real and reactive power delivered:

$$P_{Gi} - P_{Di} - V_i \sum_{j=1}^{N_B} V_j\left(G_{ij}\cos\theta_{ij} + B_{ij}\sin\theta_{ij}\right) = 0; i = 1,2,\dots N_B \tag{4.5}$$

$$Q_{Gi} - Q_{Di} - V_i \sum_{j=1}^{N_B} V_j\left(G_{ij}\sin\theta_{ij} - B_{ij}\cos\theta_{ij}\right) = 0; i = 1,2,\dots N_B \tag{4.6}$$

where N_B is the number of buses; P_{Gi}, Q_{Gi}, and P_{Di}, Q_{Di} are the real, reactive power generations and demands at the i^{th} bus, respectively; G_{ij}, B_{ij} is the conductance, susceptance of lines between buses i and j respectively;

b) Inequality constraints:

The operational limitations on generators, transformers, and shunt devices, as well as the security requirements on lines and load buses, constitute inequality constraints.

- Generator constraints: The boundary limits of real and reactive powers and voltage magnitude of the generator buses are expressed as follows:

$$P_{TGi}^{min} \le P_{TGi} \le P_{TGi}^{max}; i = 1,2,\dots N_{TG} \tag{4.7}$$

$$P_{WGi}^{min} \le P_{WGi} \le P_{WGi}^{max}; i = 1,2,\dots N_{WG} \tag{4.8}$$

$$P_{SGi}^{min} \le P_{SGi} \le P_{SGi}^{max}; i = 1,2,\dots N_{SG} \tag{4.9}$$

$$Q_{TGi}^{min} \le Q_{TGi} \le Q_{TGi}^{max}; i = 1,2,\dots N_{TG} \tag{4.10}$$

$$Q_{WGi}^{min} \le Q_{WGi} \le Q_{WGi}^{max}; i = 1,2,\dots N_{WG} \tag{4.11}$$

$$Q_{SGi}^{min} \le Q_{SGi} \le Q_{SGi}^{max}; i = 1,2,\dots N_{SG} \tag{4.12}$$

$$V_{Gi}^{min} \le V_{Gi} \le V_{Gi}^{max}; i = 1,2,\dots N_G \tag{4.13}$$

- Shunt compensator constraints: The following are the boundary values for shunt compensators:

$$Q_{Ci}^{min} \leq Q_{Ci} \leq Q_{Ci}^{max}; i = 1,2, \dots N_C \quad (4.14)$$

- Transformer constraints: The ideal operating limits for tap settings on a transformer are given as follows:

$$T_i^{min} \leq T_i \leq T_i^{max}; i = 1,2, \dots N_T \quad (4.15)$$

- Security constraints: The voltage limits of the load buses and the apparent power value of each transmission line, which can be restricted by its maximum capacity, are given as follows:

$$V_{Li}^{min} \leq V_{Li} \leq V_{Li}^{max}; i = 1,2, \dots N_{PQ} \quad (4.16)$$

$$|S_{li}| \leq S_{li}^{max};\ i = 1,2, \dots N_L \quad (4.17)$$

where N_C, N_T is the number of shunt VAR compensators and transformers respectively; S_{li} and S_{li}^{max} are the apparent power flow and its maximum limit of i^{th} line; P_{Gi}^{min},P_{Gi}^{max} are the limits on real power generation; Q_{Gi}^{min},Q_{Gi}^{max} are the limits on reactive power generation; V_{Gi}^{min},V_{Gi}^{max} are the limits on generator bus voltages; T_i^{min},T_i^{max} are the limits on transformer taps; Q_{Ci}^{min},Q_{Ci}^{max} are the limits on shunt compensator; V_{Li}^{min}, $V_{Li}^{max}$are the limits on load bus voltages;

Two equality constraints Eq. (4.5) and Eq. (4.6) are automatically satisfied when the power flow converges to an optimal solution. The generator buses' real power (excluding slack bus), transformer tap ratios, voltage limits, and shunt compensator ranges are considered to control variables that are self-limiting. The remaining inequality constraints require constraint handling techniques.

In OPF, generator reactive power capacities are significant. In recent years, WECSs with complete reactive power capability has become commercially viable [60]. WECS can deliver reactive power in the range of -0.4p.u.to 0.5p.u. The negative sign signifies the generator's ability to absorb. Rooftop SPVS is designed as load buses with zero reactive power. However, because utility-based SPVS have built-in converters, full generator modeling is required due to the converters' dynamic behavior [61]. In this study, the reactive power capabilities of SPVS are assessed between -0.4p.u and 0.5p.u.

4.3 Constraint Handling Method

The most commonly used CHM is the penalty method. When a constraint violation occurs, its solution is penalized. Owing to its simplicity and operability, the outcome of this method relying on the penalty, which must be determined by trial and error, leading the fitness value to degrade. This study deployed a new CHM called the SF technique which doesn't require any penalty coefficient.

In this work, the SF technique [62] was employed to solve the MOOPF problem with RESs. The steps followed when comparing two solutions are as follows:

(1) While comparing two non-feasible solutions, the solution having the smallest constraint violation is selected.

(2) When two feasible solutions are compared, the one with a better fitness solution is selected.

(3) When a feasible solution is compared to a non-feasible solution, the feasible solution is selected.

Comparing non-feasible solutions based on constraint violation helps push non-feasible answers into the feasible region while comparing viable solutions based on the fitness value enables solution quality to be improved.

4.4 Integration of WECS, and SPVS

4.4.1 WECS, and SPVS Modeling

a) WECS Modeling:

The wind speed at a given geographical area is most likely distributed according to Weibull PDF as given below:

$$f(v) = \left(\frac{k}{c}\right)\left(\frac{v}{c}\right)^{(k-1)}(e)^{\left(\frac{-v}{c}\right)^{k}}; 0 < v < \infty \tag{4.18}$$

where v is the wind speed (m/sec); k, c is the shape, and scale factors respectively.

The PDFs for two different shape and scale factors are given in [63]. The relationship between wind speed and power generation is as follows:

$$P_w(v) = \begin{cases} 0; v < v_{in}\ and\ v > v_{out} \\ P_{wr}\left(\frac{v - v_{in}}{v_r - v_{in}}\right) \quad ;\ v_{in} \le v_w \le v_r \\ P_{wr};\ v_r < v_w \le v_{out} \end{cases} \tag{4.19}$$

where P_{wr} is the rated wind power output; $v_{in}, v_{out},\ and\ v_r$ are the cut-in, cut-out, and rated wind speeds (m/sec) respectively;

The probability of obtaining a zero and rated power output is given by the following:

$$f_w(P_w = 0) = 1 - e^{\left(-\left(\frac{v_{in}}{c}\right)^{k}\right)} + e^{\left(-\left(\frac{v_{out}}{c}\right)^{k}\right)} \tag{4.20}$$

$$f_w(P_w = P_{wr}) = e^{\left(-\left(\frac{v_r}{c}\right)^{k}\right)} + e^{\left(-\left(\frac{v_{out}}{c}\right)^{k}\right)} \tag{4.21}$$

The probability for the linear part of the wind speed is given by the following:

$$f_w(P_w) = \left(\frac{k(v_r - v_{in})}{cP_{wr}}\right)\left(\frac{v_{in}P_{wr} + P_w(v_r - v_{in})}{cP_{wr}}\right)^{(k-1)} e^{\left(-\left(\frac{v_{in}P_{wr} + P_{wr}(v_r - v_{in})}{cP_{wr}}\right)^{k}\right)} \tag{4.22}$$

b) SPVS Modeling:

Similarly, the power output of a solar PV system (SPVS) is a factor of solar irradiance and it likely follows the Lognormal PDF [64] as follows:

$$f_G(G_s) = \frac{1}{G_S\sigma\sqrt{2\pi}} e^{\left\{\frac{-(\ln G_S - \mu)^2}{2\sigma^2}\right\}}; G_S > 0 \quad (4.23)$$

where μ and σ are the mean and standard deviation respectively; G_s is the solar irradiance (W/m^2).

The SPVS unit's solar irradiance to energy generation is as follows [65]:

$$P_S(G_S) = \begin{cases} P_{sr}\left(\frac{G_S^2}{G_{std}R_c}\right) & ; 0 < G_S < R_c \\ P_{sr}\left(\frac{G_S}{G_{std}}\right) & ; G_S \geq R_c \end{cases} \quad (4.24)$$

where G_{std} is the standard solar irradiance (W/m^2); R_c is the particular irradiance point (W/m^2); P_{sr} is the SPVS-rated power output.

4.4.2 Uncertainty cost calculation of WECS, and SPVS

Since WECS and SPVS powers are intermittent, Monte-Carlo simulations were used to account for uncertainty and calculate the uncertainty cost. The estimated cost for the intermittency of WECS and SPVS power is reflected in three ways: direct, reserve, and penalty costs. Whenever power is underestimated, extra unusable power is wasted; however, in practical power system applications, such power can be saved in an energy storage system and thus be counted as the reserve cost. The cost of overestimating power that is lower than the scheduled power is considered a penalty cost in the case of overestimation.

The direct cost associated with j^{th} WECS is as follows:

$$C_{w,j}(P_{ws,j}) = g_j P_{ws,j} \quad (4.25)$$

Similarly, the direct cost of k^{th} SPVS is as follows:

$$C_{w,k}(P_{ss,k}) = h_k P_{ss,k} \quad (4.26)$$

where $P_{ws,j}$, $P_{ss,k}$ are the scheduled powers of j^{th} WECS, k^{th} SPVS respectively; g_j, h_k are the direct cost constants of j^{th} WECS, k^{th} SPVS respectively;

If the actual output power of the wind farm is lower than the predicted value, to ensure a constant supply of electricity to the consumers, the operator requires some spinning reserve. It is called the overestimation of power from unreliable sources. The cost incurred to maintain the spinning reserve is known as the reserve cost [66].

The reserve cost of the j^{th} WECS is as follows:

$$C_{Rw,j}(P_{ws,j} - P_{wav,j}) = K_{Rw,j}(P_{ws,j} - P_{wav,j}) = K_{Rw,j}\int_0^{P_{ws,j}} (P_{ws,j} - p_{w,j}) f_w(p_{w,j}) dp_{w,j}$$

(4.27)

In contrast to the overestimation scenario, when the power output of wind exceeds the predicted output, the surplus power generated by WECS cannot be used and is wasted. This is called the underestimation of power from uncertain sources. In this case, ISO must pay a penalty for excess power.

The penalty cost of the j^{th} WECS is as follows:

$$C_{Pw,j}\left(P_{wav,j} - P_{ws,j}\right) = K_{Pw,j}(P_{wav,j} - P_{ws,j}) = K_{Pw,j}\int_{P_{ws,j}}^{P_{wr,j}}\left(P_{w,j} - p_{ws,j}\right)f_w\left(p_{w,j}\right)dp_{w,j} \tag{4.28}$$

where $K_{Rw,j}$, $K_{Pw,j}$ are the reserve, penalty cost constants of j^{th} WECS respectively; $P_{wr,j}$ and $P_{wav,j}$ are the rated and actually available powers of j^{th} WECS; $f_w\left(p_{w,j}\right)$ is the possibility of j^{th} WECS power.

Similarly to WECS, SPVS also exhibits intermittent power output. The SPVS reserve, and penalty cost expressions are provided below [67].

The reserve cost for k^{th} SPVS plant is as follows:

$$\begin{aligned} C_{Rs,k}\left(P_{ss,k} - P_{sav,k}\right) &= K_{Rs,k}\left(P_{ss,k} - P_{sav,k}\right) \\ &= K_{Rs,k} * f_s\left(P_{sav,k} < P_{ss,k}\right) * \left[P_{ss,k} - E\left(P_{sav,k} < P_{ss,k}\right)\right] \end{aligned} \tag{4.29}$$

The penalty cost for a k^{th} SPVS plant is as follows:

$$\begin{aligned} C_{Ps,k}\left(P_{sav,k} - P_{ss,k}\right) &= K_{Ps,k}\left(P_{sav,k} - P_{ss,k}\right) \\ &= K_{Ps,k} * f_s\left(P_{sav,k} > P_{ss,k}\right) * \left[E\left(P_{sav,k} > P_{ss,k}\right) - P_{ss,k}\right] \end{aligned} \tag{4.30}$$

where $K_{Rs,k}$, $K_{Ps,k}$ are the reserve, penalty cost constants of k^{th} SPVS respectively; $P_{sav,k}$ is the actual available power of k^{th} SPVS; $f_s\left(P_{sav,k} < P_{ss,k}\right)$ and $f_s\left(P_{sav,k} > P_{ss,k}\right)$ are the probabilities of SPVS power; $E\left(P_{sav,k} < P_{ss,k}\right)$, $E\left(P_{sav,k} > P_{ss,k}\right)$ are the expectations of SPVS power.

4.5 Proposed Method

In this chapter, a summation of normalized objective values (SNOV) with improved diversified selection (IDS) is integrated with the multi-objective evolution algorithm based on the decomposition (MOEA/D) [53] to solve the MOOPF problem with RES. The MOEA/D decomposes the multi-objective optimization problem into several single scalar optimization problems and optimizes them all at the same time using weight vectors. The weight vectors' distance is used to create neighborhoods. In every population evolution, information from the neighborhood is used to find a solution. The non-dominated sorting used in MOEA/D is

complex and time-taking. Some useful information may be lost if the dominant solutions are completely discarded. In addition, diversity may be lost during the search process and lead to local optima. To overcome these problems, the summation of normalized objective values with IDS [68] is employed in this work instead of non-dominated sorting selection to get a uniformly distributed Pareto front and improved convergence characteristics.

Proposed algorithm steps:

1 Randomly generate the initial population (*N*) and uniformly distributed weights using SSA [54] as given below:

$$N(D,M) = \binom{D+M-1}{M-1} \; for \; D > 0$$

2 Run the load flow, and determine the fitness value of the chosen objective function and total constraint violation.

3 Using angle criteria [55], locate neighbors with the smallest angles for each weight vector as given below:

$$\tan\theta = \frac{d_2}{d_1}$$

$$\text{where } d_1 = \frac{\|w_i^T w_j\|}{\|w_j\|}, d_2 = \left\| w_i - d_1 \frac{w_j}{\|w_j\|} \right\|$$

$i, j = 1, 2,.., N$; $i \neq j$, θ= angle between d_1 and d_2.

4 Evaluate the smaller objective values to form the present ideal point.

5 Evaluate the larger objective values to form the present nadir point.

6 Angle criteria are used to choose N pairs of mating parents**.** A set of mating parents is picked with a probability of δ each weight.

7 Crossover is used to produce offspring from mated parents. Then, the mutation is applied to produce a new population (Q_t).

8 The new population is formed by combining the original population (P_t) with the new offspring population (Q_t).

$$P_t = P_t \cup Q_t$$

9 For each objective and solution, calculate the normalized objective values.

10 By adding all of the normalized objective values for each solution, obtain the sum of the normalized objective values [68].

For *m*= 1 to *M*

Calculate the max and min objectives of *the* m^{th} objective and find its range. Normalize the m^{th} objective values using the expression:

$$f'_m(x) = \frac{f_m(x) - f_{min}}{f_{max} - f_{min}}$$

End for

For *i*= 1 to *N*

Sum up all the normalized objective values to get a unique value

End for

11 Calculate the Euclidean space between all of the solutions and the reference point.

12 Set a stopping point for the individual with the shortest path to the original point.

13 Partition the target range into 100 bins and scan each bin till you reach the stopping point. The solution having the least summation value will be picked to enter into the preferential set for each scanned bin.

14 The solutions are dominated by stopping points, and also the individuals who were not selected will be sent to the backup set.
15 Apply the fuzzy approach [56] to get the optimal values.

4.6 Results and Discussions

The proposed method was tested on IEEE 57-bus, and 118-bus systems to address the MOOPF problem incorporating WECS and SPVS uncertainties. To consider uncertainties, Monte-Carlo simulations were used to generate 1000 samples. It is programmed in MATLAB R2016a and operates on an i3 processor with 4GB RAM and the results obtained are compared with NSGA-II [57], and MOPSO [58]. The control parameters of the proposed method, NSGA-II, and MOPSO are given in Table 4.1. The various cases considered are given in Table 4.2. The description of the test systems is given in Table 4.3. PDF specifications and cost components of various sources are given in Table 4.4.

Table 4.1: Control parameters of the proposed method, NSGA-II, and MOPSO.

S. No.	Method	Control parameters
1.	**Proposed method**	***N* = 100, *D* =12, *T* = 20, P_c = 1.0, P_m = 0.05, and max. iterations= 100.**
2.	NSGA-II [57]	*N* =100, *Pc* = 0.8, *Pm* = 0.01, and max. iterations = 100.
3.	MOPSO [58]	*N* =100, *C1*= *C2* =2, *W* = 0.5, and max. iterations = 100.

Table 4.2: Various cases considered.

S. No.	Test Systems	Case #	J_1	J_2	J_3	J_4
1.	IEEE 57-bus system	Case-1	✓	✓	--	--
		Case-2	✓	✓	✓	--
		Case-3	✓	✓	✓	✓
2.	IEEE 118-bus system	Case-4	✓	--	✓	--
		Case-5	✓	--	✓	✓

Table 4.3: Test systems description.

Specifications	IEEE 57-bus system		IEEE 118-bus system	
Buses	57	[59]	118	[59]
Lines	80		186	
Thermal units	7	Buses:1,2,3,6,8,9 and 12	54	Buses: [59]
Slack bus	1	Bus:1	69	Bus: 69
Transformer tap positions	17	Lines:19,20,31,35,36,37,41,46, 54,58,59,65,66,71,73,76, and 80	9	Lines: 8,32,36, 51, 93,95,102,107 and 127
Shunt capacitors	3	Buses:18,25, and 53	12	Buses:34,44,45,46,48,74,79,82, 83, 105, 107 and 110
Control variables	37	Generator bus real powers (8) + voltages (9) + transformer tap settings (17) + shunt capacitor (3).	132	Generator bus real powers (55) + voltages (56) + transformer tap settings (9) + shunt capacitor (12).
Load	-	1250.80MW, 336.40MVAR	-	4242.00MW, 1439.00MVAR
WECS	1	45 # bus	1	81 # bus
SPVS	1	16 # bus	1	64 # bus

Table 4.4: PDF specifications and cost components of various sources.

S. No.	Specifications	WECS	SPVS
1.	PDF	Weibull	Lognormal
2.	Parameters	c =10, k =2, v_{in}=10m/sec, v_{out}=12m/sec, v_r=12m/sec	μ =6, σ = 0.6, G_{std}=800 W/m^2 , R_c=120 W/m^2
3.	Direct cost coefficients ($/MW)	1.75	1.60
4.	Reserve cost coefficients ($/MW)	3	3
5.	Penalty cost coefficients ($/MW)	1.5	1.5

4.6.1 IEEE 57-bus system

To test the efficacy of the proposed method, in solving the MOOPF problem the IEEE 57-bus system [59] was considered. It contains 7 thermal generators # 1 bus as a slack bus), 80 lines, 15 off-nominal transformers, 3 shunt VAR compensators, and real and reactive power demand of 1250.80MW and 336.40MVAR respectively. Notably, the locations of these sources were chosen from [74], by replacing load buses with the respective WECS, and SPVS.

a) Case-1: Minimize J_1 and J_2 simultaneously

In this case, J_1, and J_2 are the objectives that need to be minimized simultaneously. The optimal decision variables obtained by the proposed method are included in Table 4.5. The best-compromised values obtained by the proposed method have a total generation cost of **36195.21$/h** and emission of **1.0182ton/h.** NSGA-II [57] gives 36399.10$/h, 1.0912ton/h and MOPSO [58] gives 36733.34$/h, 1.1145ton/h as shown in Table 4.6. The Pareto-optimal fronts (PFs) observed in this are depicted in Figure 4.1.

b) Case-2: Minimize J_1, J_2 and J_3 simultaneously

In this case, J_1, J_2, and J_3 are the objectives that need minimizing simultaneously. The optimal decision variables obtained by the proposed method are included in Table 4.5. The best-compromised values obtained by the proposed method have a total generation cost of **36096.69$/h**, emission of **1.0238ton/h,** and active power loss of **10.3303MW.** NSGA-II [57] gives 36363.70$/h, 1.1288ton/h, 10.7953MW and MOPSO [58] gives 39208.74$/h, 1.0890ton/h, 11.0434MW as shown in Table 4.6. The Pareto-optimal fronts (PFs) observed in this are depicted in Figure 4.1.

c) Case-3: Minimize J_1, J_2, J_3 and J_4 simultaneously

In this case, J_1, J_2, J_3, and J_4 are the objectives that need to be minimized simultaneously. The optimal decision variables obtained by the proposed method are included in Table 4.5. The best-compromised values obtained by the proposed method have a total generation cost of **36207.21$/h**, emission of **1.0916ton/h,** active power loss of **9.9732MW**, and voltage magnitude deviation of **0.6848p.u.** NSGA-II [57] gives 36479.38$/h, 1.1382ton/h,

11.3923MW, 0.8907p.u and MOPSO [58] gives 37321.91$/h, 1.2049ton/h, 14.5232MW, 0.8323p.u. as shown in Table 4.6.

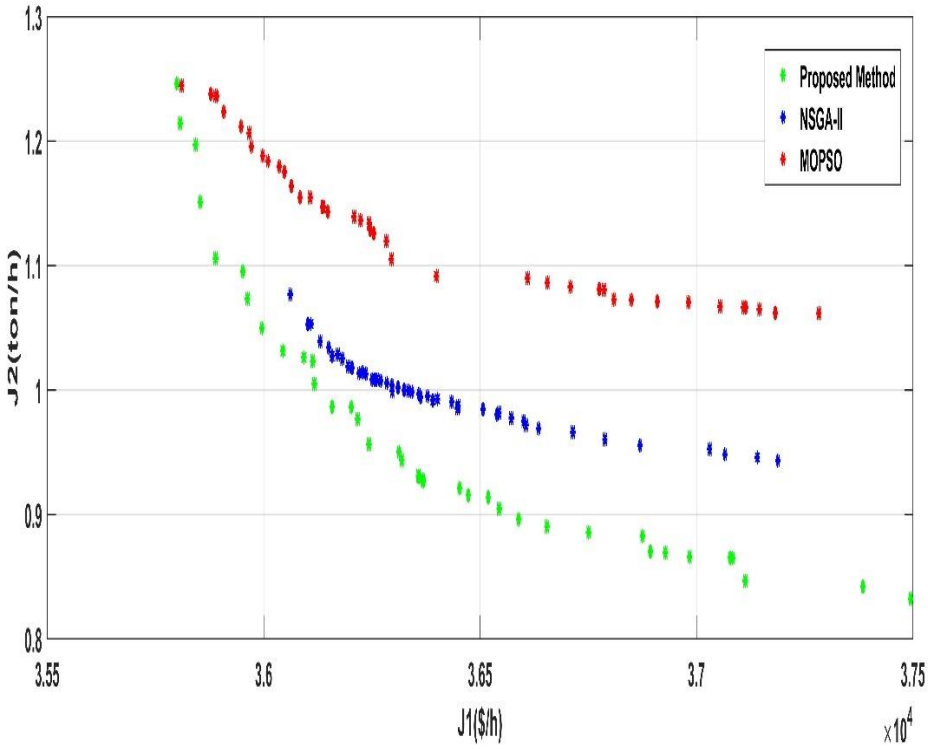

(a)

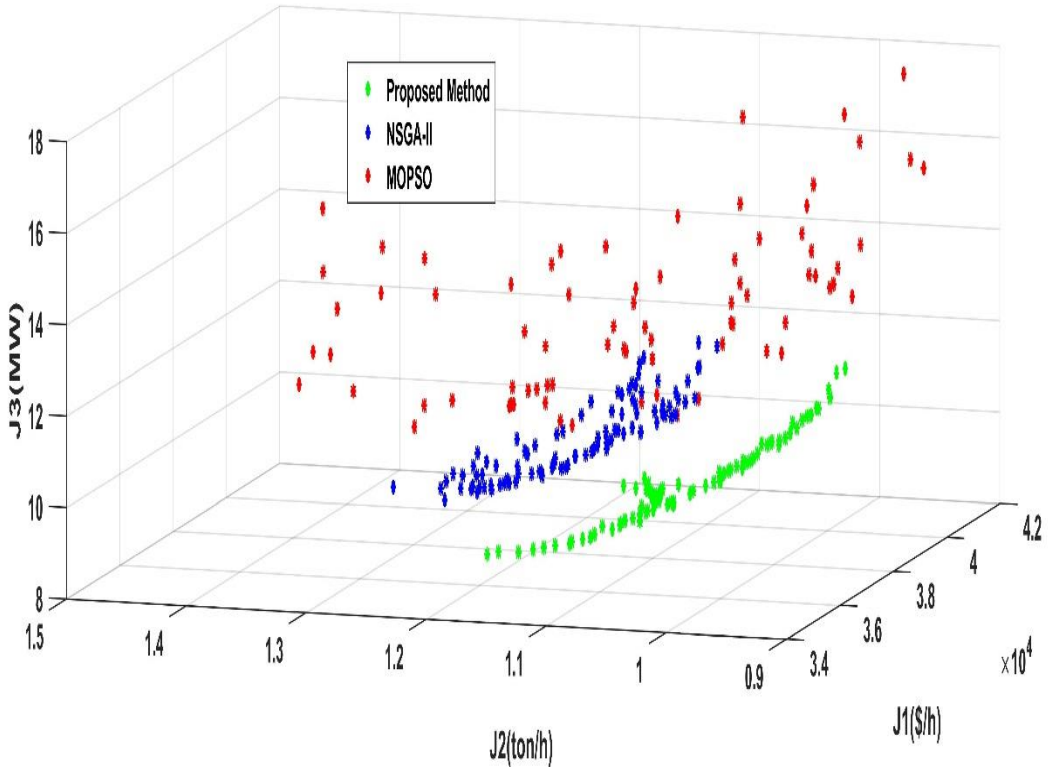

(b)

Fig. 4.1: IEEE 57-bus system: Pareto-optimal fronts. a) Case-1, and b) Case-2.

Table 4.5: IEEE 57-bus system: Optimal control variables obtained by the proposed method.

S. No.	Control variables	Limits		Case-1	Case-2	Case-3
		Min	Max			
1.	P2	0	100	98.1298	67.1046	74.8586
2.	P3		140	69.4063	55.0118	64.1958
3.	P6		100	70.9842	98.4255	52.0615
4.	P8		550	329.0458	306.7587	315.7318
5.	P9		100	72.7441	99.3728	98.8024
6.	P12		410	315.2646	341.6928	378.7730
7.	P45		80	79.6017	79.9551	79.8243
8.	P46		80	79.8919	79.9311	79.5757
9.	V1	0.95	1.1	1.0481	1.0296	1.0391
10.	V2			1.0371	1.0246	1.0333
11.	V3			1.0340	1.0227	1.0229
12.	V6			1.0275	1.0185	1.0209
13.	V8			1.0295	1.0162	1.0318
14.	V9			1.0169	1.0099	1.0160
15.	V12			1.0369	1.0268	1.0217
16.	V45			1.0471	1.0498	1.0514
17.	V46			1.0209	1.0372	1.0175
18.	T19	0.9	1.1	1.0154	1.0139	1.0056
19.	T20			0.9945	1.0497	1.0367
20.	T31			1.0183	1.0260	0.9955
21.	T35			0.9938	1.0263	0.9876
22.	T36			0.9601	0.9982	0.9821
23.	T37			0.9943	1.0176	1.0321
24.	T41			1.0225	0.9911	1.0155
25.	T46			0.9889	0.9757	0.9456
26.	T54			0.9999	0.9233	0.9049
27.	T58			0.9814	0.9802	0.9613
28.	T59			1.0108	0.9877	1.0070
29.	T65			0.9914	0.9841	0.9967
30.	T66			0.9748	0.9484	0.9140
31.	T71			0.9703	0.9756	0.9547
32.	T73			1.0158	0.9829	1.0058
33.	T76			0.9691	0.9769	0.9649
34.	T80			0.9908	0.9872	1.0199
35.	QC18	0	20	9.1150	11.4035	11.0379
36.	QC25			9.8438	10.4059	8.2934
37.	QC53			11.2830	7.1925	7.7894
1.	**J_1($/h)**	-	-	**36195.21**	**36096.69**	**36207.21**
2.	**J_2(ton/h)**	-	-	**1.0182**	**1.0238**	**1.0916**
3.	**J_3(MW)**	-	-	-	**10.3303**	**9.9732**
4.	**J_4(p.u.)**	-	-	-	-	**0.6848**

Table 4.6: IEEE 57-bus system: Comparison of the proposed method.

Case #	Objective functions	**Proposed method**	NSGA-II [57]	MOPSO [58]
Case-1	J_1($/h)	**36195.21**	36399.10	36733.34
	J_2(ton/h)	**1.0182**	1.0912	1.1145
Case-2	J_1($/h)	**36096.69**	36363.70	39208.74
	J_2(ton/h)	**1.0238**	1.1288	1.0890
	J_3(MW)	**10.3303**	10.7953	11.0434
Case-3	J_1($/h)	**36207.21**	36479.38	37321.91
	J_2(ton/h)	**1.0916**	1.1382	1.2049
	J_3(MW)	**9.9732**	11.3923	14.5232
	J_4(p.u.)	**0.6848**	0.8907	0.8323

4.6.2 IEEE 118-bus system

To show the scalability of the proposed method for a large-scale system in solving the MOOPF problem, the IEEE 118-bus system [59] is considered. It contains 54 thermal generators (# 69 bus as a slack bus), 186 lines, 9 off-nominal transformers, and 12 shunt VAR compensators. The real and reactive power demand on the system is 4242.00MW and 1439.00MVAR respectively. Notably, the locations of these sources were chosen from [74], by replacing load buses with the respective WECS, and SPVS.

a) Case-4: Minimize J_1 and J_3 simultaneously

In this case, J_1, and J_3 are the objectives that need to be minimized simultaneously. The optimal decision variables obtained by the proposed method are included in Table 4.7. The best-compromised values obtained by the proposed method have a total generation cost of **132958.66$/h,** and an active power loss of **31.2916MW**. NSGA-II [57] gives 133837.90$/h, 31.8664MW and MOPSO [58] gives 134673.5$/h, 35.3868MW as shown in Table 4.8. The Pareto-optimal fronts (PFs) observed in this are depicted in Figure 4.2.

b) Case-5: Minimize J_1, J_3 and J_4 simultaneously

In this case, J_1, J_3, and J_4 are the objectives that need minimizing simultaneously. The optimal decision variables obtained by the proposed method are included in Table 4.7. The best-compromised values obtained by the proposed method have a total generation cost of **135774.93$/h**, active power loss of **39.6333MW**, and voltage magnitude deviation of **0.4299p.u**. NSGA-II [57] gives 135912.8$/h, 45.6904MW, 0.5074p.u and MOPSO [58] gives 136459.9$/h, 48.3446MW, 0.5878p.u. as shown in Table 4.8. The Pareto optimal fronts (PFs) observed in this are depicted in Figure 4.2.

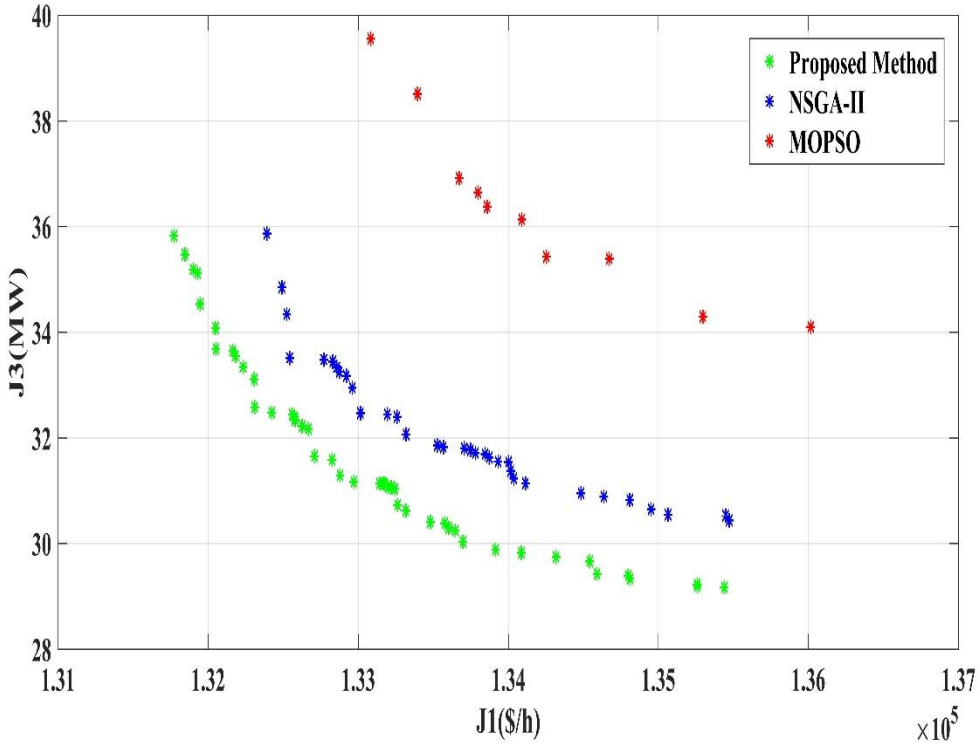

(a)

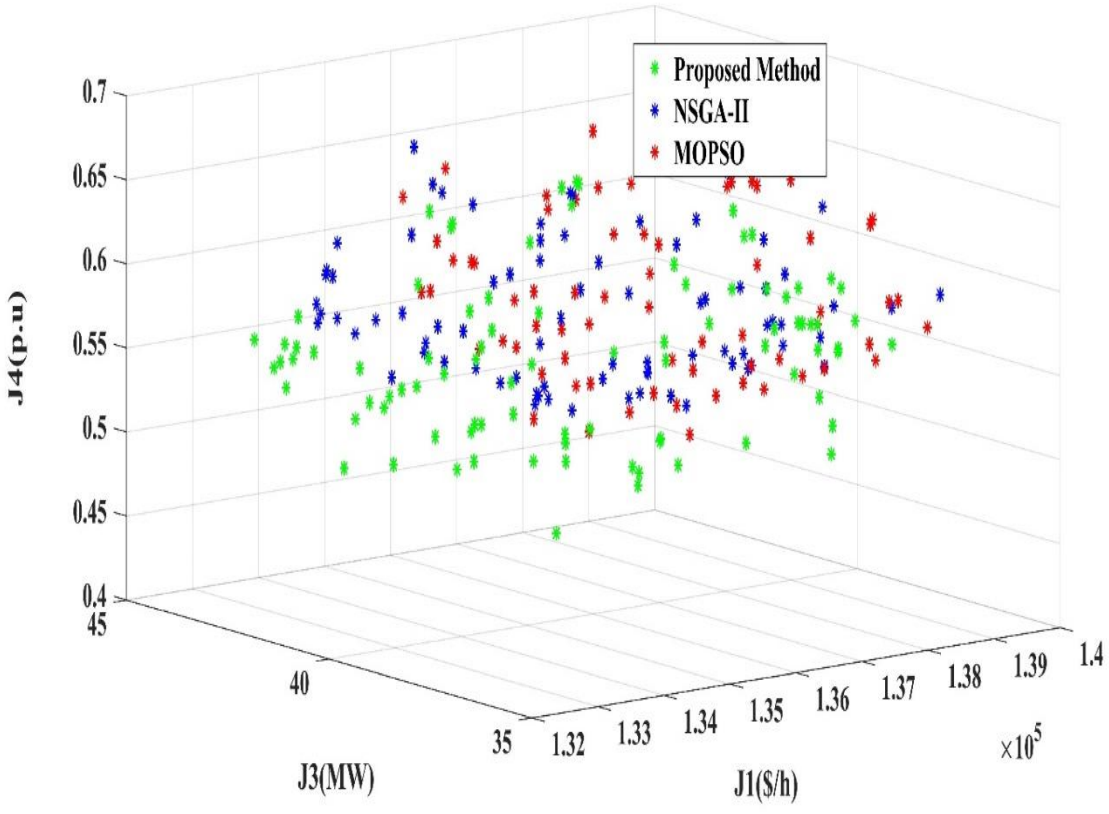

(b)

Fig. 4.2: IEEE 118-bus system: Pareto-optimal fronts. a) Case-4, and b) Case-5.

Table 4.7: IEEE 118-bus system: Optimal control variables obtained by the proposed method.

S. No.	Control variables	Limits		Case-4	Case-5	S. No.	Control variables	Limits		Case-4	Case-5
		min	max					min	max		
1.	P1	0	100	31.118	52.020	69.	V31	0.95	1.1	1.0253	1.0169
2.	P4		100	21.400	41.520	70.	V32			1.0195	1.0030
3.	P6		100	42.530	40.834	71.	V34			0.9909	1.0094
4.	P8		100	28.556	26.448	72.	V36			1.0241	1.0067
5.	P10		550	273.35	245.999	73.	V40			1.0096	1.0118
6.	P12		185	86.663	95.235	74.	V42			1.0305	1.0113
7.	P15		100	43.268	37.779	75.	V46			1.0150	1.0221
8.	P18		100	99.997	45.659	76.	V49			1.0118	1.0055
9.	P19		100	35.781	55.328	77.	V54			1.0359	1.0023
10.	P24		100	64.585	35.747	78.	V55			1.0708	1.0239
11.	P25		320	182.60	90.928	79.	V56			1.0661	1.0256
12.	P26		414	0.000	162.842	80.	V59			1.0619	1.0271
13.	P27		100	24.090	46.656	81.	V61			1.1000	1.0175
14.	P31		107	22.783	25.781	82.	V62			1.0982	0.9985
15.	P32		100	62.386	37.325	83.	V65			1.0875	1.0049
16.	P34		100	43.187	40.202	84.	V66			1.0434	1.0099
17.	P36		100	100.00	54.841	85.	V69			1.0436	1.0280
18.	P40		100	88.192	64.417	86.	V70			1.0184	1.0096
19.	P42		100	83.016	49.460	87.	V72			1.0066	1.0062
20.	P46		119	19.417	44.338	88.	V73			1.0092	1.0190
21.	P49		304	138.66	140.370	89.	V74			1.0119	1.0264
22.	P54		148	59.984	98.543	90.	V76			1.0045	1.0089
23.	P55		100	74.764	52.457	91.	V77			1.0367	1.0170
24.	P56		100	59.627	46.8259	92.	V80			1.0229	1.0183
25.	P59		255	117.12	115.881	93.	V85			0.9985	1.0125
26.	P61		260	121.66	121.893	94.	V87			0.9617	1.0290
27.	P62		100	35.517	44.630	95.	V89			1.0269	1.0266
28.	P65		491	214.33	213.346	96.	V90			1.0321	1.0253
29.	P66		492	205.83	187.419	97.	V91			1.0209	1.0221
30.	P70		100	12.582	54.0066	98.	V92			1.0237	1.0056
31.	P72		100	12.141	40.751	99.	V99			1.0297	1.0222
32.	P73		100	55.579	50.455	100.	V100			1.0412	1.0206
33.	P74		100	14.137	42.021	101.	V103			1.0269	1.0326
34.	P76		100	75.678	37.592	102.	V104			1.0484	1.0319
35.	P77		100	82.194	42.539	103.	V105			1.0531	1.0203
36.	P80		577	256.72	270.903	104.	V107			1.0380	1.0324
37.	P85		100	42.579	42.382	105.	V110			1.0685	1.0243
38.	P87		104	0.000	19.159	106.	V111			1.0854	1.0296
39.	P89		707	257.13	216.783	107.	V112			1.0619	1.0349
40.	P90		100	97.811	36.604	108.	V113			1.0228	1.0236
41.	P91		100	8.436	52.187	109.	V116			1.0519	1.0073
42.	P92		100	45.760	43.249	110.	V64			1.0160	1.0149
43.	P99		100	23.885	40.178	111.	V65			1.0453	1.0229
44.	P100		352	113.62	150.771	112.	T8	0.9	1.1	0.9897	1.0013
45.	P103		140	42.612	50.598	113.	T32			1.0611	1.0167
46.	P104		100	11.805	45.019	114.	T36			0.9508	0.9920
47.	P105		100	100.00	63.106	115.	T51			1.0001	0.9742
48.	P107		100	19.672	39.046	116.	T93			0.9995	1.0096
49.	P110		100	56.657	53.624	117.	T95			0.9000	1.0180
50.	P111		136	22.867	43.765	118.	T102			1.0099	1.0270
51.	P112		100	40.659	39.005	119.	T107			0.9262	0.9814
52.	P113		100	16.067	51.229	120.	T127			0.9770	0.9995

53.	P116		100	39.564	44.049	121.	QC34			6.1168	14.2885
54.	P64		100	99.998	74.484	122.	QC44			14.0212	11.8200
55.	P65		100	99.998	61.143	123.	QC45			24.0656	12.7371
56.	V1			1.0554	1.0093	124.	QC46			9.5124	15.7212
57.	V4			0.9500	1.0106	125.	QC48			5.8489	14.8892
58.	V6			0.9753	1.0256	126.	QC74			19.2222	10.8066
59.	V8			0.9585	1.0102	127.	QC79	0	25	0.0000	15.8930
60.	V10			1.0381	1.0205	128.	QC82			24.7411	13.8225
61.	V12			1.0502	1.0141	129.	QC83			13.9104	11.6974
62.	V15			0.9529	1.0094	130.	QC105			24.9944	13.5413
63.	V18			0.9960	1.0220	131.	QC107			19.0262	15.0743
64.	V19			1.0077	1.0321	132.	QC110			12.1782	11.1250
65.	V24			0.9956	1.0184						
66.	V25			1.0117	1.0251	**1.**	J_1 ($/h)	-	-	**132958.6**	**135774.9**
67.	V26			1.0397	1.0227	**2.**	J_3(MW)	-	-	**31.2916**	**39.6333**
68.	V27			1.0466	1.0121	**3.**	J_4 (p.u)	-	-	-	**0.4299**

Table 4.8: IEEE 118-bus system: Comparison of the proposed method.

Case #	Objective functions	**Proposed method**	NSGA-II [57]	MOPSO [58]
Case-4	J_1($/h)	**132958.66**	133837.90	134673.5
	J_3(MW)	**31.2916**	31.8664	35.3868
Case-5	J_1($/h)	**135774.93**	135912.8	136459.9
	J_3(MW)	**39.6333**	45.6904	48.3446
	J_4(p.u.)	**0.4299**	0.5074	0.5878

4.7 Summary

This work proposes a solution to the MOOPF problem with a combination of thermal, WECS, and SPVS using MOEA based on decomposition and summation of normalized objectives with an improved diversified selection method. Using the superiority of the feasible solution (SF) technique, the method also addresses the restrictions in the MOOPF problem. The generation cost of thermal generators and uncertainty cost associated with WECS and SPVS are minimized along with emission, active power loss, and voltage magnitude deviation. Monte Carlo simulations were used to assess the uncertainty of WECS and SPVS power. To show the efficacy of the proposed method, simulations were done on the IEEE 57-bus and IEEE 118-bus systems, and the results were compared with NSGA-II and MOPSO algorithms. The outcomes show that the proposed method is superior to competing methods. Therefore, the proposed approach can be effectively used in operation and control when WECS and SPVS power generation are included in the power system. This work is limited to the MOOPF problem with integration of WECS, and SPVS, to assess the impact of PEV integration on the MOOPF problem along with WECS, and SPVS next work is proposed.

Chapter 5

A New Hybrid Decomposition and Summation of Normalized Objectives with Improved Diversified Selection Based Multi-Objective Evolutionary Algorithm Including Wind, Solar, and PEV Uncertainty for the Optimal Power Flow

This work is published in:

Ravi Kumar Avvari and Vinod Kumar D.M. “A Novel Hybrid Multi-Objective Evolutionary Algorithm for Optimal Power Flow in Wind, PV, and PEV Systems.” **Journal of Operation and Automation in Power Engineering**, Vol. 11, No. 2, pp. 130-143, Aug 2023. **(Scopus).**

Chapter 5

A New Hybrid Decomposition and Summation of Normalized Objectives with Improved Diversified Selection Based Multi-Objective Evolutionary Algorithm Including Wind, Solar, and PEV Uncertainty for the Optimal Power Flow

5.1 Introduction

This chapter presents a new hybrid decomposition and summation of normalized objectives with improved diversified selection-based MOEA for the OPF problem including WECS, SPVS, and PEVs uncertainty with four conflicting objectives including minimizing total generation cost, emission, active power loss, and voltage magnitude deviation. The MOOPF problem was solved using a unique CHM that adaptively inserts the penalty and avoids the parameter relying on penalty calculation. The summation-based sorting and enhanced diverse selection are used to improve the diversity of MOEA. In addition, a fuzzy algorithm is used to determine the optimal compromise values from Pareto-optimal solutions. The impact of intermittence of WECS, SPVS, and PEVS integration was considered for optimal cost analysis. The uncertainty associated with WECS, SPVS, and PEV systems was represented using PDFs and its uncertainty cost is calculated using the Monte-Carlo simulations. To test the effectiveness of the suggested method, IEEE 57-bus and 118-bus systems were assessed, and the acquired results were compared with NSGA-II and MOPSO.

The contributions of this chapter are as follows:

i. Proposing a novel hybrid MOEA for solving the MOOPF problem based on the decomposition and summation of normalized objectives with an enhanced diverse selection.
ii. Integrating WECS, SPVS, and PEV systems into the traditional OPF to investigate the effect of the stochastic nature of the sources.
iii. Modeling uncertainty associated with WECS, SPVS, and PEV systems using PDFs, and evaluating the associated uncertain cost using Monte-Carlo simulations.
iv. Using an efficient constraint handling method called the SF method to address various constraints in the MOOPF problem.

5.2 Problem Formulation

The objectives and constraints for the considered MOOPF problem are expressed as follows:

5.2.1 Objectives

The MOOPF problem is formulated using four objectives: minimizing a) total generation cost (J_1), b) emission (J_2), c) active power loss (J_3), and d) voltage magnitude deviation (J_4).

a) Total generation cost ($/h):

The overall generating cost is the sum of the generation cost of thermal, WECS, SPVS, and PEV sources and is expressed by the following equation:

$$\begin{aligned} Min\, J_1 = & \sum_{i=1}^{N_{TG}} (a_i + b_i P_{TGi} + c_i P_{TGi}^2) \\ & + \sum_{j=1}^{N_{WG}} \left[C_{w,j}(P_{ws,j}) + C_{Rw,j}(P_{ws,j} - P_{wav,j}) + C_{Pw,j}(P_{wav,j} - P_{ws,j}) \right] \\ & + \sum_{k=1}^{N_{SG}} \left[C_{s,k}(P_{ss,k}) + C_{Rs,k}(P_{ss,k} - P_{sav,k}) + C_{Ps,k}(P_{sav,k} - P_{ss,k}) \right] \\ & + \sum_{n=1}^{N_{PEV}} \left[C_{pev,n}(P_{pevs,n}) + C_{Rpev,n}(P_{pevs,n} - P_{pevav,n}) + C_{Ppev,n}(P_{pevav,n} \right. \\ & \left. - P_{pevs,n}) \right] \end{aligned} \tag{5.1}$$

where N_{TG}, N_{WG}, N_{SG}, and N_{PEV} are the number of thermal, WECS, SPVS, and PEVS respectively; $P_{ws,j}$, $P_{ss,k}$, and $P_{pevs,n}$ are the scheduled powers of j^{th} WECS, k^{th} SPVS, and n^{th} PEVS respectively; $P_{wav,j}$, $P_{sav,k}$, and $P_{pevav,n}$ are the actual powers of j^{th} WECS, k^{th} SPVS, and n^{th} PEVS respectively; P_{TGi} is the i^{th} thermal generator output power; a_i, b_i, c_i is the i^{th} thermal generator cost coefficients;

b) Emission (ton/h):

The generation of electric power from traditional fossil fuels would result in the emission of hazardous gases into the atmosphere. The following expression describes the total emission from thermal generators:

$$MinJ_2 = \sum_{i=1}^{N_{TG}} (\alpha_i + \beta_i P_{TGi} + \gamma_i P_{TGi}^2 + \delta_i e^{\varepsilon_i P_{TGi}}) \tag{5.2}$$

where $\alpha_i, \beta_i, \gamma_i, \delta_i, \varepsilon_i$ are the i^{th} thermal generator emission coefficients;

c) Active power loss (MW):

The following equation can be used to express active power loss:

$$Min\, J_3 = \sum_{k=1}^{N_L} \left(G_k \left(V_i^2 + V_j^2 - 2V_i V_j \cos\theta_{ij} \right) \right) \tag{5.3}$$

where N_L is the number of lines; θ_{ij} shows the voltage angle between buses i and j; G_k represents the conductance of branch k; V_i, V_j is the voltage magnitudes at i^{th} and j^{th} bus respectively.

d) Voltage magnitude deviation (p.u.):

The voltage variation is the sum of all voltage variances at load buses in the network relative to the reference voltage. The mathematical expression is as follows:

$$Min\, J_4 = \sum_{i=1}^{N_{PQ}} \left|\left(V_i - V_{ref}\right)\right| \tag{5.4}$$

where N_{PQ} is the number of PQ buses; V_{ref} is the reference voltage set to 1 p.u.; V_i is the i^{th} load bus voltage.

5.2.2 Constraints

The MOOPF objectives are subjected to the following equality and inequality constraints.

a) Equality constraints:

The equality restrictions are power-balancing equations in which the sum of the generations of the real and reactive powers is equal to their corresponding demands and losses.

- Power flow constraints

The overall demand and losses throughout the system are equal to the total real and reactive power delivered:

$$P_{Gi} - P_{Di} - V_i \sum_{j=1}^{N_B} V_j\left(G_{ij}\cos\theta_{ij} + B_{ij}\sin\theta_{ij}\right) = 0; i = 1,2,\dots N_B \tag{5.5}$$

$$Q_{Gi} - Q_{Di} - V_i \sum_{j=1}^{N_B} V_j\left(G_{ij}\sin\theta_{ij} - B_{ij}\cos\theta_{ij}\right) = 0; i = 1,2,\dots N_B \tag{5.6}$$

where N_B is the number of buses; P_{Gi}, Q_{Gi}, and P_{Di}, Q_{Di} are the real, reactive power generations and demands at the i^{th} bus, respectively; G_{ij}, B_{ij} is the conductance, susceptance of lines between buses i and j respectively;

b) Inequality constraints:

The operational limitations on generators, transformers, and shunt devices, as well as the security requirements on lines and load buses, constitute inequality constraints.

- Generator constraints: The boundary limits of real and reactive powers and the voltage magnitude of the generator buses are expressed as follows:

$$P_{TGi}^{min} \le P_{TGi} \le P_{TGi}^{max}; i = 1,2,\dots N_{TG} \tag{5.7}$$

$$P_{WGi}^{min} \le P_{WGi} \le P_{WGi}^{max}; i = 1,2,\dots N_{WG} \tag{5.8}$$

$$P_{SGi}^{min} \le P_{SGi} \le P_{SGi}^{max}; i = 1,2,\dots N_{SG} \tag{5.9}$$

$$P_{PEVGi}^{min} \le P_{PEVGi} \le P_{PEVGi}^{max}; i = 1,2,\dots N_{PEV} \tag{5.10}$$

$$Q_{TGi}^{min} \le Q_{TGi} \le Q_{TGi}^{max}; i = 1,2,\dots N_{TG} \tag{5.11}$$

$$Q_{WGi}^{min} \leq Q_{WGi} \leq Q_{WGi}^{max}; i = 1,2, \dots N_{WG} \quad (5.12)$$

$$Q_{SGi}^{min} \leq Q_{SGi} \leq Q_{SGi}^{max}; i = 1,2, \dots N_{SG} \quad (5.13)$$

$$V_{Gi}^{min} \leq V_{Gi} \leq V_{Gi}^{max}; i = 1,2, \dots N_{G} \quad (5.14)$$

- Shunt compensator constraints: The following are the boundary values for shunt compensators:

$$Q_{Ci}^{min} \leq Q_{Ci} \leq Q_{Ci}^{max}; i = 1,2, \dots N_{C} \quad (5.15)$$

- Transformer constraints: The ideal operating limits for tap settings on a transformer are given as follows:

$$T_{i}^{min} \leq T_{i} \leq T_{i}^{max}; i = 1,2, \dots N_{T} \quad (5.16)$$

- Security constraints: The voltage limits of the load buses and the apparent power value of each transmission line, which can be restricted by its maximum capacity, are given as follows:

$$V_{Li}^{min} \leq V_{Li} \leq V_{Li}^{max}; i = 1,2, \dots N_{PQ} \quad (5.17)$$

$$|S_{li}| \leq S_{li}^{max};\ i = 1,2, \dots N_{L} \quad (5.18)$$

where N_C,and N_T is the number of shunt compensators and transformers respectively; S_{li} and S_{li}^{max} are the apparent power flow and its maximum limit of i^{th} line; P_{Gi}^{min},P_{Gi}^{max} are the limits on real power generation; Q_{Gi}^{min},Q_{Gi}^{max} are the limits on reactive power generation; V_{Gi}^{min},V_{Gi}^{max} are the limits on generator bus voltages; T_{i}^{min},T_{i}^{max} are the limits on transformer taps; Q_{Ci}^{min},Q_{Ci}^{max} are the limits on shunt compensator; V_{Li}^{min}, $V_{Li}^{max}$are the limits on load bus voltages;

Two equality constraints Eq. (5.5) and Eq. (5.6) are automatically satisfied when the power flow converges to an optimal solution. The generator buses' real power (excluding slack bus), transformer tap ratios, voltage limits, and shunt compensator ranges are considered to control variables that are self-limiting. The remaining inequality constraints require constraint handling techniques.

In OPF, generator reactive power capacities are significant. In recent years, WECSs with complete reactive power capability has become commercially viable [60]. WECS can deliver reactive power in the range of -0.4p.u.to 0.5p.u. The negative sign signifies the generator's ability to absorb. Rooftop solar PV is designed as load buses with zero reactive power. However, because utility-based Solar PVs have converters built-in, full generator modeling is required due to the converters' dynamic behavior [61]. In this study, the reactive power capabilities of SPVS are assessed between -0.4p.u and 0.5p.u.

5.3 Constraint Handling Method

A proper CHM must be used in conjunction with an evolutionary algorithm to guide the search process toward a globally optimal solution. Among the many CHMs, the most frequently employed is the penalty approach, which involves adding a penalty to the fitness of a non-feasible solution. Despite its simplicity and ease of implementation, this method's performance is highly dependent on the penalty factor, which must be calibrated through trial and error. To tackle this difficulty, in this study, a new parameter-free CHM superiority of feasible solution (SF) is introduced in the study for solving the MOOPF problem.

In [62], Deb introduced the SF method for handling different constraints efficiently. In the SF method, a comparison is drawn between a pair of solutions. When a pair of solutions are compared, the following cases emerge:

(1) While comparing two non-feasible solutions, the solution having the smallest constraint violation is selected.
(2) When two feasible solutions are compared, the one with a better fitness solution is selected.
(3) When a feasible solution is compared to a non-feasible solution, the feasible solution is selected.

Comparing non-feasible solutions based on constraint violation helps push non-feasible answers into the feasible region while comparing viable solutions based on the fitness value enables solution quality to be improved.

5.4 Integration of WECS, SPVS, and PEV Systems

5.4.1 WECS, SPVS, and PEV Modeling

In this part, the WECS, SPVS, and PEV systems are integrated into the conventional OPF problem.

a) WECS Modeling:

The wind speed at a given geographical area is most likely distributed according to Weibull PDF as given below:

$$f(v) = \left(\frac{k}{c}\right)\left(\frac{v}{c}\right)^{(k-1)} (e)^{\left(\frac{-v}{c}\right)^{k}} ; 0 < v < \infty \tag{5.19}$$

where v is the wind speed (m/sec); $k,$ and c is the shape, and scale factors respectively.

The PDFs for two different shape and scale factors are given in [63]. The relationship between wind speed and power generation is as follows:

$$P_w(v) = \begin{cases} 0; v < v_{in} \; and \; v > v_{out} \\ P_{wr}\left(\frac{v - v_{in}}{v_r - v_{in}}\right) \quad ; \; v_{in} \le v_w \le v_r \\ P_{wr}; \; v_r < v_w \le v_{out} \end{cases} \tag{5.20}$$

where P_{wr} is the rated wind power; v_{in}, v_{out}, v_r are the cut-in, cut-out, and rated wind speeds (m/sec) respectively;

The probability of obtaining a zero and rated power output is given by the following:

$$f_w(P_w = 0) = 1 - e^{\left(-\left(\frac{v_{in}}{c}\right)^k\right)} + e^{\left(-\left(\frac{v_{out}}{c}\right)^k\right)} \tag{5.21}$$

$$f_w(P_w = P_{wr}) = e^{\left(-\left(\frac{v_r}{c}\right)^k\right)} + e^{\left(-\left(\frac{v_{out}}{c}\right)^k\right)} \tag{5.22}$$

The probability for the linear part of the wind speed is given by the following:

$$f_w(P_w) = \left(\frac{k(v_r - v_{in})}{cP_{wr}}\right)\left(\frac{v_{in}P_{wr} + P_w(v_r - v_{in})}{cP_{wr}}\right)^{(k-1)} e^{\left(-\left(\frac{v_{in}P_{wr} + P_{wr}(v_r - v_{in})}{cP_{wr}}\right)^k\right)} \tag{5.23}$$

b) SPVS Modeling:

Similarly, the power output of a solar energy system is a factor of solar irradiance and it likely follows the Lognormal PDF [64] as follows:

$$f_G(G_s) = \frac{1}{G_S\sigma\sqrt{2\pi}} e^{\left\{\frac{-(\ln G_S - \mu)^2}{2\sigma^2}\right\}}; G_S > 0 \tag{5.24}$$

where μ and σ are the mean and standard deviation respectively; G_s is the solar irradiance (W/m^2).

The SPVS unit's solar irradiance to energy generation is as follows [65]:

$$P_S(G_S) = \begin{cases} P_{sr}\left(\frac{G_S^2}{G_{std}R_c}\right) & ; 0 < G_S < R_c \\ P_{sr}\left(\frac{G_S}{G_{std}}\right) & ; G_S \geq R_c \end{cases} \tag{5.25}$$

where G_{std} is the standard solar irradiance (W/m^2); R_c is the particular irradiance point (W/m^2); P_{sr} is the SPVS-rated power output.

c) PEV Modeling:

In recent days, public transport electric vehicles ply most of the time during the day and are charged during off-peak periods and so are not suitable for V2G application. Privately-owned PEVs are generally idle most of the time during the day and hence PEVs are suitable for the vehicle-to-grid (V2G) power-fed capability. The availability of electric vehicles as V2G source follows the normal PDF as follows [69]:

$$f_{pev} = \frac{1}{\sqrt{2\pi\varphi^2}} e^{-\left\{\frac{(P_{pev} - \mu)^2}{2\varphi^2}\right\}} \tag{5.26}$$

where μ and φ are the mean and standard deviation of normal PDF respectively; P_{pev} is the available V2G power;

Here, the PEVs are used as a source of power feeding the grid through suitable infrastructure. The following assumptions are made regarding the use of PEV as a power source.

- All PEVs supply battery power to the power network through DC/AC inverter.
- All PEVs represent one big V2G charging/discharging station.
- V2G system acts as a power source controller.

Depending on the probability of PEVs availability, the direct, reserve, and penalty costs are calculated.

5.4.2 Uncertainty cost calculation of WECS, SPVS, and PEV Systems

Since WECS, SPVS, and PEVS are intermittent, the Monte-Carlo simulations are used to account for uncertainty and to calculate the uncertainty cost. The estimated cost for the intermittency of WECS, SPVS, and PEVS powers is reflected in three ways: direct, reserve, and penalty costs. Whenever power is underestimated, extra unusable power is wasted; however, in practical power system applications, such power can be saved in an energy storage system and thus be counted as the reserve cost. The cost of overestimating power that is lower than the scheduled power is considered a penalty cost in the case of overestimation.

The direct cost associated with j^{th} WECS is as follows:

$$C_{w,j}(P_{ws,j}) = g_j P_{ws,j} \tag{5.27}$$

The direct cost of k^{th} SPVS is as follows:

$$C_{w,k}(P_{ss,k}) = h_k P_{ss,k} \tag{5.28}$$

Similarly, the direct cost of n^{th} PEVS is as follows:

$$C_{pev,n}(P_{pevs,n}) = d_n P_{pevs,n} \tag{5.29}$$

where $P_{ws,j}$, $P_{ss,k}$, and $P_{pevs,n}$ are the scheduled powers of j^{th} WECS, k^{th} SPVS, and n^{th}PEVS respectively; $g_j, h_{k,}$ and d_n are the direct cost coefficients of j^{th} WECS, k^{th} SPVS, and n^{th} PEVS respectively;

When the wind farm's actual output falls short of the predicted value, the system operator must maintain a spinning reserve to ensure that consumers receive uninterrupted power. This is called the overestimation of power delivered from uncertain sources and the cost incurred to maintain the spinning reserve is known as reserve cost [66].

The reserve cost of the j^{th} WECS is as follows:

$$C_{Rw,j}(P_{ws,j} - P_{wav,j}) = K_{Rw,j}(P_{ws,j} - P_{wav,j}) = K_{Rw,j}\int_0^{P_{ws,j}} (P_{ws,j} - p_{w,j}) f_w(p_{w,j}) dp_{w,j} \tag{5.30}$$

In contrast to the overestimation case, when the actual power output of the wind exceeds the predicted output, the surplus power is squandered if it cannot be utilized. As a result, the

ISO is required to pay a penalty fee for excess power. This is referred to as the underestimation of power delivered from uncertain sources.

The penalty cost of the j^{th} WECS is as follows:

$$C_{Pw,j}\left(P_{wav,j} - P_{ws,j}\right) = K_{Pw,j}(P_{wav,j} - P_{ws,j}) = K_{Pw,j}\int_{P_{ws,j}}^{P_{wr,j}}\left(P_{w,j} - p_{ws,j}\right)f_w\left(p_{w,j}\right)dp_{w,j} \tag{5.31}$$

where $K_{Rw,j}$, $K_{Pw,j}$ are the reserve, penalty cost coefficients of j^{th} WECS respectively; $P_{wr,j}$, $P_{wav,j}$ are the rated, actually available powers of j^{th} WECS; $f_w\left(p_{w,j}\right)$ be the possibility of j^{th} WECS.

Like the WECS, SPVS power also shows intermittency in output power. The approach to calculating the over and underestimation cost of SPVS is as follows [67].

The reserve cost for k^{th} SPVS is as follows:

$$\begin{aligned} C_{Rs,k}\left(P_{ss,k} - P_{sav,k}\right) &= K_{Rs,k}\left(P_{ss,k} - P_{sav,k}\right) \\ &= K_{Rs,k} * f_s\left(P_{sav,k} < P_{ss,k}\right) * \left[P_{ss,k} - E\left(P_{sav,k} < P_{ss,k}\right)\right] \end{aligned} \tag{5.32}$$

The penalty cost for a k^{th} SPVS is as follows:

$$\begin{aligned} C_{Ps,k}\left(P_{sav,k} - P_{ss,k}\right) &= K_{Ps,k}\left(P_{sav,k} - P_{ss,k}\right) \\ &= K_{Ps,k} * f_s\left(P_{sav,k} > P_{ss,k}\right) * \left[E\left(P_{sav,k} > P_{ss,k}\right) - P_{ss,k}\right] \end{aligned} \tag{5.33}$$

where $K_{Rs,k}$, $K_{Ps,k}$ is the reserve, penalty cost constants of k^{th} SPVS respectively; $P_{sav,k}$ is the actually available power of k^{th} SPVS; $f_s\left(P_{sav,k} < P_{ss,k}\right)$ and $f_s\left(P_{sav,k} > P_{ss,k}\right)$ are the probabilities of SPVS power; $E\left(P_{sav,k} < P_{ss,k}\right)$, $E\left(P_{sav,k} > P_{ss,k}\right)$ are the expectations of SPVS power.

Similarly, PEVS also shows intermittency in output power. The approach to calculating the over and underestimation cost of PEVS is as follows [70, 71].

Reserve cost associated with n^{th} PEV is defined as:

$$\begin{aligned} C_{Rpev,n}\left(P_{pevs,n} - P_{pevav,n}\right) &= K_{Rpev,n}\left(P_{pevs,n} - P_{pevav,n}\right) \\ &= K_{Rpev,n}\int_0^{P_{pevs,n}}\left(P_{pevs,n} - p_{pev,n}\right)f_{pev}\left(p_{pev,n}\right)dp_{pev,n} \end{aligned} \tag{5.34}$$

Penalty cost associated with n^{th} PEV is defined as:

$$\begin{aligned} C_{Ppev,n}\left(P_{pevav,n} - P_{pevs,n}\right) &= K_{Ppev,n}\left(P_{pevav,n} - P_{pevs,n}\right) \\ &= K_{Ppev,n}\int_{P_{pevs,n}}^{P_{pevr,n}}\left(p_{pev,n} - P_{pevs,n}\right)f_{pev}\left(p_{pev,n}\right)dp_{pev,n} \end{aligned} \tag{5.35}$$

where $K_{Rpev,n}$, $K_{Ppev,n}$ is the reserve, penalty cost constants of n^{th} PEVS respectively; $P_{pevr,n}$, $P_{pevav,n}$ are the rated, actually available powers of n^{th} PEVS; $f_{pev}(p_{pev,n})$ is the n^{th} PEVS power probability.

5.5 Proposed Method

In this chapter, a summation of normalized objective values (SNOV) with improved diversified selection (IDS) is proposed and integrated with the multi-objective evolution algorithm based on the decomposition (MOEA/D) [53] method to solve the MOOPF problem. The MOEA/D method decomposes the multi-objective optimization problem into several single scalar optimization problems and optimizes them all at the same time using weight vectors. The weight vectors' distance is used to create neighborhoods. In every population evolution, information from the neighborhood is used to find a solution. The non-dominated sorting used in MOEA/D is complex and time-taking. Some useful information may be lost if the dominant solutions are completely discarded. In addition, diversity may be lost during the search process and lead to local optima. To overcome these problems, the summation of normalized objective values [68] with IDS is employed in this work instead of non-dominated sorting selection to get a uniformly distributed Pareto front and improved convergence characteristics.

The proposed MOEA comprises initialization, reproduction, investigation of feasible solutions, normalization and selection, and termination phases.

1. Initialization:

- Initialize the population (Pt) of size 'N'.
- The uniformly distributed weights are produced using SSA in the following manner:

$$\mathrm{N(D,M)} = \binom{\mathrm{D+M-1}}{\mathrm{M-1}} \text{ for } \mathrm{D} > 0 \tag{5.36}$$

- Run the load flow, and calculate the fitness of the selected objective and total constraint violation.
- Using angle criteria, locate neighbors with the smallest angles for each weight vector [55] as follows:

$$\tan\varphi = \frac{d_2}{d_1}$$

$$where\ d_1 = \frac{\|w_i^T.w_j\|}{\|w_j\|}\ and\ d_2 = \left\|w_i - d_1\frac{w_j}{\|w\|}\right\|$$

$$where\ i,j = 1,2,\dots\dots,N\ and\ i \neq j \tag{5.37}$$

Where w indicates the weight vector, φ indicates the angle between d_1 and d_2.

- Find the smallest objective values to form the present ideal point.
- Find the largest objective values to form the present nadir point.
- Set iteration count=1.

2. Reproduction:

- Use an angle criterion to choose N pair of mating parents. A set of mating parents is picked from neighbors with a probability for each weight vector.
- Perform two-point crossover and mutation operations to generate a new population (Qt).
- Calculate the fitness values for the newly generated population (Qt).
- Compute the total constraint violation for the new population (Qt).
- Merge the original population (Pt) and the new population (Qt).

3. Investigation of feasible solutions:

- Sort the total population ascending by total constraint violation values.
- Discover feasible solutions.
- If the number of viable solutions is lower than the population (N), move on to **Step 5.**
- If at least N solutions exist in the total population, move on to **Step 4.**

4. Normalization and selection:

- Apply the equation below to each objective and solution to determine the normalized objective value[68, 72].

$$f_i^{"}(x^m) = \frac{f_i(x^m) - f_{i,min}}{f_{i,max} - f_{i,min}} \tag{5.38}$$

  where $f_i^{"}(x^m)$ is the normalized value of x^m for i^{th} objective, $f_{i,max}$, $f_{i,min}$ are the i^{th} objective limits.

- Obtain a summation of the normalized objective values for all solutions [68, 72].

$$F^{"}(x^m) = \sum_{i=1}^{M} f_i^{"}(x^m) \tag{5.39}$$

- Calculate the Euclidian distance between the origin and the sum of all normalized objective values. The stopping point is defined by the solution that yields total normalized objective values near to the origin.
- Equally, divide the objective space into 100 bins where scanning of the bins should continue until the scanning procedure reaches a stopping point. For every

scanned bin, the solution with the smallest sum of normalized objective values is entered into the preferred set.

- The backup set includes unselected solutions as well as solutions dominated by the stopping point.

5. Termination:

- Increase iteration number by one i.e. iter=iter+1.
- If the stopping requirement is met, Stop else **Go to Step 2.**

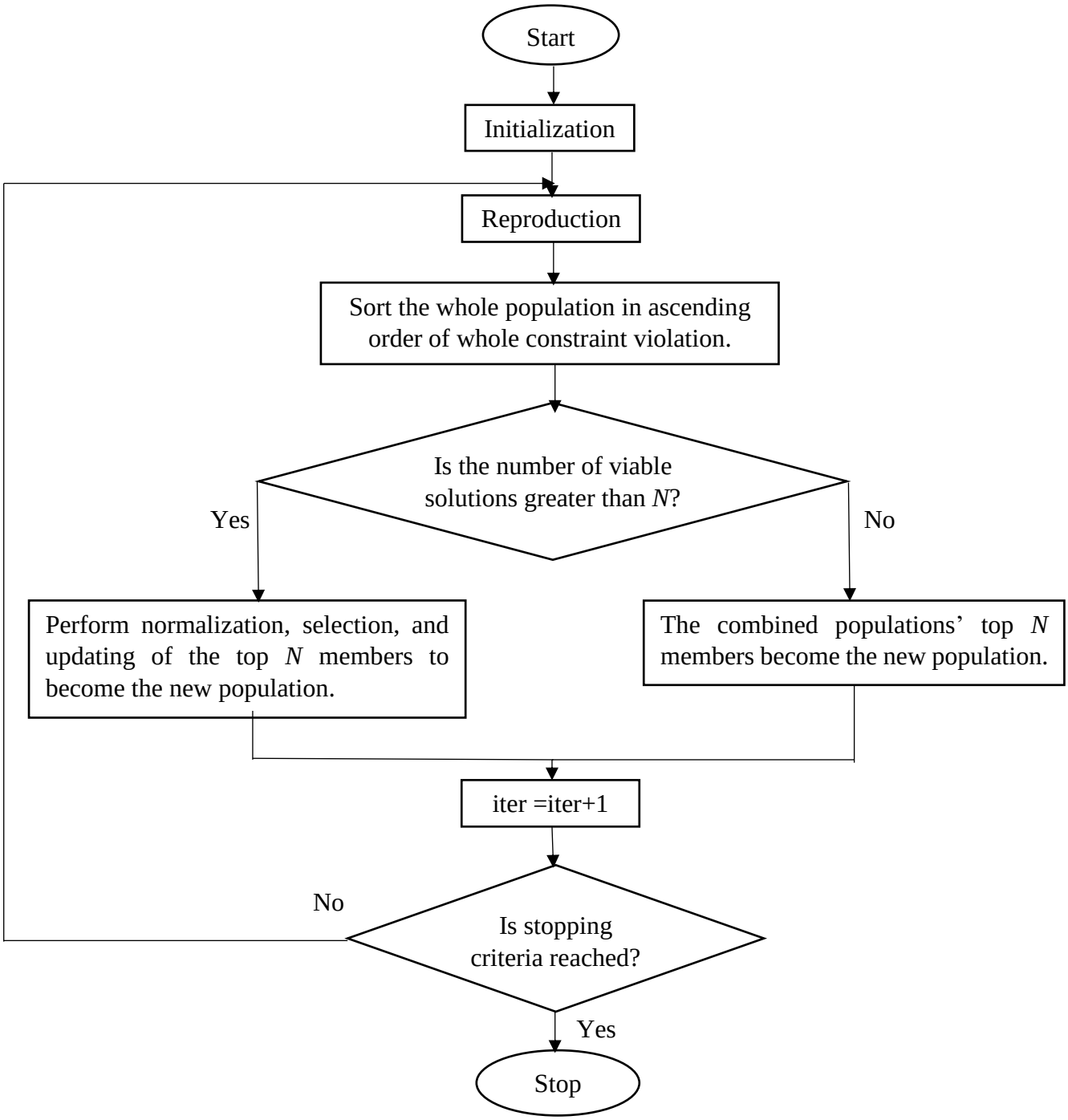

Fig. 5.1: Flowchart of the proposed method.

5.6 Results and Discussions

To analyze the robustness and efficacy of the proposed method, IEEE 57-bus, and 118-bus systems were chosen. The proposed method was implemented in MATLAB R2016a, and simulations were conducted over an i3-Processor having 4 GB RAM. To verify the efficacy of the proposed method, comparisons were made with NSGA-II [57] and MOPSO [58]. In this work, the stochastic nature of WECS, SPVS, and PEV sources was taken into account to study the impact of these sources on the MOOPF problem. To consider uncertainties, Monte-Carlo simulations were used to generate 1000 samples. The control parameters of the proposed method, NSGA-II, and MOPSO are given in Table 5.1. The various cases considered are given in Table 5.2. The description of the test systems is given in Table 5.3. PDF specifications and cost components of various sources are given in Table 5.4.

Table 5.1: Control parameters of the proposed method, NSGA-II, and MOPSO.

S. No.	Method	Control parameters
1.	**Proposed method**	***N* =100, *D* =12, *T* =20, P_c =1.0, P_m =0.05, and max. iterations=100.**
2.	NSGA-II [57]	*N* =100, P_c =0.8, P_m =0.01, and max. iterations=100.
3.	MOPSO [58]	*N* =100, *C1= C2* =2, *W*=0.5, and max. iterations=100.

Table 5.2: Various cases considered.

S. No	Test Systems	Case #	J_1	J_2	J_3	J_4
1.	IEEE 57-bus system	Case-1	✓	✓	--	--
		Case-2	✓	✓	✓	--
		Case-3	✓	✓	✓	✓
2.	IEEE 118-bus system	Case-4	✓	--	✓	--
		Case-5	✓	--	✓	✓

Table 5.3: Test systems description.

Specifications	IEEE 57-bus system		IEEE 118-bus system	
Buses	57	[59]	118	[59]
Lines	80		186	
Thermal units	7	Buses:1,2,3,6,8,9 and 12	54	Buses: [59]
Slack bus	1	Bus:1	69	Bus: 69
Transformer tap positions	17	Lines:19,20,31,35,36,37,41,46, 54,58,59,65,66,71,73,76, and 80	9	Lines: 8,32,36, 51, 93,95,102,107 and 127
Shunt capacitors	3	Buses:18,25, and 53	12	Buses:34,44,45,46,48,74,79,82, 83, 105, 107 and 110
Control variables	36	Generator bus real powers (9) + voltages (7) + transformer tap settings (17) + shunt capacitor (3).	131	Generator bus real powers (56) + voltages (54) + transformer tap settings (9) + shunt capacitor (12).
Load	-	1250.8MW, 336.4MVAR	-	4242.0MW, 1439.0MVAR
WECS	1	45 #bus	1	81 #bus
SPVS	1	16 #bus	1	64 #bus
PEVS	1	49 #bus	1	117 #bus

Table 5.4: PDF specifications and cost components of various sources.

S. No.	Specifications	WECS	SPVS	PEVS
1.	PDF	Weibull	Lognormal	Normal
2.	Parameters	c =10, k =2, v_{in}=10m/sec, v_{out}=12m/sec, v_r=12m/sec	μ =6, σ = 0.6, G_{std}=800 W/m^2 , R_c=120 W/m^2	μ = 3.2, φ = 0.88
3.	Direct cost coefficient ($/MW)	1.75	1.60	1.60
4.	Reserve cost coefficient ($/MW)	3	3	3
5.	Penalty cost coefficient ($/MW)	1.5	1.5	1.5

5.6.1 IEEE 57-bus system

The proposed method was tested on an IEEE 57-bus system [59], it has 7 thermal generators (# 1 bus acts as a slack bus), 80 lines, 15 off-nominal transformers, 3 shunt VAR compensators, and real and reactive power demand of 1250.80MW and 336.40MVAR respectively. Notably, the locations of these sources were chosen from [74], by replacing load buses with the respective WECS, SPVS, and PEV sources.

a) Case-1: Minimize J_1 and J_2 simultaneously.

In this case, J_1 and J_2 are the objectives that need to be minimized simultaneously. The optimal decision variables obtained by the proposed method are included in Table 5.5. The best-compromised values obtained using the proposed method have a total generation cost of **35815.04$/h** and emission of **0.8950ton/h**. The best-compromised values achieved using NSGA-II [57] and MOPSO [58] are 35850.00$/h, 0.9928ton/h, and 35910.00$/h, 1.0120ton/h respectively as reported in Table 5.6. The Pareto-optimal fronts (PFs) observed are depicted in Figure 5.2.

b) Case-2: Minimize J_1, J_2 and J_3 simultaneously.

In this case, J_1, J_2, and J_3 are the objectives that need minimizing simultaneously. The optimal decision variables obtained by the proposed method are included in Table 5.5. The best-compromised values obtained using the proposed method have a total generation cost of **35558.26$/h**, emission of **0.9673ton/h,** and active power loss of **10.0796MW**. The best compromised values achieved using NSGA-II [57] and MOPSO [58] are 36336.00$/h, 1.2498ton/h, 11.0813MW and 36402.69$/h, 1.0450ton/h, 12.5591MW respectively as reported in Table 5.6. The Pareto-optimal fronts (PFs) observed are depicted in Figure 5.2.

c) Case-3: Minimize J_1, J_2, J_3 and J_4 simultaneously.

In this case, J_1, J_2, J_3 and J_4 are the objectives that need to be minimized simultaneously. The optimal decision variables obtained by the proposed method are included in Table 5.5. The best-compromised values obtained using the proposed method have a total generation cost of

35980.02$/h, emission of **1.1696ton/h,** active power loss of **10.5229MW**, and voltage magnitude deviation of **0.8308p.u.** The best-compromised values achieved using NSGA-II [57] and MOPSO [58] are 36250.00$/h, 1.4175ton/h, 12.3871MW, 1.0481p.u. and 36662.59$/h, 0.9367ton/h, 14.1833MW, 1.0669p.u respectively as reported in Table 5.6.

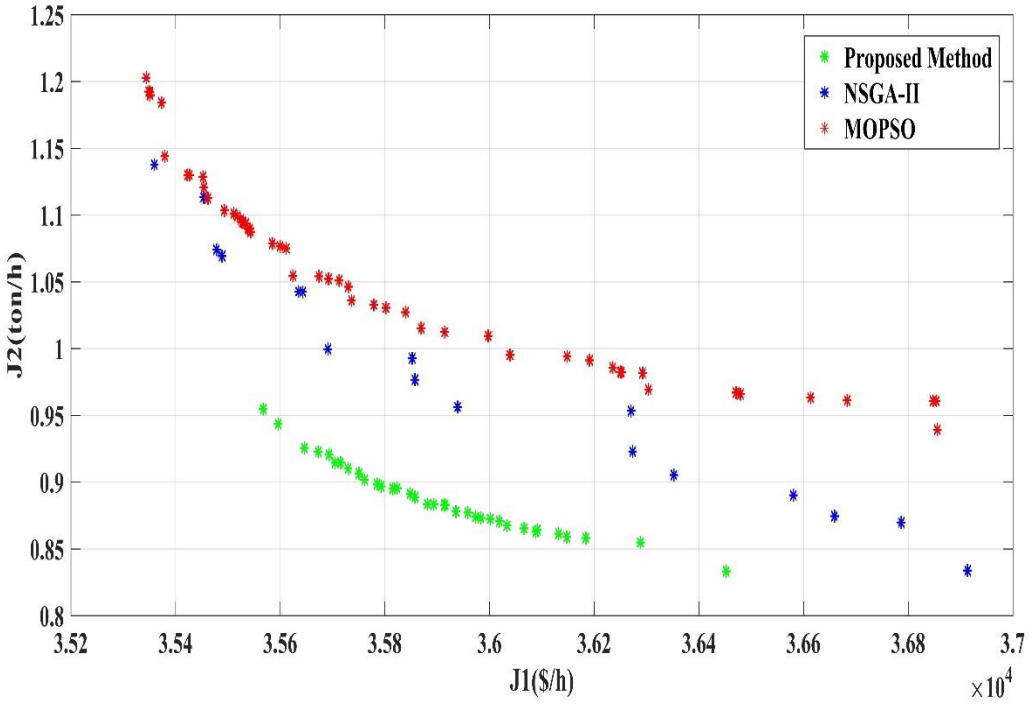

(a)

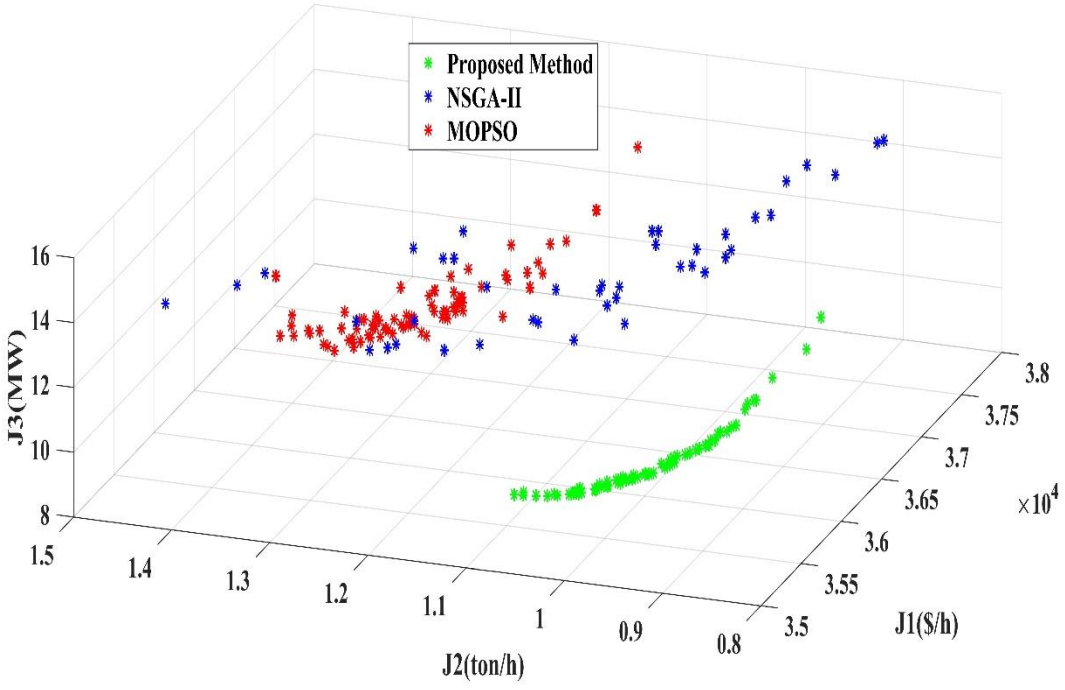

(b)

Fig. 5.2: IEEE 57-bus system: Pareto-optimal fronts. a) Case-1, and b) Case-2.

Table 5.5: IEEE 57-bus system: Optimal control variables obtained by the proposed method.

S. No.	Control variables	Limits		Case-1	Case-2	Case-3
		min	max			
1.	P2	0	100	95.7907	84.1793	57.9085
2.	P3		140	69.0738	53.1935	80.1009
3.	P6		100	97.6214	95.7712	57.4498
4.	P8		550	304.0230	302.8312	329.5786
5.	P9		100	82.3521	98.7022	64.9448
6.	P12		410	294.0245	331.1684	379.1110
7.	P45		80	79.8467	79.7886	78.2859
8.	P16		80	79.7469	79.9465	78.5326
9.	P49		20	19.3799	19.8993	14.6734
10.	V1	0.95	1.1	1.0385	1.0340	1.0226
11.	V2			1.0279	1.0286	1.0102
12.	V3			1.0313	1.0252	1.0144
13.	V6			1.0343	1.0203	1.0127
14.	V8			1.0394	1.0201	1.0224
15.	V9			1.0214	1.0123	1.0125
16.	V12			1.0341	1.0353	1.0421
17.	T19	0.9	1.1	1.0362	1.0016	1.0101
18.	T20			1.0250	0.9939	0.9964
19.	T31			1.0036	0.9826	1.0142
20.	T35			1.0307	1.0275	0.9855
21.	T36			0.9769	0.9881	0.9927
22.	T37			1.0448	1.0359	1.0270
23.	T41			1.0065	0.9990	1.0064
24.	T46			0.9927	0.9800	0.9956
25.	T54			1.0014	0.9536	0.9065
26.	T58			0.9821	0.9724	0.9780
27.	T59			0.9530	0.9719	0.9732
28.	T65			0.9719	0.9847	0.9799
29.	T66			0.9873	0.9485	0.9536
30.	T71			0.9720	0.9750	0.9620
31.	T73			0.9815	1.0087	1.0091
32.	T76			0.9844	0.9706	0.9641
33.	T80			1.0118	0.9973	1.0106
34.	QC18	0	20	11.6868	8.9393	11.0809
35.	QC25			10.5195	10.2799	11.1002
36.	QC53			10.8182	6.1637	8.4158
1.	**J_1($/h)**	**-**	**-**	**35815.04**	**35558.26**	**35980.02**
2.	**J_2(ton/h)**	**-**	**-**	**0.8950**	**0.9673**	**1.1696**
3.	**J_3(MW)**	**-**	**-**	**-**	**10.0796**	**10.5229**
4.	**J_4(p.u.)**	**-**	**-**	**-**	**-**	**0.8308**

Table 5.6: IEEE 57-bus system: Comparison of the proposed method.

Case #	Objective functions	**Proposed method**	NSGA-II [57]	MOPSO [58]
Case-1	J_1($/h)	**35815.04**	35850.00	35910.00
	J_2(ton/h)	**0.8950**	0.9928	1.0120
Case-2	J_1($/h)	**35558.26**	36336.00	36402.69
	J_2(ton/h)	**0.9673**	1.2498	1.0450
	J_3(MW)	**10.0796**	11.0813	12.5591

Case-3	J_1($/h)	**35980.02**	36250.00	36662.59
	J_2(ton/h)	**1.1696**	1.4175	0.9367
	J_3(MW)	**10.5229**	12.3871	14.1833
	J_4(p.u.)	**0.8308**	1.0481	1.0669

5.6.2 IEEE 118-bus system

The proposed technique has been examined on an IEEE 118-bus system [59], it has 54 thermal generators (# 69 bus as a slack bus), 186 lines, 9 off-nominal transformers, 12 shunt VAR compensators, and real and reactive power demand of 4242.00 MW and 1439.00 MVAR respectively. Notably, the locations of these sources were chosen from [74], by replacing load buses with the respective WECS, SPVS, and PEV sources.

a) Case-4: Minimize J_1 and J_3 simultaneously.

In this case, J_1 and J_3 are the objectives that need to be minimized simultaneously. The optimal decision variables obtained by the proposed method are included in Table 5.7. The best-compromised values obtained using the proposed method have a total generation cost of **129019.12$/h** and an active power loss of **36.7616MW**. The best-compromised values achieved using NSGA-II [57] and MOPSO [58] are 129582.23$/h, 37.3464MW, and 130673.5$/h, 38.0368MW respectively as reported in Table 5.8. The Pareto-optimal fronts (PFs) observed are depicted in Figure 5.3.

b) Case-5: Minimize J_1, J_3 and J_4 simultaneously.

In this case, J_1, J_3, and J_4 are the objectives that need to be minimized simultaneously. The optimal decision variables obtained by the proposed method are included in Table 5.7. The best-compromised values obtained using the proposed method have a total generation cost of **130796.33$/h**, active power loss of **32.5358MW,** and voltage magnitude deviation of **0.5165p.u.**. The best-compromised values achieved using NSGA-II [57] and MOPSO [58] are 134395.5$/h, 40.0724MW, 0.6876p.u. and 133574.6$/h, 41.3020MW, 0.9706p.u. respectively as reported in Table 5.8. The Pareto-optimal fronts (PFs) observed are depicted in Figure 5.3.

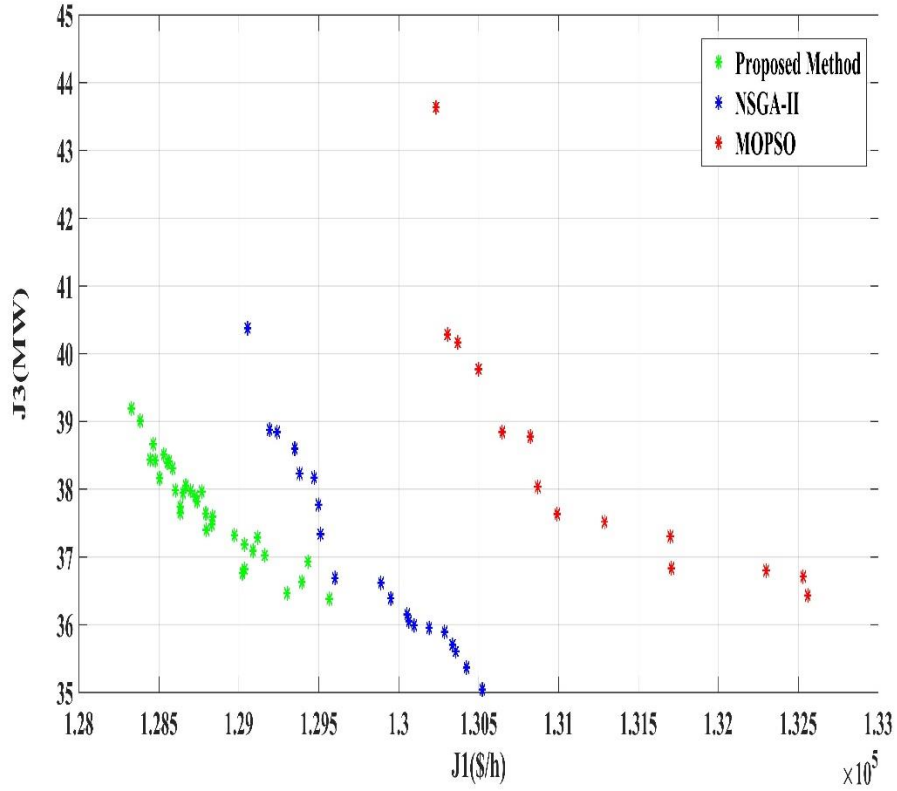

(a)

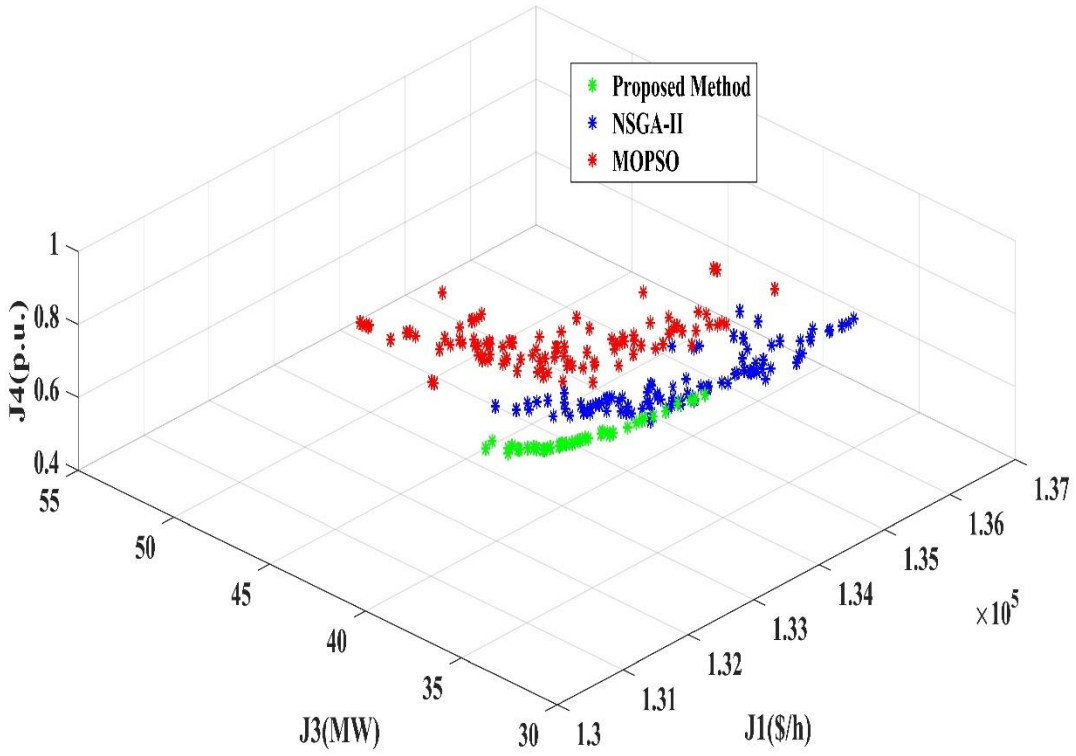

(b)

Fig. 5.3: IEEE 118-bus system: Pareto-optimal fronts. a) Case-4, and b) Case-5.

Table 5.7: IEEE 118-bus system: Optimal control variables obtained by the proposed method.

S. No.	Control variables	Limits		Case-4	Case-5	S. No.	Control variables	Limits		Case-4	Case-5
		min	max					min	max		
1.	P1	0	100	40.0447	63.4515	68.	V26	0.95	1.1	1.0157	1.0212
2.	P4		100	49.9982	35.6629	69.	V27			1.0335	1.0080
3.	P6		100	59.1167	35.0138	70.	V31			1.0378	1.0260
4.	P8		100	45.0837	47.8259	71.	V32			1.0211	1.0335
5.	P10		550	193.352	164.224	72.	V34			1.0259	1.0250
6.	P12		185	66.1489	76.0734	73.	V36			1.0379	1.0142
7.	P15		100	48.9935	56.2799	74.	V40			1.0346	1.0075
8.	P18		100	43.7256	39.0496	75.	V42			1.0239	1.0040
9.	P19		100	28.7879	70.2897	76.	V46			1.0123	1.0215
10.	P24		100	33.8075	48.7321	77.	V49			1.0274	0.9947
11.	P25		320	120.040	60.8414	78.	V54			1.0252	1.0138
12.	P26		414	120.644	169.915	79.	V55			1.0079	1.0267
13.	P27		100	46.2456	61.7409	80.	V56			1.0059	1.0278
14.	P31		107	22.3999	22.4692	81.	V59			1.0022	1.0261
15.	P32		100	55.1251	27.1559	82.	V61			1.0346	1.0459
16.	P34		100	51.6765	56.3221	83.	V62			1.0200	1.0243
17.	P36		100	55.7278	26.4301	84.	V65			1.0282	1.0170
18.	P40		100	58.4597	54.2550	85.	V66			1.0376	1.0277
19.	P42		100	61.1690	78.9208	86.	V69			1.0270	1.0202
20.	P46		119	42.4237	36.1427	87.	V70			1.0283	1.0337
21.	P49		304	178.039	177.089	88.	V72			1.0330	1.0119
22.	P54		148	68.7727	93.0152	89.	V73			1.0417	1.0283
23.	P55		100	41.4856	64.4180	90.	V74			1.0268	1.0272
24.	P56		100	56.0731	39.1371	91.	V76			1.0088	1.0119
25.	P59		255	141.029	133.894	92.	V77			1.0187	1.0314
26.	P61		260	106.400	112.972	93.	V80			1.0252	1.0404
27.	P62		100	60.9986	56.6838	94.	V85			1.0134	1.0240
28.	P65		491	220.874	232.485	95.	V87			1.0207	1.0161
29.	P66		492	204.311	137.571	96.	V89			1.0214	1.0363
30.	P70		100	57.4597	45.9800	97.	V90			1.0218	1.0280
31.	P72		100	40.2247	35.5260	98.	V91			1.0264	1.0480
32.	P73		100	33.4507	40.8232	99.	V92			1.0262	1.0312
33.	P74		100	62.6285	52.5801	100.	V99			1.0083	1.0415
34.	P76		100	58.4179	60.1585	101.	V100			1.0155	1.0291
35.	P77		100	58.7759	47.9148	102.	V103			1.0270	1.0226
36.	P80		577	277.432	307.393	103.	V104			1.0178	1.0103
37.	P85		100	45.6938	50.9420	104.	V105			1.0316	1.0118
38.	P87		104	8.7870	9.0718	105.	V107			1.0132	1.0042
39.	P89		707	265.920	217.226	106.	V110			1.0212	1.0117
40.	P90		100	37.1972	40.2967	107.	V111			1.0209	0.9956
41.	P91		100	38.8539	31.8664	108.	V112			1.0184	1.0163
42.	P92		100	48.4612	49.3316	109.	V113			1.0333	1.0343
43.	P99		100	37.8606	30.9745	110.	V116			1.0418	1.0108
44.	P100		352	97.0986	130.965	111.	T8	0.9	1.1	1.0165	0.9994
45.	P103		140	71.3612	50.4524	112.	T32			1.0025	0.9958
46.	P104		100	54.0455	51.1611	113.	T36			0.9948	0.9237
47.	P105		100	37.9765	43.3539	114.	T51			1.0136	0.9826
48.	P107		100	46.0688	38.7497	115.	T93			0.9876	0.9304
49.	P110		100	41.2868	31.8345	116.	T95			0.9931	0.9980
50.	P111		136	30.3153	42.3214	117.	T102			1.0057	0.9999
51.	P112		100	38.6270	34.9093	118.	T107			0.9818	0.9784
52.	P113		100	51.6430	44.9313	119.	T127			0.9806	0.9861
53.	P116		100	43.0444	42.0291	120.	QC34			11.3179	14.5351

54.	P81		150	95.3791	128.314	121.	QC44			10.0859	14.2184
55.	P64		150	134.122	142.181	122.	QC45			14.7235	9.0981
56.	P117		40	15.9465	19.7354	123.	QC46			13.0587	6.1809
57.	V1			1.0263	1.0471	124.	QC48			11.7728	14.5904
58.	V4			1.0310	1.0050	125.	QC74			12.4274	14.0292
59.	V6			1.0355	1.0291	126	QC79			12.0556	6.2538
60.	V8			1.0093	1.0193	127	QC82	0	25	16.3087	16.4578
61.	V10			1.0374	1.0024	128	QC83			11.7913	11.4913
62.	V12			1.0158	1.0224	129.	QC105			12.6136	10.6581
63.	V15			1.0206	1.0179	130.	QC107			8.8002	12.8524
64.	V18			1.0285	1.0259	131.	QC110			11.7193	15.2300
65.	V19			1.0193	1.0269	**1.**	**J_1($/h)**	-	-	**129019.1**	**130796.3**
66.	V24			1.0230	1.0235	**2.**	**J_3(MW)**	-	-	**36.7616**	**32.5358**
67.	V25			1.0278	0.9998	**3.**	**J_4(p.u)**	-	-	-	**0.5165**

Table 5.8: IEEE 118-bus system: Comparison of the proposed method.

Case #	Objective functions	**Proposed method**	NSGA-II [57]	MOPSO [58]
Case-4	J_1($/h)	**129019.12**	129582.23	130673.5
	J_3(MW)	**36.7616**	37.3464	38.0368
Case-5	J_1($/h)	**130796.33**	134395.5	133574.6
	J_3(MW)	**32.5358**	40.0724	41.3020
	J_4(p.u.)	**0.5165**	0.6876	0.9706

5.7 Summary

The approach for the MOEA is based on decomposition and summing up normalized objectives with an improved diverse selection mechanism. It also addresses the superiority of the feasible solution (SF) technique for dealing with the MOOPF problem constraints. The cost of thermal energy and the cost uncertainty associated with WECS, SPVS, and PEV systems are minimized along with the minimization of emission, active power loss, and voltage magnitude deviation. Monte Carlo simulations were used to assess the uncertainty of WECS, SPVS, and PEV power. To show the efficacy of the proposed method, simulations were done on the IEEE 57-bus and IEEE 118-bus systems, and the results were compared with NSGA-II and MOPSO algorithms. The outcomes show that the proposed method is superior to competing methods. Therefore, the proposed approach can be effectively used in operation when WECS, SPVS, and PEVS power generations are included in the power system. The proposed method may provide an optimal solution, but to further improve the evolutionary process a new hybrid MOEA is proposed in the next work.

Chapter 6

A Novel Hybrid Multi-Objective Evolutionary Algorithm Based on Decomposition and Invasive Weed Optimization Including Wind, Solar, and PEV Uncertainty for the Optimal Power Flow

This work is published in:

Ravi Kumar Avvari and Vinod Kumar D.M. "A New Hybrid Evolutionary Algorithm for Multi-Objective Optimal Power Flow in an Integrated WE, PV, and PEV Power System." **Electric Power Systems Research**, Elsevier, Vol. 214, 108870, Jan 2023. **(SCIE, IF:3.818).**

Chapter 6

A Novel Hybrid Multi-Objective Evolutionary Algorithm Based on Decomposition and Invasive Weed Optimization Including Wind, Solar, and PEV Uncertainty for the Optimal Power Flow

6.1 Introduction

This chapter proposes a novel hybrid decomposition and invasive weed optimization (IWO) based MOEA for the OPF problem. The standard OPF problem was transformed into a stochastic OPF by incorporating the uncertainty of WECS, SPVS, and PEV systems. This chapter presents a new CHM that adaptively inserts the penalty and avoids the parameter relying on penalty calculation. The IWO technique's selection qualities were utilized to increase the diversity of MOEA. The MOOPF problem includes minimization of the total generation cost, emission, active power loss, and voltage magnitude deviation as objectives. The generation cost of WECS, SPVS, and PEVS was examined using Monte Carlo simulations to reduce the total generation cost. Weibull, Lognormal, and Normal PDFs were used to characterize the unpredictability of WECS, SPVS, and PEVS, respectively. The impact of WECS, SPVS, and PEV uncertainties, was taken into account to validate the proposed method. The superiority of the proposed method was validated by comparing it with NSGA-II, and MOPSO algorithms and tested using IEEE 57-bus and IEEE 118-bus systems.

The contributions of this chapter are as follows:

i. Introducing a novel hybrid decomposition and invasive weed optimization (IWO) based MOEA for the OPF problem.
ii. Integrating the stochastic nature of WECS, SPVS, and PEVS with normal OPF to address the influence of the sources' unpredictable nature.
iii. Modeling the uncertainty of WECS, SPVS, and PEV energy systems using PDF and computing its uncertainty cost with Monte Carlo simulations.
iv. Using an effective CHM known as the SF method to handle constraints in the MOOPF problem.

6.2 Problem Formulation

The objectives and constraints for the considered MOOPF problem are expressed as follows:

6.2.1 Objectives

The MOOPF problem is formulated by considering four objectives which involve minimizing a) total generation cost (J_1), b) emission (J_2), c) active power loss (J_3), and d) voltage magnitude deviation (J_4).

a) Total generation cost ($/h):

The overall generating cost is the sum of the generation cost of thermal, WECS, SPVS, and PEV sources and is expressed by the following equation:

$$\begin{aligned} Min\, J_1 = & \sum_{i=1}^{N_{TG}} (a_i + b_i P_{TGi} + c_i P_{TGi}^2) \\ & + \sum_{j=1}^{N_{WG}} \left[C_{w,j}(P_{ws,j}) + C_{Rw,j}(P_{ws,j} - P_{wav,j}) + C_{Pw,j}(P_{wav,j} - P_{ws,j}) \right] \\ & + \sum_{k=1}^{N_{SG}} \left[C_{s,k}\left(P_{ss,k}\right) + C_{Rs,k}\left(P_{ss,k} - P_{sav,k}\right) + C_{Ps,k}\left(P_{sav,k} - P_{ss,k}\right) \right] \\ & + \sum_{n=1}^{N_{PEV}} \left[C_{pev,n}(P_{pevs,n}) + C_{Rpev,n}(P_{pevs,n} - P_{pevav,n}) + C_{Ppev,n}(P_{pevav,n} \right. \\ & \left. - P_{pevs,n}) \right] \end{aligned} \tag{6.1}$$

where N_{TG}, N_{WG}, N_{SG}, and N_{PEV} are the number of thermal, WECS, SPVS, and PEVS respectively; $P_{ws,j}$, $P_{ss,k}$, and $P_{pevs,n}$ are the scheduled powers of j^{th} WECS, k^{th} SPVS, and n^{th} PEVS respectively; $P_{wav,j}$, $P_{sav,k}$, and $P_{pevav,n}$ are the actual powers of j^{th} WECS, k^{th} SPVS, and n^{th} PEVS respectively; P_{TGi} is the i^{th} thermal generator output power; a_i, b_i, c_i is the i^{th} thermal generator cost coefficients;

b) Emission (ton/h):

The generation of electric power from traditional fossil fuels would result in the emission of hazardous gases into the atmosphere. The following expression describes the total emission from thermal generators:

$$Min J_2 = \sum_{i=1}^{N_{TG}} (\alpha_i + \beta_i P_{TGi} + \gamma_i P_{TGi}^2 + \delta_i e^{\varepsilon_i P_{TGi}}) \tag{6.2}$$

where $\alpha_i, \beta_i, \gamma_i, \delta_i, \varepsilon_i$ are the i^{th} generator emission coefficients;

c) Active power loss (MW):

The following equation can be used to express active power loss:

$$Min\, J_3 = \sum_{k=1}^{N_L} \left(G_k \left(V_i^2 + V_j^2 - 2V_i V_j \cos\theta_{ij} \right) \right) \tag{6.3}$$

where N_L is the number of lines; θ_{ij} indicates voltage angles between buses i and j; G_k shows the conductance of branch k; V_i, V_j is the voltage magnitudes at i^{th} and j^{th} bus respectively.

d) Voltage magnitude deviation (p.u.):

The voltage variation is the sum of all voltage variances at load buses in the network relative to the reference voltage. The mathematical expression is as follows:

$$Min\ J_4 = \sum_{i=1}^{N_{PQ}} \left|\left(V_i - V_{ref}\right)\right| \tag{6.4}$$

where N_{PQ} is the number of PQ buses; V_{ref} is the reference voltage set to 1 p.u.; V_i is the i^{th} load bus voltage.

6.2.2 Constraints

The MOOPF objectives are subjected to the following equality and inequality constraints.

a) Equality constraints:

The equality restrictions are power-balancing equations in which the sum of the generations of the real and reactive powers is equal to their corresponding demands and losses.

- Power flow constraints

The overall demand and losses throughout the system are equal to the total real and reactive power delivered:

$$P_{Gi} - P_{Di} - V_i \sum_{j=1}^{N_B} V_j\left(G_{ij}\cos\theta_{ij} + B_{ij}\sin\theta_{ij}\right) = 0; i = 1,2,\dots N_B \tag{6.5}$$

$$Q_{Gi} - Q_{Di} - V_i \sum_{j=1}^{N_B} V_j\left(G_{ij}\sin\theta_{ij} - B_{ij}\cos\theta_{ij}\right) = 0; i = 1,2,\dots N_B \tag{6.6}$$

where N_B is the number of buses; P_{Gi}, Q_{Gi}, and P_{Di}, Q_{Di} are the real, reactive power generations and demands at the i^{th} bus, respectively; G_{ij}, B_{ij} is the conductance, susceptance of lines between buses i and j respectively;

b) Inequality constraints:

The operational limitations on generators, transformers, and shunt devices, as well as the security requirements on lines and load buses, constitute inequality constraints.

- Generator constraints: The boundary limits of real and reactive powers and the voltage magnitude of the generator buses are expressed as follows:

$$P_{TGi}^{min} \le P_{TGi} \le P_{TGi}^{max}; i = 1,2,\dots N_{TG} \tag{6.7}$$

$$P_{WGi}^{min} \le P_{WGi} \le P_{WGi}^{max}; i = 1,2,\dots N_{WG} \tag{6.8}$$

$$P_{SGi}^{min} \le P_{SGi} \le P_{SGi}^{max}; i = 1,2,\dots N_{SG} \tag{6.9}$$

$$P_{PEVGi}^{min} \le P_{PEVGi} \le P_{PEVGi}^{max}; i = 1,2,\dots N_{PEV} \tag{6.10}$$

$$Q_{TGi}^{min} \le Q_{TGi} \le Q_{TGi}^{max}; i = 1,2,\dots N_{TG} \tag{6.11}$$

$$Q_{WGi}^{min} \le Q_{WGi} \le Q_{WGi}^{max}; i = 1,2,\dots N_{WG} \tag{6.12}$$

$$Q_{SGi}^{min} \leq Q_{SGi} \leq Q_{SGi}^{max}; i = 1,2, \dots N_{SG} \quad (6.13)$$

$$V_{Gi}^{min} \leq V_{Gi} \leq V_{Gi}^{max}; i = 1,2, \dots N_{G} \quad (6.14)$$

- Shunt VAR compensator constraints: The following are the boundary values for shunt compensators:

$$Q_{Ci}^{min} \leq Q_{Ci} \leq Q_{Ci}^{max}; i = 1,2, \dots N_{C} \quad (6.15)$$

- Transformer constraints: The ideal operating limits for tap settings on a transformer are given as follows:

$$T_{i}^{min} \leq T_{i} \leq T_{i}^{max}; i = 1,2, \dots N_{T} \quad (6.16)$$

- Security constraints: The voltage limits of the load buses and the apparent power value of each transmission line, which can be restricted by its maximum capacity, are given as follows:

$$V_{Li}^{min} \leq V_{Li} \leq V_{Li}^{max}; i = 1,2, \dots N_{PQ} \quad (6.17)$$

$$|S_{li}| \leq S_{li}^{max}; i = 1,2, \dots N_{L} \quad (6.18)$$

where N_C,and N_T is the number of shunt compensators and transformers respectively; S_{li} and S_{li}^{max} are the apparent power flow and its maximum limit of i^{th} line; P_{Gi}^{min},P_{Gi}^{max} are the real power generation limits; Q_{Gi}^{min},Q_{Gi}^{max} are the reactive power generation limits; V_{Gi}^{min},V_{Gi}^{max} are the generator bus voltage limits; T_{i}^{min},T_{i}^{max} are the transformer tap limits; Q_{Ci}^{min},Q_{Ci}^{max} are the shunt compensator limits; V_{Li}^{min}, $V_{Li}^{max}$are the load bus voltage limits;

Two equality constraints Eq. (6.5) and Eq. (6.6) are automatically satisfied when the power flow converges to an optimal solution. The generator buses' real power (excluding slack bus), transformer tap ratios, voltage limits, and shunt compensator ranges are considered to control variables that are self-limiting. The remaining inequality constraints require constraint handling techniques.

In OPF, generator reactive power capacities are significant. In recent years, WECSs with complete reactive power capability has become commercially viable [60]. WECS can deliver reactive power in the range of -0.4p.u.to 0.5p.u. The negative sign signifies the generator's ability to absorb. Rooftop solar PV is designed as load buses with zero reactive power. However, because utility-based Solar PVs have built-in converters, full generator modeling is required due to the converters' dynamic behavior [61]. In this study, the reactive power capabilities of SPVS are assessed between -0.4p.u and 0.5p.u.

6.3 Constraint Handling Method

Since MOOPF is a constrained optimization problem, it requires a better-constrained handling method. In this work, the SF technique [62] was employed to solve the MOOPF problem with RESs. The steps followed when comparing two solutions are as follows:

1) While comparing two non-feasible solutions, the solution having the smallest constraint violation is selected.
2) When two feasible solutions are compared, the one with a better fitness solution is selected.
3) When a feasible solution is compared to a non-feasible solution, the feasible solution is selected.

Comparing non-feasible solutions based on constraint violation helps push non-feasible answers into the feasible region while comparing viable solutions based on the fitness value enables solution quality to be improved.

6.4 Integration of WECS, SPVS, and PEV Sources

6.4.1 WECS, SPVS, and PEV Modeling

a) WECS Modeling:

The wind speed at a given geographical area is most likely distributed according to Weibull PDF as given below:

$$f(v) = \left(\frac{k}{c}\right)\left(\frac{v}{c}\right)^{(k-1)} (e)^{\left(\frac{-v}{c}\right)^k}; 0 < v < \infty \tag{6.19}$$

where v is the wind speed (m/sec); $k,$ and c is the shape, and scale factors respectively.

The PDFs for two different shape and scale factors are given in [63]. The relationship between wind speed and power generation is as follows:

$$P_w(v) = \begin{cases} 0; v < v_{in} \; and \; v > v_{out} \\ P_{wr}\left(\frac{v - v_{in}}{v_r - v_{in}}\right) \quad ; \; v_{in} \le v_w \le v_r \\ P_{wr}; \; v_r < v_w \le v_{out} \end{cases} \tag{6.20}$$

where P_{wr} is the rated wind power; v_{in}, v_{out}, v_r are the cut-in, cut-out, and rated wind speeds (m/sec) respectively;

The probability of obtaining a zero and rated power output is given by the following:

$$f_w(P_w = 0) = 1 - e^{\left(-\left(\frac{v_{in}}{c}\right)^k\right)} + e^{\left(-\left(\frac{v_{out}}{c}\right)^k\right)} \tag{6.21}$$

$$f_w(P_w = P_{wr}) = e^{\left(-\left(\frac{v_r}{c}\right)^k\right)} + e^{\left(-\left(\frac{v_{out}}{c}\right)^k\right)} \tag{6.22}$$

The probability for the linear part of the wind speed is given by the following:

$$f_w(P_w) = \left(\frac{k(v_r - v_{in})}{cP_{wr}}\right)\left(\frac{v_{in}P_{wr} + P_w(v_r - v_{in})}{cP_{wr}}\right)^{(k-1)} e^{\left(-\left(\frac{v_{in}P_{wr} + P_{wr}(v_r - v_{in})}{cP_{wr}}\right)^k\right)} \tag{6.23}$$

b) SPVS Modeling:

Similarly, the power output of an SPVS is a factor of solar irradiance and it likely follows the Lognormal PDF [64] as follows:

$$f_G(G_s) = \frac{1}{G_S\sigma\sqrt{2\pi}} e^{\left\{\frac{-(\ln G_S-\mu)^2}{2\sigma^2}\right\}}; G_S > 0 \quad (6.24)$$

where μ and σ are the mean and standard deviation respectively; G_s is the solar irradiance (W/m^2).

The SPVS unit's solar irradiance to energy generation is as follows [65]:

$$P_S(G_S) = \begin{cases} P_{sr}\left(\frac{G_S^2}{G_{std}R_c}\right) & ; 0 < G_S < R_c \\ P_{sr}\left(\frac{G_S}{G_{std}}\right) & ; G_S \geq R_c \end{cases} \quad (6.25)$$

where G_{std} is the standard solar irradiance (W/m^2); R_c is the particular irradiance point (W/m^2); P_{sr} is the SPVS-rated power output.

c) PEV Modeling:

In recent days, public transport electric vehicles ply most of the time during the day and are charged during off-peak periods and so are not suitable for V2G application. Privately-owned PEVs are generally idle most of the time during the day and hence PEVs are suitable for the vehicle-to-grid (V2G) power-fed capability. The availability of electric vehicles as V2G source follows the normal PDF as follows [69]:

$$f_{pev} = \frac{1}{\sqrt{2\pi\varphi^2}} e^{-\left\{\frac{(P_{pev}-\mu)^2}{2\varphi^2}\right\}} \quad (6.26)$$

where μ and φ are the mean and standard deviation of normal PDF respectively; P_{pev} is the available V2G power;

Here, the PEVs are used as a source of power feeding the grid through suitable infrastructure. The following assumptions are made regarding the use of PEV as a power source.

- All PEVs supply battery power to the power network through DC/AC inverter.
- All PEVs represent one big V2G charging/discharging station.
- V2G system acts as a power source controller.

Depending on the probability of PEVs availability, the direct, reserve, and penalty costs are calculated

6.4.2 Uncertainty cost calculation of WECS, SPVS, and PEV Sources

Since WECS, SPVS, and PEVS are intermittent, the Monte Carlo simulations are used to account for uncertainty and to calculate the uncertainty cost. The estimated cost for the

intermittency of WECS, SPVS, and PEVS powers is reflected in three ways: direct, reserve, and penalty costs. Whenever power is underestimated, extra unusable power is wasted; however, in practical power system applications, such power can be saved in an energy storage system and thus be counted as the reserve cost. The cost of overestimating power that is lower than the scheduled power is considered a penalty cost in the case of overestimation.

The direct cost of j^{th} WECS is as follows:

$$C_{w,j}(P_{ws,j}) = g_j P_{ws,j} \tag{6.27}$$

The direct cost of k^{th} SPVS is as follows:

$$C_{w,k}(P_{ss,k}) = h_k P_{ss,k} \tag{6.28}$$

The direct cost of n^{th} PEV unit is as follows:

$$C_{pev,n}(P_{pevs,n}) = d_n P_{pevs,n} \tag{6.29}$$

where $P_{ws,j}$, $P_{ss,k}$, and $P_{pevs,n}$ are the scheduled powers of j^{th} WECS, k^{th} SPVS, and n^{th} PEVS respectively; g_j, h_k, and d_n are the direct cost coefficients of j^{th} WECS, k^{th} SPVS, and n^{th} PEV systems respectively;

The approach to calculating the over and underestimation cost of WECS is as follows [66].

The reserve cost of the j^{th} WECS is as follows:

$$C_{Rw,j}(P_{ws,j} - P_{wav,j}) = K_{Rw,j}(P_{ws,j} - P_{wav,j}) = K_{Rw,j}\int_0^{P_{ws,j}} (P_{ws,j} - p_{w,j}) f_w(p_{w,j}) dp_{w,j} \tag{6.30}$$

The penalty cost of the j^{th} WECS is as follows:

$$C_{Pw,j}(P_{wav,j} - P_{ws,j}) = K_{Pw,j}(P_{wav,j} - P_{ws,j}) = K_{Pw,j}\int_{P_{ws,j}}^{P_{wr,j}} (P_{w,j} - p_{ws,j}) f_w(p_{w,j}) dp_{w,j} \tag{6.31}$$

where $K_{Rw,j}$ and $K_{Pw,j}$ are the reserve and penalty cost coefficients of j^{th} WECS respectively; $P_{wr,j}$ and $P_{wav,j}$ are rated and actually available powers of j^{th} WECS; $f_w(p_{w,j})$ be the possibility of j^{th} WECS.

The approach to calculating the over and underestimation cost of SPVS is as follows [67].

The reserve cost for k^{th} SPVS is as follows:

$$\begin{aligned} C_{Rs,k}(P_{ss,k} - P_{sav,k}) &= K_{Rs,k}(P_{ss,k} - P_{sav,k}) \\ &= K_{Rs,k} * f_s(P_{sav,k} < P_{ss,k}) * [P_{ss,k} - E(P_{sav,k} < P_{ss,k})] \end{aligned} \tag{6.32}$$

The penalty cost for a k^{th} SPVS is as follows:

$$C_{Ps,k}(P_{sav,k} - P_{ss,k}) = K_{Ps,k}(P_{sav,k} - P_{ss,k}) = K_{Ps,k} * f_s(P_{sav,k} > P_{ss,k}) * [E(P_{sav,k} > P_{ss,k}) - P_{ss,k}] \quad (6.33)$$

where $K_{Rs,k}$ and $K_{Ps,k}$ are the reserve and penalty cost constants of k^{th} SPVS respectively; $P_{sav,k}$ is the actual available power of k^{th} SPVS; $f_s(P_{sav,k} < P_{ss,k})$ and $f_s(P_{sav,k} > P_{ss,k})$ are the probabilities of SPVS power; $E(P_{sav,k} < P_{ss,k})$, $E(P_{sav,k} > P_{ss,k})$ are the expectations of SPVS power.

The approach to calculating the over and underestimation cost of PEVS is as follows [70, 71]. Reserve cost associated with n^{th} PEV is defined as:

$$C_{Rpev,n}(P_{pevs,n} - P_{pevav,n}) = K_{Rpev,n}(P_{pevs,n} - P_{pevav,n}) = K_{Rpev,n} \int_0^{P_{pevs,n}} (P_{pevs,n} - p_{pev,n}) f_{pev}(p_{pev,n}) dp_{pev,n} \quad (6.34)$$

Penalty cost associated with n^{th} PEVS is defined as:

$$C_{Ppev,n}(P_{pevav,n} - P_{pevs,n}) = K_{Ppev,n}(P_{pevav,n} - P_{pevs,n}) = K_{Ppev,n} \int_{P_{pevs,n}}^{P_{pevr,n}} (p_{pev,n} - P_{pevs,n}) f_{pev}(p_{pev,n}) dp_{pev,n} \quad (6.35)$$

where $K_{Rpev,n}$ and $K_{Ppev,n}$ are the reserve and penalty cost constants of n^{th} PEVS respectively; $P_{pevr,n}$ and $P_{pevav,n}$ are the rated and actually available powers of n^{th} PEVS; $f_{pev}(p_{pev,n})$ is the n^{th} PEVS power probability. $f_{pev}(p_{pev,n})$ is the n^{th} PEVS power probability.

6.5 Proposed Method

In this chapter, the modified IWO [73] for multi-objective optimization and then include in MOEA/D [53], which provides a decomposition-based multi-objective optimization method with invasive weed colonies, to merge their exceptional qualities in the proposed hybrid method. The flowchart of the proposed method is shown in Figure 6.1.

The proposed method decomposes a multi-objective issue into a large number of scalar optimization sub-problems and solves them simultaneously. In each sub-problem, an adaptive IWO search was used to minimize the aggregation function of all objectives under consideration. Each sub-problem has a unique aggregation weight that generates a distinct aggregation function from those of others. The population size at each generation is equal to the number of decomposed sub-problems. If *N* is specified as the population size, then *N* sub-problems must be simultaneously optimized. The objective function of i^{th} sub-problem can be expressed as follows.

$$g^{te}(x|\lambda^i, z^*) = max\{\lambda_j^i | f_j(x) - z_j^*|\}; 1 \le j \le m \quad (6.36)$$

Where $\lambda^i = \left(\lambda_1^i, \lambda_2^i, \dots \lambda_m^i\right)^T$, m is the number of objectives and $z^* = (z_1^*, z_2^*, \dots z_m^*)^T$, $z_i^* = min\{f_i(x) | x \in [l, u]\}, i = 1,2, \dots m$ is the point of reference.

The proposed method steps are as follows:

Input: N: population size;
T: neighborhood size, $0 < T < N$;
$\lambda^1, \lambda^2, \dots \lambda^N$: weight vectors;
Output: PO solutions;

1. Initialization:
2. $x^1, x^2, \dots x^N$ is randomly selected between $[l, u]$ $FV^j = F(x^j)$;
3. For each $j = 1: N$ *do* $neb(j) = \{a, b, \dots t\}$;
4. reference point $z = (z_1, z_2, \dots z_m)^T$.
5. Do while (loop is not met)
6. For $j = 1: N$
7. $U \leftarrow IWO\left(x^j, std_{iter}^j\right)$;
8. $V \leftarrow IWO\left(x^k, std_{iter}^k\right)$;
/ k is chosen from $neb(j)$ /
9. For each $y \in U \cup V$ do
10. If $y \notin [l, u]$ then
11. y repair (y);
12. End
13. For each $i = 1$ *to* m do
14. If $z_i > f_i(y)$ then
15. $z_i = f_i(y)$;
16. End
17. End
18. For each $i \in neb(j)$ do
19. If $g^{te}\left(y|\lambda^i, z\right) < g^{te}\left(x^i|\lambda^i, z\right)$then
20. $x^i = y$;
21. $FV^i = F(y)$;
22. End
23. End
24. End
25. End
26. End Do
27. Use fuzzy theory to get best-compromised values [55].

In line 7 of the pseudo-code, $U \leftarrow IWO\left(x^i, std_{iter}^i\right)$expresses the procedure of producing x^i seeds. U Contains the children's seeds generated byx^i. Suppose$U = \{y^1, y^2, \dots y^k\}$; then k is the size of children seeds generated byx^i, which is calculated using Eq. (6.37).

$$S_{num} = floor\left(\frac{g_{max}^{te} - g^{te}}{g_{max}^{te} - g_{min}^{te}}(S_{max} - S_{min}) + S_{min}\right) \tag{6.37}$$

where g_{min}^{te}, $g_{max}^{te}$are obtained as follows:

$$g_{min}^{te} = min\left\{g^{te}\left(x^k\middle|\lambda^i, z^*\right)\middle|\, x^k \in B(i)\right\} \tag{6.38}$$

$$g_{max}^{te} = max\{g^{te}(x^k|\lambda^i, z^*)|\ x^k \in B(i)\} \tag{6.39}$$

where std_{iter}^{i} represents the adaptive standard deviation (SD) of x^i and its value can be obtained through Eq. (6.40) and Eq. (6.41).

$$\sigma_{iter} = \sigma_{final} + \left(\frac{iter_{max}-iter}{iter_{max}}\right)^{pow} . (\sigma_{initial} - \sigma_{final}) \tag{6.40}$$

It is evident from Eq. (6.40) that σ_{iter} reduces with increasing iterations. However, for each parent seed in a single generation, the value σ_{iter}remains constant. This does not promote exploration or efficient exploration. Each parent should have weed characteristics that are distinct from those of other parents. In this study, an adaptive standard deviation (SD) $std_{iter}$was employed, whose σ_{iter} value fluctuates with iteration and rank. The SD can be characterized as follows:

$$std_{iter} = \begin{cases} \left(1 + Q\,\frac{g^{te}-g_{mean}^{te}}{g_{max}^{te}-g_{mean}^{te}}\right) * \sigma_{iter}; & g^{te} \geq g_{mean}^{te} \\ \left(1 - Q\,\frac{g_{mean}^{te}-g^{te}}{g_{mean}^{te}-g_{min}^{te}}\right) * \sigma_{iter}; & otherwise \end{cases} \tag{6.41}$$

Where $g_{mean}^{te}$is formulated as follows:

$$g_{mean}^{te} = \frac{\sum\{g^{te}(x^k|\ \lambda^i, z^*)|\ x^k \in B(i)\}}{|B(i)|} \tag{6.42}$$

Where g^{te} be the value of the weed's aggregated scalar function, $g_{min}^{te}, g_{max}^{te}$ and g_{mean}^{te} are the lowest, highest, and mean values of weeds in the present iteration respectively, and Q is the regulatory parameter whose value ranges from 0 to 0.5. $|B(i)|$ is the number of neighbors of i^{th} sub-problem. Similarly, the same model was applied to the neighbors of x^i in line 8 of the algorithm.

Let $x^i = (x_1^i, x_2^i, \ldots x_n^i)^T$ is the i^{th} parent individual, $y = (y_1, y_2, \ldots y_n)^T$ are the seeds generated byx^i; where each element y_j is produced as follows:

$$y_j = x_j^i + N(0, std_{iter}^2); j = 1,2, \ldots n. \tag{6.43}$$

Then the trade-off objective optimal value is selected using the fuzzy method [56].

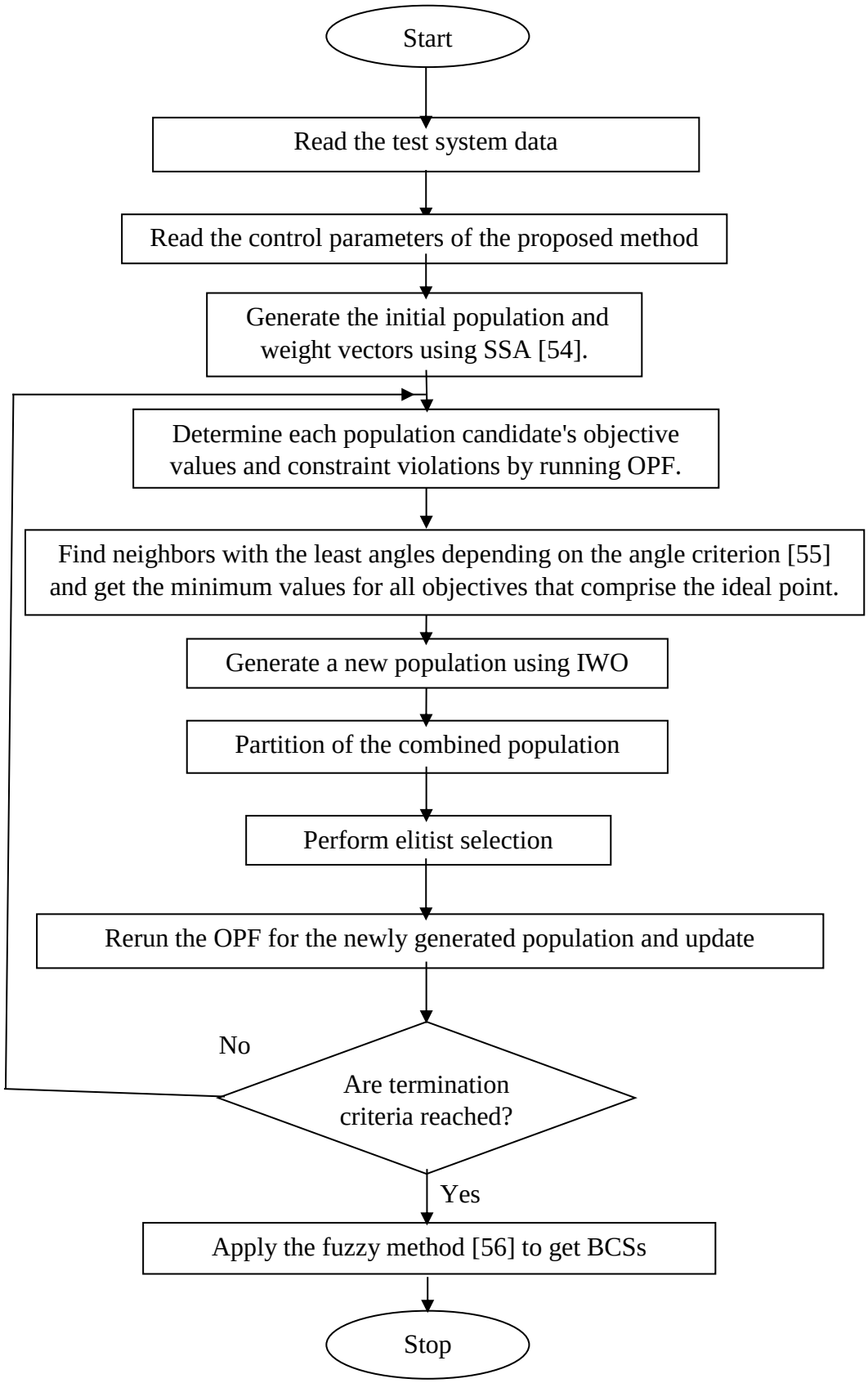

Fig.6.1: Flowchart of the proposed method

6.6 Results and Discussions

To analyze the robustness and efficacy of the suggested method, IEEE 57-bus and 118-bus systems were taken into account. The proposed method was implemented in MATLAB R2016a, and simulations were conducted over an i3-Processor having 4 GB RAM. To verify the efficacy of the proposed method, comparisons were made with NSGA-II [57] and MOPSO [58]. In this work, the stochastic nature of WECS, SPVS, and PEV sources was taken into account to study the impact of these sources on the MOOPF problem. To consider uncertainties, Monte-Carlo simulations were used to generate 1000 samples. The control parameters of the proposed method, NSGA-II, and MOPSO are given in Table 6.1. The various cases considered are given in Table 6.2. The description of the test systems was given in Table 6.3. PDF specifications and cost components of various sources are given in Table 6.4.

Table 6.1: Control parameters of the proposed method, NSGA-II, and MOPSO.

S. No.	Method	Control parameters
1.	**Proposed method**	***N* =100, *D* =12, *T* =20, P_c =1.0, P_m =0.05, max. iterations=100.**
2.	NSGA-II [57]	N =100, P_c =0.8, P_m =0.01, and max. iterations=100.
3.	MOPSO [58]	N =100, $C1$= $C2$= 2, W=0.5, and max. iterations=100.

Table 6.2: Various cases considered.

S. No.	Test Systems	Case #	J_1	J_2	J_3	J_4
1.	IEEE 57-bus system	Case 1	✓	✓	--	--
		Case 2	✓	✓	✓	--
		Case 3	✓	✓	✓	✓
2.	IEEE 118-bus system	Case 4	✓	--	✓	--
		Case 5	✓	--	✓	✓

Table 6.3: Test systems description.

Specifications	IEEE 57-bus system		IEEE 118-bus system	
Buses	57	[59]	118	[59]
Lines	80		186	
Thermal units	7	Buses:1,2,3,6,8,9 and 12	54	Buses: [59]
Slack bus	1	Bus:1	69	Bus: 69
Transformer tap positions	17	Lines:19,20,31,35,36,37,41,46, 54,58,59,65,66,71,73,76, and 80	9	Lines: 8,32,36, 51, 93,95,102,107 and 127
Shunt capacitors	3	Buses:18,25, and 53	12	Buses:34,44,45,46,48,74,79,82, 83, 105, 107 and 110
Control variables	36	Generator bus real powers (9) + voltages (7) + transformer tap settings (17) + shunt capacitor (3).	131	Generator bus real powers (56) + voltages (54) + transformer tap settings (9) + shunt capacitor (12).
Load	-	1250.8MW, 336.4MVAR	-	4242.0MW, 1439.0MVAR
WECS	1	45 #bus	1	81 #bus
SPVS	1	16 #bus	1	64 #bus
PEVS	1	49 #bus	1	117 #bus

Table 6.4: PDF specifications and cost components of various sources.

S. No.	Specifications	WECS	SPVS	PEVS
1.	PDF	Weibull	Lognormal	Normal
2.	Parameters	c =10, k =2, v_{in}=10m/sec, v_{out}=12m/sec, v_r=12m/sec	μ =6, σ = 0.6, G_{std}=800 W/m^2 , R_c=120 W/m^2	μ = 3.2, φ = 0.88
3.	Direct cost coefficient ($/MW)	1.75	1.60	1.60
4.	Reserve cost coefficient ($/MW)	3	3	3
5.	Penalty cost coefficient ($/MW)	1.5	1.5	1.5

6.6.1 IEEE 57-bus system

The IEEE 57-bus system [59] was investigated to demonstrate the performance of the proposed method for solving the MOOPF problem. The information about the IEEE 57-bus system incorporating WECS, SPVS, and PEV sources used is given in Table 6.3. Notably, the locations of these sources were chosen from [74], by replacing load buses with the respective WECS, SPVS, and PEV sources.

a) Case-1: Minimize J_1, and J_2 simultaneously

In this case, the proposed method was simulated by considering two objectives J_1 and J_2. The Pareto-optimal fronts (PFs) observed are depicted in Figure 6.2. The optimal decision variables obtained by the proposed method are presented in Table 6.5. The proposed method obtains a total generation cost of **35780.28$/h**, and emission of **0.8702ton/h**. NSGA-II [57] gives 35850.00$/h, 0.9928ton/h and MOPSO [58] gives 35910.00$/h, 1.0120ton/h respectively as shown in Table 6.6.

b) Case-2: Minimize J_1, J_2, and J_3 simultaneously

In this case, the proposed method was simulated by considering three objectives J_1, J_2, and J_3. The Pareto-optimal fronts (PFs) observed are depicted in Figure 6.2. The optimal decision variables obtained by the proposed method are presented in Table 6.5. The proposed method obtains a total generation cost of **36111.28$/h**, emission of **0.9568ton/h,** and active power loss of **10.3543MW**. NSGA-II [57] gives 36336.00$/h, 1.2498ton/h, 11.0813MW and MOPSO [58] gives 36402.69$/h, 1.0450ton/h, 12.5591MW respectively as shown in Table 6.6.

c) Case-3: Minimize J_1, J_2, J_3, and J_4 simultaneously

In this case, the proposed method was simulated by considering four objectives J_1, J_2, J_3, and J_4. The optimal decision variables obtained by the proposed method are presented in Table 6.5. The proposed method obtains a total generation cost of **36340.27$/h**, emission of **1.1009ton/h**, active power loss of **10.9504MW**, and voltage magnitude deviation of **0.8519p.u.** NSGA-II

[57] gives 36250.00$/h, 1.4175ton/h, 12.3871MW, 1.0481p.u. and MOPSO [58] gives 36662.59$/h, 0.9367ton/h, 14.1833MW, 1.0669p.u. respectively as shown in Table 6.6.

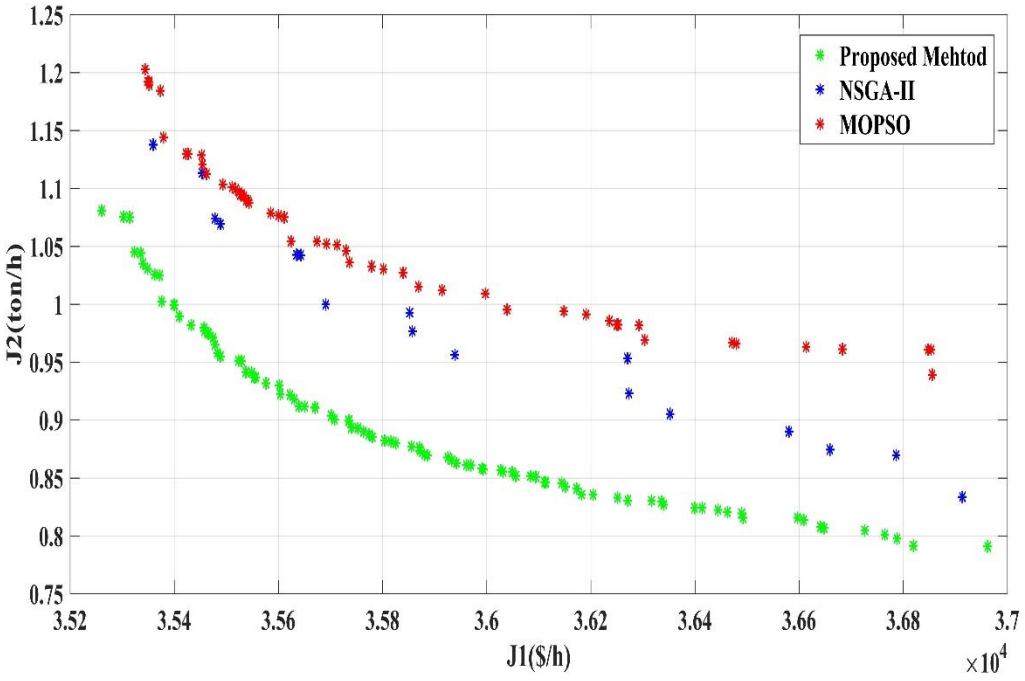

(a)

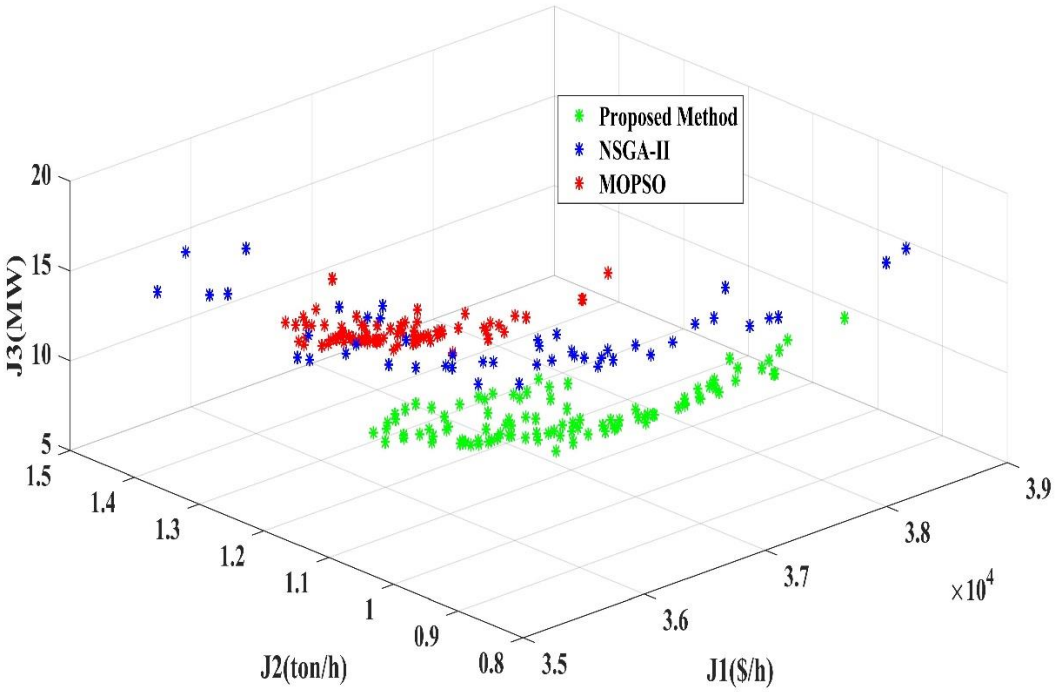

(b)

Fig. 6.2: IEEE 57-bus system: Pareto-optimal fronts. a) Case-1, and b) Case-2.

Table 6.5: IEEE 57-bus system: Optimal control variables obtained by the proposed method.

S. No.	Control variables	Limits		Case-1	Case-2	Case-3
		min	max			
1.	P2	0	100	98.6033	74.3511	66.6157
2.	P3		140	68.1994	84.8910	73.7500
3.	P6		100	94.1666	76.8214	64.6217
4.	P8		550	302.9663	306.6662	343.0574
5.	P9		100	97.5424	96.5544	86.5482
6.	P12		410	281.1485	323.7556	333.9688
7.	P45		80	79.8163	76.7799	64.5531
8.	P16		80	79.6213	77.8880	76.2239
9.	P49		20	19.0489	20.0000	12.9058
10.	V1	0.95	1.1	1.0336	1.0292	1.0217
11.	V2			1.0426	1.0307	1.0395
12.	V3			1.0359	1.0209	1.0209
13.	V6			1.0238	1.0152	1.0068
14.	V8			1.0281	1.0278	1.0267
15.	V9			1.0301	1.0322	1.0334
16.	V12			0.9964	1.0293	1.0281
17.	T19	0.9	1.1	0.9699	1.0169	0.9913
18.	T20			1.0061	0.9466	0.9981
19.	T31			0.9952	1.0297	1.0208
20.	T35			1.0185	1.0392	0.9834
21.	T36			0.9865	0.9587	1.0104
22.	T37			1.0302	1.0210	0.9945
23.	T41			0.9931	0.9793	1.0133
24.	T46			0.9980	0.9517	0.9548
25.	T54			0.9789	1.0221	0.9580
26.	T58			1.0155	0.9831	0.9625
27.	T59			0.9985	0.9873	0.9783
28.	T65			0.9916	0.9903	0.9809
29.	T66			0.9863	0.9828	0.9328
30.	T71			1.0063	0.9541	1.0035
31.	T73			1.0113	1.0138	0.9825
32.	T76			0.9938	0.9960	0.9718
33.	T80			0.9709	0.9940	1.0180
34.	QC18	0	20	9.4263	8.5916	8.6920
35.	QC25			7.8862	9.9315	10.1887
36.	QC53			9.5980	8.2526	7.1468
1.	**J_1($/h)**	**-**	**-**	**35780.28**	**36111.28**	**36340.27**
2.	**J_2(ton/h)**	**-**	**-**	**0.8702**	**0.9568**	**1.1009**
3.	**J_3(MW)**	**-**	**-**	**-**	**10.3543**	**10.9504**
4.	**J_4(p.u.)**	**-**	**-**	**-**	**-**	**0.8519**

Table 6.6: IEEE 57-bus system: Comparison of the proposed method.

Case #	Objective functions	**Proposed method**	NSGA-II [57]	MOPSO [58]
Case-1	J_1($/h)	**35780.28**	35850.00	35910.00
	J_2(ton/h)	**0.8702**	0.9928	1.0120
Case-2	J_1($/h)	**36111.28**	36336.00	36402.69
	J_2(ton/h)	**0.9568**	1.2498	1.0450
	J_3(MW)	**10.3543**	11.0813	12.5591
Case-3	J_1($/h)	**36340.27**	36250.00	36662.59
	J_2(ton/h)	**1.1009**	1.4175	0.9367
	J_3(MW)	**10.9504**	12.3871	14.1833
	J_4(p.u.)	**0.8519**	1.0481	1.0669

6.6.2 IEEE 118-bus system

The IEEE 118-bus system [59] was considered to demonstrate the efficacy of the proposed method on a big system. The information about the IEEE 118-bus system incorporating WECS, SPVS, and PEV sources used is given in Table 6.3. Notably, the locations of these sources were chosen from [74], by replacing load buses with the respective WECS, SPVS, and PEV sources.

a) Case-4: Minimize J_1, and J_3 simultaneously

In this case, the proposed method was simulated by considering two objectives J_1, and J_3. The Pareto-optimal fronts (PFs) observed are depicted in Figure 6.3. The optimal decision variables obtained by the proposed method are presented in Table 6.7. The proposed method obtains a total generation cost of **127890.61$/h**, and an active power loss of **33.3705MW**. NSGA-II [57] gives 129582.23$/h, 37.3464MW and MOPSO [58] gives 130673.5$/h, 38.0368MW respectively as shown in Table 6.8.

b) Case-5: Minimize J_1, J_3, and J_4 simultaneously

In this case, the proposed method was simulated by considering three objectives J_1, J_3, and J_4. The Pareto-optimal fronts (PFs) observed are depicted in Figure 6.3. The optimal decision variables obtained by the proposed method are presented in Table 6.7. The proposed method obtains a total generation cost of **130749.11$/h**, active power loss of **38.2259MW,** and voltage magnitude deviation of **0.4511p.u.** NSGA-II [57] gives 134395.5$/h, 40.0724MW, 0.6876p.u. and MOPSO [58] gives 133574.6$/h, 41.3020MW, 0.9706p.u. respectively as shown in Table 6.8.

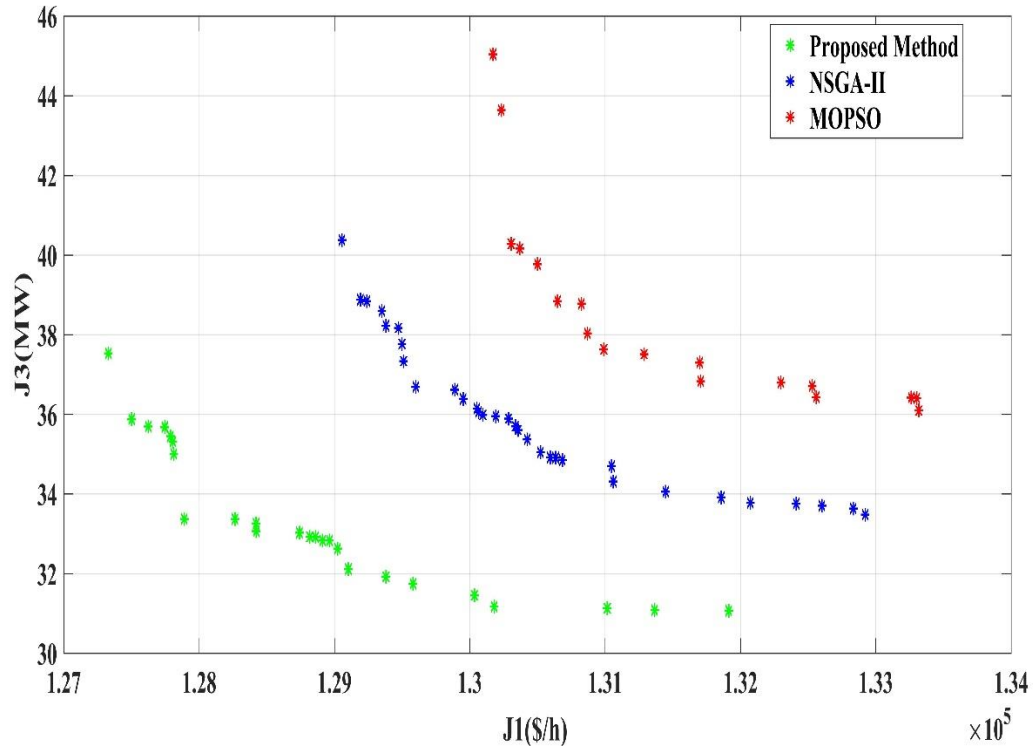

(a)

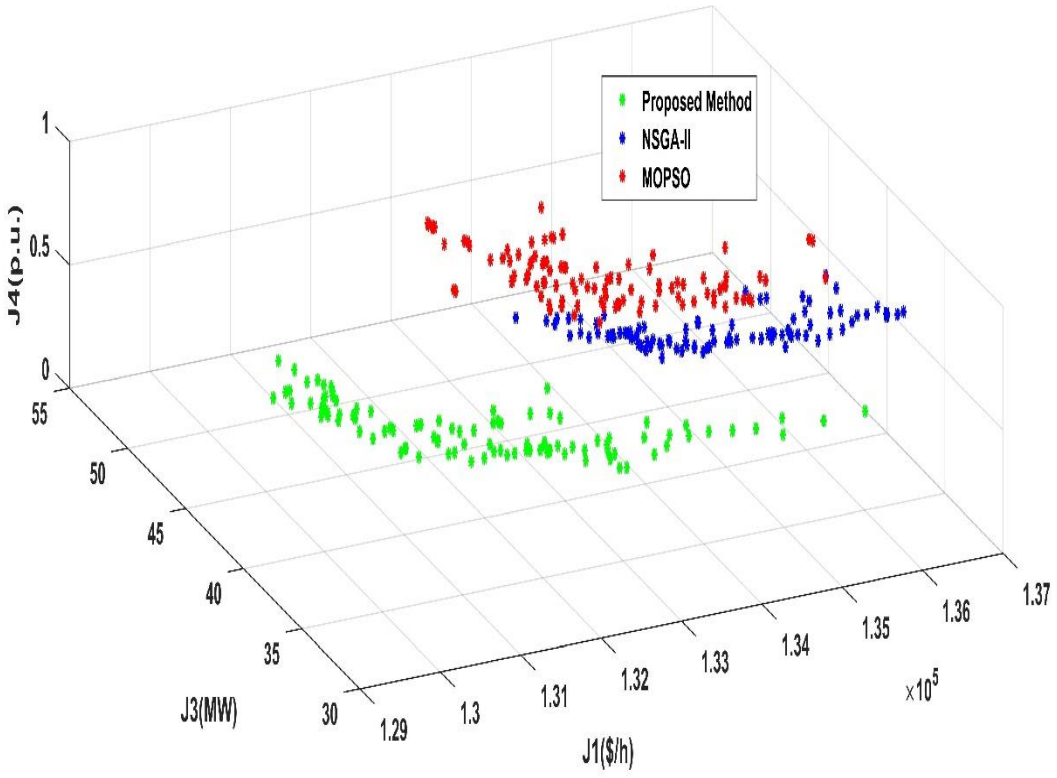

(b)

Fig. 6.3: IEEE 118-bus system: Pareto-optimal fronts. a) Case-4, and b) Case-5.

Table 6.7: IEEE 118-bus system: Optimal control variables obtained by the proposed method.

S. No.	Control variables	Limits		Case-4	Case-5	S. No.	Control variables	Limits		Case-4	Case-5
		min	max					min	max		
1.	P1	0	100	55.9460	48.6240	68.	V26	0.95	1.1	1.0178	1.0307
2.	P4		100	39.0503	43.6199	69.	V27			1.0297	1.0318
3.	P6		100	56.3835	56.3541	70.	V31			1.0184	1.0121
4.	P8		100	54.5506	37.2383	71.	V32			1.0182	1.0019
5.	P10		550	173.927	181.510	72.	V34			1.0243	1.0045
6.	P12		185	67.0061	85.3627	73.	V3			1.0429	1.0027
7.	P15		100	48.2205	48.2502	74.	V40			1.0352	1.0122
8.	P18		100	45.9455	40.6351	75.	V42			1.0165	1.0207
9.	P19		100	51.4212	38.9266	76.	V46			1.0292	1.0287
10.	P24		100	45.6110	43.8313	77.	V49			1.0177	1.0110
11.	P25		320	88.1517	107.417	78.	V54			1.0228	1.0018
12.	P26		414	139.941	143.538	79.	V55			1.0168	1.0151
13.	P27		100	56.0018	53.8079	80.	V56			1.0154	1.0180
14.	P31		107	18.1830	10.9532	81.	V59			1.0193	1.0160
15.	P32		100	51.1361	44.4332	82.	V61			1.0296	1.0011
16.	P34		100	42.2086	53.2355	83.	V62			1.0245	1.0068
17.	P36		100	41.1170	51.3992	84.	V65			1.0144	1.0007
18.	P40		100	66.2173	43.2414	85.	V66			1.0162	1.0112
19.	P42		100	59.6259	64.8196	86.	V69			1.0250	1.0095
20.	P46		119	35.3173	53.9039	87.	V70			1.0266	1.0118
21.	P49		304	142.501	162.688	88.	V72			0.9897	1.0338
22.	P54		148	85.1966	79.4450	89.	V73			1.0493	1.0116
23.	P55		100	43.7812	46.0740	90.	V74			1.0115	1.0220
24.	P56		100	73.7154	64.3958	91.	V76			1.0384	1.0181
25.	P59		255	142.951	121.802	92.	V77			1.0260	1.0069
26.	P61		260	112.737	102.575	93.	V80			1.0323	1.0154
27.	P62		100	32.7737	33.4058	94.	V85			1.0222	1.0083
28.	P65		491	219.553	185.720	95.	V87			1.0175	1.0229
29.	P66		492	210.691	173.373	96.	V89			1.0459	1.0158
30.	P70		100	44.5214	39.1977	97.	V90			1.0331	1.0215
31.	P72		100	28.1889	38.9919	98.	V91			1.0313	1.0356
32.	P73		100	45.6510	33.4913	99.	V92			1.0322	1.0073
33.	P74		100	52.7319	54.0390	100.	V99			1.0288	1.0398
34.	P76		100	57.4716	59.8387	101.	V100			1.0363	1.0168
35.	P77		100	49.0969	49.5707	102.	V103			1.0262	1.0155
36.	P80		577	264.626	215.734	103.	V104			1.0230	1.0330
37.	P85		100	38.1422	53.5711	104.	V105			1.0227	1.0089
38.	P87		104	9.2807	8.5961	105.	V107			1.0192	1.0293
39.	P89		707	226.574	247.730	106.	V110			1.0160	1.0135
40.	P90		100	44.6105	47.3346	107.	V111			1.0152	1.0249
41.	P91		100	45.9099	42.2742	108.	V112			1.0099	1.0278
42.	P92		100	35.3494	34.6101	109.	V113			1.0405	1.0139
43.	P99		100	38.3796	53.0877	110.	V116			1.0306	1.0077
44.	P100		352	136.606	150.785	111.	T8	0.9	1.1	0.9871	1.0178
45.	P103		140	56.5448	47.0893	112.	T32			0.9952	1.0190
46.	P104		100	33.6492	60.5636	113.	T36			0.9914	0.9827
47.	P105		100	56.5368	30.3130	114.	T51			1.0251	0.9933
48.	P107		100	28.6504	58.8769	115.	T93			1.0069	1.0144
49.	P110		100	52.2132	35.2832	116.	T95			0.9791	0.9795
50.	P111		136	32.2479	38.7994	117.	T102			1.0044	0.9924
51.	P112		100	25.2790	44.2174	118.	T107			0.9813	0.9928
52.	P113		100	23.7058	44.1563	119.	T127			1.0172	0.9870

53.	P116		100	46.6905	45.1908	120.	QC34			11.6919	13.8154
54.	P81		150	116.444	139.032	121.	QC44			11.2106	10.0945
55.	P64		150	126.922	104.668	122.	QC45			14.6353	15.2303
56.	P117		40	19.4935	21.7456	123.	QC46			9.9899	12.5583
57.	V1			1.0190	1.0200	124.	QC48			11.2227	10.7383
58.	V4			1.0210	1.0063	125.	QC74			17.2265	13.3213
59.	V6			1.0217	1.0128	126.	QC79	0	25	12.3653	12.9234
60.	V8			1.0246	1.0092	127.	QC82			7.8219	14.5555
61.	V10			1.0313	0.9973	128.	QC83			9.2042	11.3947
62.	V12			1.0286	1.0310	129.	QC105			10.8933	17.0364
63.	V15			1.0220	1.0048	130.	QC107			11.7149	11.3518
64.	V18			1.0210	1.0177	131.	QC110			11.1915	11.8901
65.	V19			1.0287	1.0345	**1.**	**J_1($/h)**	-	-	**127890.6**	**130749.1**
66.	V24			1.0250	1.0231	**2.**	**J_3(MW)**	-	-	**33.3705**	**38.2259**
67.	V25			0.9987	1.0055	**3.**	**J_4(p.u)**	-	-	**-**	**0.4511**

Table 6.8: IEEE 118-bus system: Comparison of the proposed method.

Case #	Objective functions	**Proposed method**	NSGA-II [57]	MOPSO [58]
Case-4	J_1($/h)	**127890.61**	129582.23	130673.5
	J_3(MW)	**33.3705**	37.3464	38.0368
Case-5	J_1($/h)	**130749.11**	134395.5	133574.6
	J_3(MW)	**38.2259**	40.0724	41.3020
	J_4(p.u.)	**0.4511**	0.6876	0.9706

6.7 Summary

This chapter introduced a solution to the MOOPF problem in a thermal, WECS, SPVS, and PEV integrated power system using hybrid MOEA based on decomposition and IWO methods. It also addressed the constraints of the MOOPF problem with the superiority of the feasible solution (SF) method. In conjunction with the minimization of emission, active power loss, and voltage magnitude deviation, the generation cost of thermal generators and the uncertainty cost of WECS, SPVS, and PEV systems were reduced. The unpredictability of WECS, SPVS, and PEV powers was assessed with Monte Carlo simulations. To illustrate the efficacy of the proposed technique, simulations were done on the IEEE 57-bus and IEEE 118-bus systems, and the results were compared with NSGA-II and MOPSO algorithms. The outcomes indicate that the proposed technique is much more reliable and superior to existing techniques.

Chapter 7

Conclusions

Chapter 7

Conclusions

In this thesis, the power system OPF problem was solved using new hybrid MOEAs. The thesis explored the new multi-objective frameworks such as decomposition-based MOEAs and their application to the MOOPF problem. Furthermore, stochastic WECS, SPVS, and PEV systems were integrated into the conventional OPF to study the impact of uncertainty. Since MOOPF is a constrained problem, in this thesis, effective constraint handling methods were proposed for solving the OPF problem. A fuzzy method was used to obtain the best-compromised solution among the solutions obtained. This chapter presents the important findings proposed through the research work and discusses future extensions of the proposed research work.

7.1 Summary of Important Findings

The following conclusions were arrived at from the research work carried out and reported in previous chapters of this thesis.

1) A new hybrid decomposition and local dominance-based MOEA was proposed for the OPF problem.
   - The MOOPF problem was modeled with four objectives: minimizing total generation cost, emission, active power loss, and voltage magnitude deviation.
   - The hybridization of decomposition and dominance methodologies increased the Pareto front's convergence and diversity of solutions.
   - The MOOPF problem constraints were handled using a static-penalty method, in which a penalty is imposed to the fitness of the infeasible solutions with this all infeasible solutions are discarded and only considers feasible ones, and this would help in achieving the global optimal solution.
   - The results of the proposed method were compared with NSGA-II and MOPSO and demonstrated on IEEE 57-bus and IEEE 118-bus systems.
2) A new hybrid decomposition and summation of normalized objectives with improved diversified selection-based MOEA were proposed for solving the OPF problem including the WECS, and SPVS uncertainty.
   - Integrating RESs like WECS and SPVS sources with conventional OPF to consider the impact of the uncertain nature of these sources. The uncertain nature of RESs was modeled using PDFs and their uncertainty cost was calculated using Monte-Carlo simulations.

- A new constraint handling method was adopted so that it enhances the quality of the solution and eliminates the parameter dependence in handling constraints.
- The proposed method was tested on IEEE 57-bus and IEEE 118-bus systems. The findings obtained demonstrate that the proposed strategy is superior to NSGA-II and MOPSO.

3) A novel hybrid decomposition and summation of normalized objectives with improved diversified selection-based MOEA was proposed for OPF problems including WECS, SPVS, and PEV system uncertainty.
   - The MOOPF problem was designed with four objectives: minimizing total generation cost, emission, active power loss, and voltage magnitude deviation.
   - A new constraint handling method was adopted so that it enhances the quality of the solution and eliminates the parameter dependence in handling constraints.
   - The impact of WECS, SPVS generation, as well as PEV uncertainties, was taken into account to validate the proposed method.
   - The proposed method was tested on IEEE 57-bus and IEEE 118-bus systems. The findings obtained demonstrate that the proposed strategy is superior to NSGA-II and MOPSO.
4) A new hybrid decomposition and invasive weed optimization (IWO) based MOEA was proposed for OPF including WECS, SPVS, and PEV system uncertainty.
   - The MOOPF problem was designed with four objectives: minimizing total generation cost, emission, active power loss, and voltage magnitude deviation.
   - A new constraint handling method was adopted so that it enhances the quality of the solution and eliminates the parameter dependence in handling constraints.
   - The impact of WECS, SPVS generation, as well as PEV uncertainties, was taken into account to validate the proposed method.
   - The proposed method was tested on IEEE 57-bus and IEEE 118-bus systems. The findings obtained demonstrate that the proposed strategy is superior to NSGA-II and MOPSO.

7.2 Scope of the Future Work

The present research can be extended for future research. The probable areas where research can be contemplated are:

- Big data, data analytics techniques, and machine learning methods can be used to model multi-objective framework design to adopt problem-specific and computationally complex problems like the MOOPF problems.
- To evaluate the efficacy of MOEAs for multi-objective optimization problems, other CHM such as epsilon constraint (EC), and stochastic ranking (SR) can be combined.
- To discover the best-compromised solutions, more sophisticated decision-making techniques may be utilized, such as the pseudo-weight method, and Lp metric.
- Future research will continue to focus on the dynamic optimal power flow (DOPF) problem, which takes into account the ramping rate of generators, variations in load needs across time, the stochastic character of all renewable sources, and all network restrictions.

References

[1] W. Warid, H. Hizam, N. Mariun, and N. I. A. Wahab. “A novel quasi-oppositional modified Jaya algorithm for multi-objective optimal power flow solutions.” Appl. Soft Comput., Vol. 65, pp. 360-373, 2018.

[2] E. Lobato, L. Rouco, M.I.Navarrete, R. Casanova, and G. Lopez. “An LP-based optimal power flow for transmission losses and generator reactive margin minimization.” IEEE Porto Power Tech Conference 10-13, Sept., Porto, Portugal, 2001.

[3] W. Yan, J. Yu, C.Y. David, and K. Bhattarai. “A new optimal reactive power flow model in rectangular form and its solution by a predictor-corrector primal-dual interior-point method.” IEEE Trans. Power Syst., Vol. 21, No. 1, pp. 61-67, 2006.

[4] H. W. Dommel, and W. F. Tinney. “Optimal power flow solutions.” IEEE Trans. Power Appar. Syst., Vol. 87, No. 10, pp. 1866-1876, 1968.

[5] C. Haiyan, C. Jinfu, and D. X. Zhong. “Multi-stage dynamic optimal power flow in wind power integrated system.” IEEE/PES Transmission and Distribution Conf. and Exhibition: Asia and Pacific, Dalian, China, pp. 1-5, 2005.

[6] Domingo, Pedro, M. P. M. “Optimal power flow including wind generation.” Instituto Superior Tecnico, Technical University of Lisbon, Potugal, pp. 1-10, 2012.

[7] D. Xiaoying, W. Xifan, S. Yonghua, and G. Jian. “The interior-point branch and cut method for optimal power flow.” IEEE Int. Conf. Power Syst. Tech., Vol. 1, pp. 651-655, 2002.

[8] X. Yan, and V. H. Quintana. “Improving an interior point based OPF by dynamic adjustments of step sizes and tolerances.” IEEE Trans. Power Syst., Vol. 14, No. 2, pp. 709-717, 1999.

[9] K. P. Wong, A. Li, and M. Y. Law. “Development of constrained-genetic algorithm load flow method.” IEE Gener. Transm. Distrb., Vol. 144, No. 2, pp. 91-99, 1997.

[10] J. Yuryevich, and K. P.Wong. “Evolutionary programming based optimal power flow algorithm.” IEEE Trans. Power Syst., Vol. 14, No. 4, pp. 1245-1250, 1999.

[11] S. Duman, J. Li, L.Wu, and N. Yorukeren. “Symbiotic organisms search algorithm-based security-constrained AC-DC OPF regarding uncertainty of wind, PV and PEV systems.” Soft Computing, Vol. 25, pp. 9389-9426, 2021.

[12] J. Sarda, K. Pandya, and K. Y. Lee. “Dynamic optimal power flow with cross entropy covariance matrix adaption evolutionary strategy for systems with electric vehicles and renewable generators.” Int. J. Energy Res., pp. 1-13, 2021.

[13] S. Duman, J Li, and L Wu. “AC optimal power flow with thermal-wind-solar-tidal systems using the symbiotic organisms search algorithm.” IET Renew. Power Gener. Vol. 15, pp. 278-296, 2021.

[14] H. J. Ben, T. Chambers, and J. Lee. “Solving constrained optimal power flow with renewables using hybrid modified imperialist competitive algorithm and sequential quadratic programming.” Elect. Power Syst. Research, Vol. 177, 105989, 2019.

[15] P. P. Biswas, P. N. Suganthan, and G. A. J. Amaratunga. “Optimal power flow solutions incorporating stochastic wind and solar power.” Energy Convers. Manage. Vol. 148: pp. 1194-1207, 2017.

[16] C. Mishra, S. P. Singh, and J. Rokadia."Optimal power flow in the presence of wind power using modified cuckoo search." IET Gener. Transm. Distrb., Vol. 9, No. 7, pp. 615-626, 2015.

[17] M. H. Sulaiman, Z. Mustaffa, A. J. Mohamad, M. M. Saari, and M. R. Mohamed. "Optimal power flow with stochastic solar power using barnacles mating optimizer." Int. Trans. Electr. Energy Syst., Vol. 66, pp. 88-93, 2021.

[18] D. H. Wolpert, and W. G. Macready. "No free lunch theorems for optimization." IEEE Trans. Evol. Comput., Vol. 1, No. 1, pp. 67-82, 1997.

[19] A. Trivedi, D. Srinivasan, K. Sanyal, and A. Ghosh. "A survey of multi-objective evolutionary algorithms based on decomposition." IEEE Trans. Evol. Comput., Vol. 21, No. 3, pp. 440-462, 2017.

[20] A. E. Chaib, H. R. E. H. Bouchekara, R. Mehasni, and M. A. Abido. "Optimal power flow with emission and non-smooth cost functions using backtracking search optimization algorithm." Int. J. Electr. Power Energy Syst., Vol. 81, pp. 64-77, 2016.

[21] A. A. A. Mohamed, Y. S. Mohamed, A. A. M. El-Gaafary, and A. M. Hemeida. "Optimal power flow using moth swarm algorithm." Electr. Power Syst. Research, Vol. 142, pp. 190-206, 2017.

[22] H. R. E. H. Bouchekana, A. E. Chaib, M. A. Abido, and R. A. El-Sehiemy. "Optimal power flow using an improved colliding bodies optimization algorithm." Appl. Soft Comput., Vol. 42, pp. 119-131, 2016.

[23] M. R. Adaryani, and A. Karami. "Artificial bee colony algorithm for solving multi-objective optimal power flow." Int. J. Electr. Power Energy Syst., Vol. 53, pp. 219-230, 2013.

[24] H. R. E. H. Bouchekana, M. A. Abido, and M. Boucherma. "Optimal power flow using teaching-learning-based optimization technique." Electr. Power Syst. Research, Vol. 144, pp. 49-59, 2014.

[25] M. A. Taher, S. Kamel, F. Jurado, and M. Ebeed. "An improved moth-flame optimization algorithm for solving optimal power flow problem." Int. Trans. Electr. Energy Syst., Vol. 29, No. 3, e2743, 2019.

[26] A. A. A. El Ela, M. A. Abido, and S. R. Spea. "Optimal power flow using differential evolution algorithm." Electr. Power Syst. Research, Vol. 80, No. 7, pp. 878-885, 2010.

[27] P. K. Roy, and C. Paul. "An improved moth-flame optimization algorithm for solving optimal power flow problem." Int. Trans. Electr. Energy Syst., Vol. 25, No. 8, pp. 1397-1419, 2015.

[28] A. Ozan. "A improved Archimedes optimization algorithm for multi/single-objective optimal power flow." Electr. Power Syst. Research, Vol. 206, 107796, 2022.

[29] A. A. El-Fergany, and H. M. Hasanien. "Single and multi-objective optimal power flow using grey wolf optimizer and differential evolution algorithms." Electr. Power Comp. Syst., Vol. 43, No. 13, pp. 1548-1559, 2015.

[30] I. U. Khan, N. Javaid, K. A. A. Gamage, C. J. Taylor, S. Baig, and X. Ma. "Heuristic algorithm based optimal power flow model incorporating stochastic renewable energy sources." IEEE Acess, Vol. 8, pp. 148622-643, 2020.

[31] M. A. Abido, and J. M. Bakhashwain. " Optimal VAR dispatch using a multi-objective evolutionary algorithm." Int. J. Electr. Power Energy Syst., Vol. 27, No. 1, pp. 13-20, 2005.

[32] S. Jeyadevi, S. Baskar, C. K. Babulal, and M. W. Iruthayarajan. “Solving multi-objective optimal reactive power dispatch using modified NSGA-II.” Int. J. Electr. Power Energy Syst., Vol. 33, No. 2, pp. 219-228, 2011.

[33] T. Niknam, M. R. Narimani, J. Aghaei, and R. Azizipanah-Abarghooee.“Improved particle swarm optimization for multi-objective optimal power flow considering the cost, loss, emission, and voltage stability index.” IET Gener. Transm. Distrib., Vol. 6, No. 6, pp. 515-527, 2012.

[34] H. Pulluri, R. Naresh, and V. Sharma. “An enhanced self-adaptive differential evolution based solution methodology for multi-objective optimal power flow.” Appl. Soft Comput., Vol. 54, pp. 229-245, 2017.

[35] A. R. Bhowmik, and A.K. Chakraborty. “Solution of optimal power flow using nondominated sorting multi-objective opposition based gravitational search algorithm.” Int. J. Electr. Power Energy Syst., Vol. 64, pp. 1237-1250, 2015.

[36] M. Varadarajan, and K. S. Swarup. “Solving multi-objective optimal power flow using differential evolution.” IET Gener. Transm. Distrb., Vol. 2, No. 5, pp. 720-30, 2008.

[37] A. A. El-Fergancy, and H. M. Hasanien. “Single and multi-objective optimal power flow using Grey Wolf optimizer and differential evolution algorithms.” Electr. Power Compon. Syst., Vol. 43, pp. 1548-59, 2015.

[38] A. E. Chaib, H. R. E. H. Bouchekara, R. Mehasni, and M. A. Abido. “Optimal power flow with emission and non-smooth cost functions using backtracking search optimization algorithm.” Int. J. Electr. Power Energy Syst., Vol. 81, pp. 64-77, 2016.

[39] X. Yuan, B. Zhang, P. Wang, J. Liang, Y. Yuan, and Y. Huang. “Multi-objective optimal power flow based on improved strength Pareto evolutionary algorithm.” Energy, Vol. 122, pp. 70-82, 2017.

[40] A. Panda, and M. Tripathy. “Optimal power flow solution of wind integrated power system using modified bacteria foraging algorithm.” Int. J. Electr. Power Energy Syst., Vol. 54, pp. 306-314, 2014.

[41] A. Panda, and M. Tripathy. “Security constrained optimal power flow solution of wind-thermal generation system using modified bacteria foraging algorithm.” Energy, Vol. 93, pp. 816-827, 2015.

[42] R. A. Jabr, and B. C. Pal. “Intermittent wind generation in optimal power flow dispatching.” IET Gener. Transm. Distrb., Vol. 3, No. 1, pp. 66-74, 2009.

[43] S. Mishra, Y. Mishra, and S. Vignesh. “Security constrained economic dispatch considering wind energy conversion systems.” Power and Energy Society General Meeting, IEEE, 2011.

[44] H. Tazvinga, B. Zhu, and X. Xia. “Optimal power flow management for distributed energy resources with batteries.” Energy Convers. Manage., Vol. 102, pp. 104-110, 2015.

[45] K. Kusakana. “Optimal scheduling for distributed hybrid system with pumped hydro storage.” Energy Convers. Manage., Vol. 111, pp. 253-260, 2016.

[46] K. Li, K. Deb, Q. Zhang, and S. Kwong. “An evolutionary many-objective optimization algorithm based on dominance and decomposition.” IEEE Trans. Evol. Comput., Vol. 19, No. 5, pp. 694–716, 2015.

[47] S. Yang, M. Li, X. Liu and J. Zheng. “A grid-based evolutionary algorithm for many-objective optimization.” IEEE Trans. Evol. Comput., Vol. 17, No. 5, pp. 721-736, 2013.

[48] X. Zhang, Y. Tian and Y. Jin. “A knee point-driven evolutionary algorithm for many-objective optimization.” IEEE Trans. Evol. Comput., Vol. 19, No. 6, pp. 761-776, 2015.

[49] J. Zhang, S. Wang, Q. Tang, Y. Zhou, and T. Zeng. “An improved NSGA-III integrating adaptive elimination strategy to solution of many-objective optimal power flow problem.” Energy. Vol. 172, pp. 945-957, 2019.

[50] K. Li, K. Deb, Q. Zhang, and S. Kwong. “An evolutionary many-objective optimization algorithm based on dominance and decomposition.” IEEE Trans. Evol. Comput. Vol. 19, No. 5, pp. 694-716, 2015.

[51] J. Zhang, Q. Tang, P. Li, D. Deng, and Y. Chen. “A modified MOEA/D approach to the solution of multi-objective optimal power flow problem.” Appl. Soft Comput., Vol. 47, pp. 494-514, 2016.

[52] K. Li, K. Deb, Q. Zhang, and S. Kwong. “An evolutionary many-objective optimization algorithm based on dominance and decomposition.” IEEE Trans. Evol. Comput., Vol. 19, No. 5, pp. 694-716, 2015.

[53] Q. Zhang and H. Li. “MOEA/D: A multiobjective evolutionary algorithm based on decomposition.” IEEE Trans. Evol. Comput., Vol. 11, No. 6, pp. 712-731, 2007.

[54] I. Das and J. E. Dennis. “Normal-boundary intersection: A new method for generating Pareto optimal points in multicriteria optimization problems.” SIAM J. Optim., Vol. 8, No. 3, pp. 631–657, 1998.

[55] Y. Zhang, Y. Li, Q. K. Panb, and P. N. Suganthan. “A many-objective evolutionary algorithm based on decomposition and local dominance.” arXiv preprint arXiv:1807.10275, 2018.

[56] M. A. Abido. “Environmental/economic power dispatch using multi-objective evolutionary algorithms: a comparative study.” IEEE Trans. Power Syst., Vol. 1, No. 4, pp. 1529-1537, 2003.

[57] K. Deb, A. Pratap, S. Agarwal, and T. Meyarivan. “A fast and elitist multi objective genetic algorithm: NSGA-II.” IEEE Trans. Evol. Comput., Vol. 6, No. 2, pp. 182–197, 2002.

[58] C. A. C. Coello, G. T. Pulido, and M. S. Lechuga. “Handling multiple objectives with particle swarm optimization.” IEEE Trans. Evol. Comput., Vol. 8, No. 3, pp. 256-279, 2004.

[59] Zimmerman R D, Murillo-Sanchez C E, and Thomas R J. “MATPOWER: steady-state operations, planning, and analysis tools for power systems research and education.” IEEE Trans. Power Syst., Vol. 26, No. 1, pp. 12-19, 2011.

[60] T. Ackermann. “Wind power in power system.” John Wiley & Sons; 2012. Chapter 43.

[61] S. Eftekharnejad, V. Vittal, G. T. Heydt, B. Keel, and J. Loehr. “Impact of increased penetration of photovoltaic generation on power systems.” IEEE Trans. Power Syst., Vol. 28, No. 2, pp. 893-901, 2013.

[62] K. Deb. “An efficient constraint handling method for genetic algorithms.” Comput. Methods Appl. Mech. Engrg., Vol. 186, pp. 311-338, 2000.

[63] J. Hetzer, D.C. Yu, and K. Bhattarai. “An economic dispatch model incorporating wind power.” IEEE Trans. Energy Convers., Vol. 23, No. 2, pp. 603-611, 2008.

[64] T. P. Chang. “Investigation on frequency distribution of global radiation using different probability density functions.” Int. J. of Appl. Science and Engg., Vol. 8, No. 2, pp. 99-107, 2010.

[65] S. S. Reddy, P. R. Bijwe, and A. R. Abhyankar. “Real-time economic dispatch considering renewable power generation variability and uncertainty over scheduling period.” IEEE Systems Journal. Vol. 9, No. 4, pp. 1440-1451, 2015.

[66] M. J. Morshed, J. B. Hmida, and A. Fekih. “A probabilistic multi-objective approach for optimal power flow optimization in hybrid wind-PV-PEV systems.” Appl. Energy, Vol. 211, pp. 1136-1149, 2018.

[67] L. Shi, C. Wang, L. Yao, Y. Ni, and M. Bazargan. “Optimal power flow solution incorporating wind power.” IEEE Systems Journal. Vol. 6, No. 2, pp. 233-241, 2012.

[68] B. Y. Qu, and P. N. Suganthan. “Multi-objective differential evolution based on the summation of normalized objectives and improved selection method.” IEEE Symposium. 1-8, 2011.

[69] J. Zhao, F. Wen, Z. Y. Dong, Y. Xue, and K. P.Wong. “Optimal dispatch of electric vehicles and wind power using enhanced particle swarm optimization.” IEEE Trans. Indus. Inform., Vol. 8, No. 4, pp. 889-899, 2012.

[70] P. Hanemann, M. Behnert, and T. Bruckner. “Effects of electric vehicle charging strategies on the German power system.” Appl. Energy, Vol. 203, pp. 608-622, 2017.

[71] T. Wu, Q. Yang, Z. Bao, and W. Yan. “Coordinated energy dispatching in micro grid with wind power generation and plug-in electric vehicles.” IEEE Trans. Smart Grid. Vol. 4, No. 3, pp. 1453-1463, 2013.

[72] B. Y. Qu, and P. N. Suganthan. “Multi-objective evolutionary algorithms based on the summation of normalized objectives and diversified selection.” Infor. Sciences. Vol. 180, No. 17, pp. 3170-3181, 2010.

[73] M. A. Reza, and C. Lucas. “A novel numerical optimization algorithm inspired from weed colonization.” Eco. Info., Vol. 1, No. 4, pp. 355-366, 2006.

[74] T. H. B. Huy, T.P. Nguyen, N. M. Nor, I. Elamvazuthi, T. Ibrahim, and D. N. Vo. “Performance Improvement of Multiobjective Optimal Power Flow-Based Renewable Energy Sources Using Intelligent Algorithm.” IEEE Access, Vol. 10, pp. 48379-48404, 2022.

Appendix-A

IEEE 57-bus system data

Number of buses: 57

Number of lines: 80

Total active power load: 1250.80 MW

Total reactive power load: 336.40 MVAR

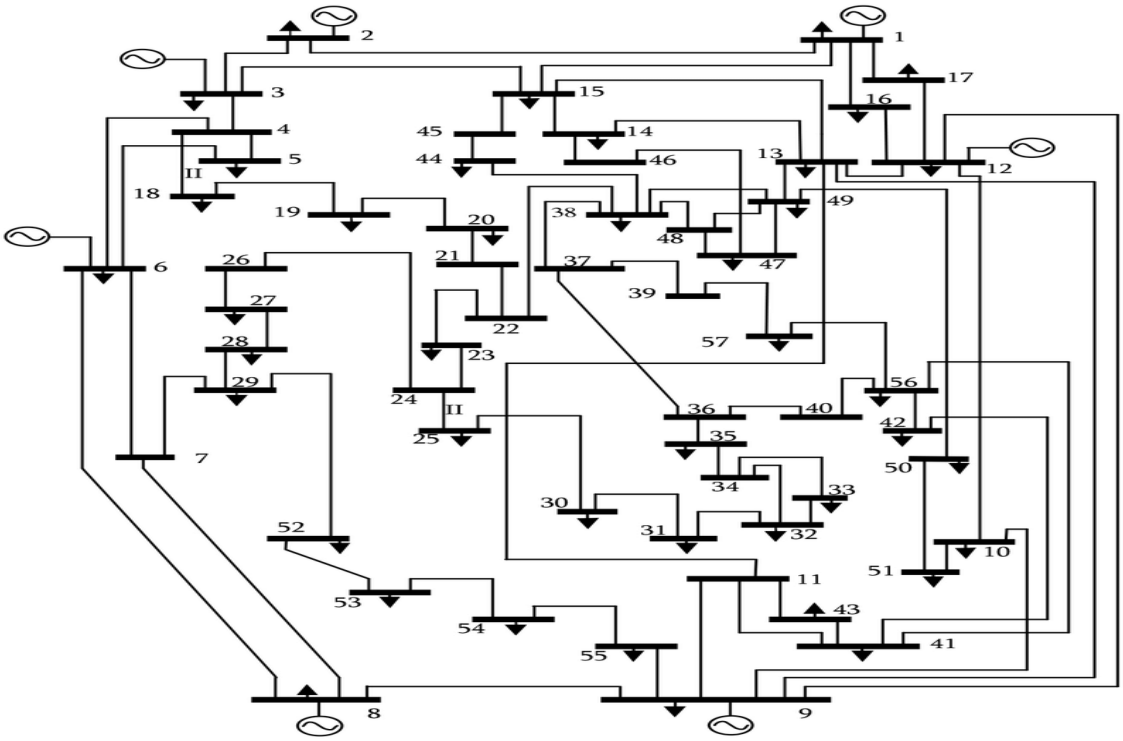

Fig. A.1: Single-line diagram of IEEE 57-bus system

Table A.1: Line data of IEEE 57-bus system

Line No.	From	To	R (in pu)	X (in pu)	B (in pu)
1	1	2	0.0083	0.0280	0.1290
2	2	3	0.0298	0.0850	0.0818
3	3	4	0.0112	0.0366	0.0380
4	4	5	0.0625	0.1320	0.0258
5	4	6	0.0430	0.1480	0.0348
6	6	7	0.0200	0.1020	0.0276
7	6	8	0.0339	0.1730	0.0470
8	8	9	0.0099	0.0505	0.0548
9	9	10	0.0369	0.1679	0.0440
10	9	11	0.0258	0.0848	0.0218
11	9	12	0.0648	0.2950	0.0772
12	9	13	0.0481	0.1580	0.0406

13	13	14	0.0132	0.0434	0.0110
14	13	15	0.0269	0.0869	0.0230
15	1	15	0.0178	0.0910	0.0988
16	1	16	0.0454	0.2060	0.0546
17	1	17	0.0238	0.1080	0.0286
18	3	15	0.0162	0.0530	0.0544
19	4	18	0	0.5550	0
20	4	18	0	0.4300	0
21	5	6	0.0302	0.0641	0.0124
22	7	8	0.0139	0.0712	0.0194
23	10	12	0.0277	0.1262	0.0328
24	11	13	0.0223	0.0732	0.0188
25	12	13	0.0178	0.0580	0.0604
26	12	16	0.0180	0.0813	0.0216
27	12	17	0.0397	0.1790	0.0476
28	14	15	0.0171	0.0547	0.0148
29	18	19	0.4610	0.6850	0
30	19	20	0.2830	0.4340	0
31	21	20	0	0.7767	0
32	21	22	0.0736	0.1170	0
33	22	23	0.0099	0.0152	0
34	23	24	0.1660	0.2560	0.0084
35	24	25	0	1.1820	0
36	24	25	0	1.2300	0
37	24	26	0	0.0473	0
38	26	27	0.1650	0.2540	0
39	27	28	0.0618	0.0954	0
40	28	29	0.0418	0.0587	0
41	7	29	0	0.0648	0
42	25	30	0.1350	0.2020	0
43	30	31	0.3260	0.4970	0
44	31	32	0.5070	0.7550	0
45	32	33	0.0392	0.0360	0
46	34	32	0	0.9530	0
47	34	35	0.0520	0.0780	0.0032
48	35	36	0.0430	0.0537	0.0016
49	36	37	0.0290	0.0366	0
50	37	38	0.0651	0.1009	0.0020
51	37	39	0.0239	0.0379	0
52	36	40	0.0300	0.0466	0
53	22	38	0.0192	0.0295	0
54	11	41	0	0.7490	0
55	41	42	0.2070	0.3520	0

56	41	43	0	0.4120	0
57	38	44	0.0289	0.0585	0.0020
58	15	45	0	0.1042	0
59	14	46	0	0.0735	0
60	46	47	0.0230	0.0680	0.0032
61	47	48	0.0182	0.0233	0
62	48	49	0.0834	0.1290	0.0048
63	49	50	0.0801	0.1280	0
64	50	51	0.1386	0.2200	0
65	10	51	0	0.0712	0
66	13	49	0	0.1910	0
67	29	52	0.1442	0.1870	0
68	52	53	0.0762	0.0984	0
69	53	54	0.1878	0.2320	0
70	54	55	0.1732	0.2265	0
71	11	43	0	0.1530	0
72	44	45	0.0624	0.1242	0.0040
73	40	56	0	1.1950	0
74	56	41	0.5530	0.5490	0
75	56	42	0.2125	0.3540	0
76	39	57	0	1.3550	0
77	57	56	0.1740	0.2600	0
78	38	49	0.1150	0.1770	0.0030
79	38	48	0.0312	0.0482	0
80	9	55	0	0.1205	0

Table A.2: Bus data of IEEE 57-bus system

Bus No.	P (MW)	Q (MVAR)
1	55	17
2	3	88
3	411	21
4	0	0
5	0	4
6	75	2
7	0	0
8	150	22
9	121	26
10	5	2
11	0	0
12	377	24
13	18	2.3
14	10.5	5.3

15	22	5
16	43	3
17	42	8
18	27.2	9.8
19	3.3	0.6
20	2.3	1
21	0	0
22	0	0
23	6.3	2.1
24	0	0
25	6.3	3.2
26	0	0
27	9.3	0.5
28	4.6	2.3
29	17	2.6
30	3.6	1.8
31	5.8	2.9
32	1.6	0.8
33	3.8	1.9
34	0	0
35	6	3
36	0	0
37	0	0
38	14	7
39	0	0
40	0	0
41	6.3	3
42	7.1	4.4
43	2	1
44	12	1.8
45	0	0
46	0	0
47	29.7	11.6
48	0	0
49	18	8.5
50	21	10.5
51	18	5.3
52	4.9	2.2
53	20	10
54	4.1	1.4
55	6.8	3.4
56	7.6	2.2
57	6.7	2

Table A.3: IEEE 57-bus system: Cost and Emission coefficients

S.No.	Bus No.	Cost coefficients			Emission coefficients				
		a	b	c	α	β	γ	δ	ε
1.	1	0	20	0.0775795	0.040	-0.05	0.060	0.00002	0.5
2.	2	0	40	0.01	0.030	-0.06	0.050	0.00005	1.5
3.	3	0	20	0.25	0.040	-0.05	0.040	0.00001	1.0
4.	6	0	40	0.01	0.035	-0.03	0.035	0.00002	0.5
5.	8	0	20	0.0222222	0.050	-0.05	0.045	0.00004	2.0
6.	9	0	40	0.01	0.045	-0.04	0.050	0.00001	2.0
7.	12	0	20	0.0322581	0.060	-0.05	0.050	0.00001	1.5

Appendix-B

IEEE 118-bus system data

Number of buses: 118

Number of lines: 186

Total active power load: 4242.00 MW

Total reactive power load: 1439.00 MVAR

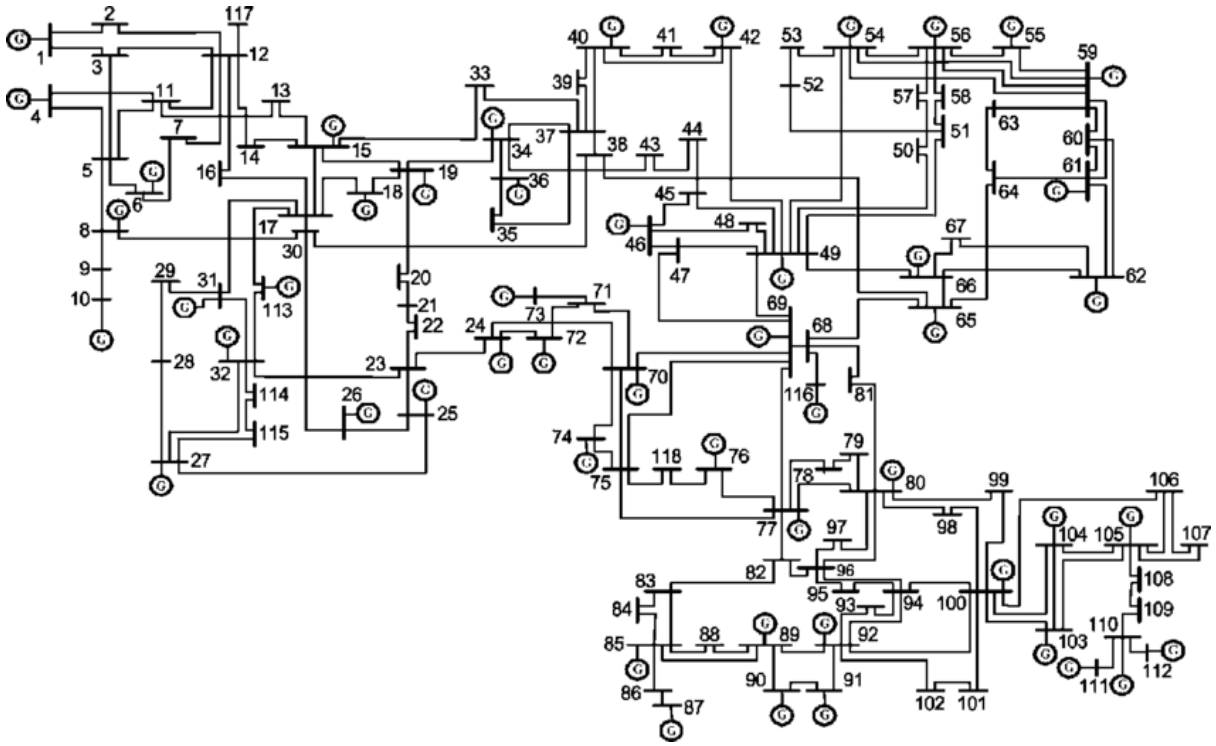

Fig. B.1: Single-line diagram of IEEE 118-bus system

Table B.1: Line data of IEEE 118-bus system

Line No.	From	To	R (in pu)	X (in pu)	B (in pu)
1	1	2	0.0303	0.0999	0.0254
2	1	3	0.0129	0.0424	0.0108
3	4	5	0.00176	0.00798	0.0021
4	3	5	0.0241	0.1080	0.0284
5	5	6	0.0119	0.0540	0.0142
6	6	7	0.00459	0.0208	0.0055
7	8	9	0.00244	0.0305	1.1620
8	8	5	0	0.0267	0
9	9	10	0.00258	0.0322	1.2300
10	4	11	0.0209	0.0688	0.01748
11	5	11	0.0203	0.0682	0.01738
12	11	12	0.00595	0.0196	0.00502

13	2	12	0.0187	0.0616	0.01572
14	3	12	0.0484	0.1600	0.0406
15	7	12	0.00862	0.0340	0.00874
16	11	13	0.02225	0.0731	0.01876
17	12	14	0.0215	0.0707	0.01816
18	13	15	0.0744	0.2444	0.06268
19	14	15	0.0595	0.1950	0.0502
20	12	16	0.0212	0.0834	0.0214
21	15	17	0.0132	0.0437	0.0444
22	16	17	0.0454	0.1801	0.0466
23	17	18	0.0123	0.0505	0.01298
24	18	19	0.01119	0.0493	0.01142
25	19	20	0.0252	0.1170	0.0298
26	15	19	0.0120	0.0394	0.0101
27	20	21	0.0183	0.0849	0.0216
28	21	22	0.0209	0.0970	0.0246
29	22	23	0.0342	0.1590	0.0404
30	23	24	0.0135	0.0492	0.0498
31	23	25	0.0156	0.0800	0.0864
32	26	25	0	0.0382	0
33	25	27	0.0318	0.1630	0.1764
34	27	28	0.01913	0.0855	0.0216
35	28	29	0.0237	0.0943	0.0238
36	30	17	0	0.0388	0
37	8	30	0.00431	0.0504	0.5140
38	26	30	0.00799	0.0860	0.9080
39	17	31	0.0474	0.1563	0.0399
40	29	31	0.0108	0.0331	0.0083
41	23	32	0.0317	0.1153	0.1173
42	31	32	0.0298	0.0985	0.0251
43	27	32	0.0229	0.0755	0.01926
44	15	33	0.0380	0.1244	0.03194
45	19	34	0.0752	0.2470	0.0632
46	35	36	0.00224	0.0102	0.00268
47	35	37	0.0110	0.0497	0.0131
48	33	37	0.0415	0.1420	0.0366
49	34	36	0.00871	0.0268	0.00568
50	34	37	0.00256	0.0094	0.00984
51	38	37	0	0.0375	0
52	37	39	0.0321	0.1060	0.0270
53	37	40	0.0593	0.1680	0.0420
54	30	38	0.00464	0.0540	0.4220
55	39	40	0.0184	0.0605	0.01552

56	40	41	0.0145	0.0487	0.01222
57	40	42	0.0555	0.1830	0.0466
58	41	42	0.0410	0.1350	0.0344
59	43	44	0.0608	0.2454	0.06068
60	34	43	0.0413	0.1681	0.04226
61	44	45	0.0224	0.0901	0.0224
62	45	46	0.0400	0.1356	0.0332
63	46	47	0.0380	0.1270	0.0316
64	46	48	0.0601	0.1890	0.0472
65	47	49	0.0191	0.0625	0.01604
66	42	49	0.0715	0.3230	0.0860
67	42	49	0.0715	0.3230	0.0860
68	45	49	0.0684	0.1860	0.0444
69	48	49	0.0179	0.0505	0.01258
70	49	50	0.0267	0.0752	0.01874
71	49	51	0.0486	0.1370	0.0342
72	51	52	0.0203	0.0588	0.01396
73	52	53	0.0405	0.1635	0.04058
74	53	54	0.0263	0.1220	0.0310
75	49	54	0.073	0.289	0.0738
76	49	54	0.0869	0.291	0.073
77	54	55	0.0169	0.0707	0.0202
78	54	56	0.00275	0.00955	0.00732
79	55	56	0.00488	0.0151	0.00374
80	56	57	0.0343	0.0966	0.0242
81	50	57	0.0474	0.134	0.0332
82	56	58	0.0343	0.0966	0.0242
83	51	58	0.0255	0.0719	0.01788
84	54	59	0.0503	0.2293	0.0598
85	56	59	0.0825	0.251	0.0569
86	56	59	0.0803	0.239	0.0536
87	55	59	0.04739	0.2158	0.05646
88	59	60	0.0317	0.145	0.0376
89	59	61	0.0328	0.15	0.0388
90	60	61	0.00264	0.0135	0.01456
91	60	62	0.0123	0.0561	0.01468
92	61	62	0.00824	0.0376	0.0098
93	63	59	0	0.0386	0
94	63	64	0.00172	0.02	0.216
95	64	61	0	0.0268	0
96	38	65	0.00901	0.0986	1.046
97	64	65	0.00269	0.0302	0.38
98	49	66	0.018	0.0919	0.0248

99	49	66	0.018	0.0919	0.0248
100	62	66	0.0482	0.218	0.0578
101	62	67	0.0258	0.117	0.031
102	65	66	0	0.037	0
103	66	67	0.0224	0.1015	0.02682
104	65	68	0.00138	0.016	0.638
105	47	69	0.0844	0.2778	0.07092
106	49	69	0.0985	0.324	0.0828
107	68	69	0	0.037	0
108	69	70	0.03	0.127	0.122
109	24	70	0.00221	0.4115	0.10198
110	70	71	0.00882	0.0355	0.00878
111	24	72	0.0488	0.196	0.0488
112	71	72	0.0446	0.18	0.04444
113	71	73	0.00866	0.0454	0.01178
114	70	74	0.0401	0.1323	0.03368
115	70	75	0.0428	0.141	0.036
116	69	75	0.0405	0.122	0.124
117	74	75	0.0123	0.0406	0.01034
118	76	77	0.0444	0.148	0.0368
119	69	77	0.0309	0.101	0.1038
120	75	77	0.0601	0.1999	0.04978
121	77	78	0.00376	0.0124	0.01264
122	78	79	0.00546	0.0244	0.00648
123	77	80	0.017	0.0485	0.0472
124	77	80	0.0294	0.105	0.0228
125	79	80	0.0156	0.0704	0.0187
126	68	81	0.00175	0.0202	0.808
127	81	80	0	0.037	0
128	77	82	0.0298	0.0853	0.08174
129	82	83	0.0112	0.03665	0.03796
130	83	84	0.0625	0.132	0.0258
131	83	85	0.043	0.148	0.0348
132	84	85	0.0302	0.0641	0.01234
133	85	86	0.035	0.123	0.0276
134	86	87	0.02828	0.2074	0.0445
135	85	88	0.02	0.102	0.0276
136	85	89	0.0239	0.173	0.047
137	88	89	0.0139	0.0712	0.01934
138	89	90	0.0518	0.188	0.0528
139	89	90	0.0238	0.0997	0.106
140	90	91	0.0254	0.0836	0.0214
141	89	92	0.0099	0.0505	0.0548

142	89	92	0.0393	0.1581	0.0414
143	91	92	0.0387	0.1272	0.03268
144	92	93	0.0258	0.0848	0.0218
145	92	94	0.0481	0.158	0.0406
146	93	94	0.0223	0.0732	0.01876
147	94	95	0.0132	0.0434	0.0111
148	80	96	0.0356	0.182	0.0494
149	82	96	0.0162	0.053	0.0544
150	94	96	0.0269	0.0869	0.023
151	80	97	0.0183	0.0934	0.0254
152	80	98	0.0238	0.108	0.0286
153	80	99	0.0454	0.206	0.0546
154	92	100	0.0648	0.295	0.0472
155	94	100	0.0178	0.058	0.0604
156	95	96	0.0171	0.0547	0.01474
157	96	97	0.0173	0.0885	0.024
158	98	100	0.0397	0.179	0.0476
159	99	100	0.018	0.0813	0.0216
160	100	101	0.0277	0.1262	0.0328
161	92	102	0.0123	0.0559	0.01464
162	101	102	0.0246	0.112	0.0294
163	100	103	0.016	0.0525	0.0536
164	100	104	0.0451	0.204	0.0541
165	103	104	0.0466	0.1584	0.0407
166	103	105	0.0535	0.1625	0.0408
167	100	106	0.0605	0.229	0.062
168	104	105	0.00994	0.0378	0.00986
169	105	106	0.014	0.0547	0.01434
170	105	107	0.053	0.183	0.0472
171	105	108	0.0261	0.0703	0.01844
172	106	107	0.053	0.183	0.0472
173	108	109	0.0105	0.0288	0.0076
174	103	110	0.03906	0.1813	0.0461
175	109	110	0.0278	0.0762	0.0202
176	110	111	0.022	0.0755	0.02
177	110	112	0.0247	0.064	0.062
178	17	113	0.00913	0.0301	0.00768
179	32	113	0.0615	0.203	0.0518
180	32	114	0.0135	0.0612	0.01628
181	27	115	0.0164	0.0741	0.01972
182	114	115	0.0023	0.0104	0.00276
183	68	116	0.00034	0.00405	0.164
184	12	117	0.0329	0.14	0.0358

185	75	118	0.0145	0.0481	0.01198
186	76	118	0.0164	0.0544	0.01356

Table B.2: Bus data of IEEE 118-bus system

Bus No.	P (MW)	Q (MVAR)
1	51	27
2	20	9
3	39	10
4	39	12
5	0	0
6	52	22
7	19	2
8	28	0
9	0	0
10	0	0
11	70	23
12	47	10
13	34	16
14	14	1
15	90	30
16	25	10
17	11	3
18	60	34
19	45	25
20	18	3
21	14	8
22	10	5
23	7	3
24	13	0
25	0	0
26	0	0
27	71	13
28	17	7
29	24	4
30	0	0
31	43	27
32	59	23
33	23	9
34	59	26
35	33	9
36	31	17
37	0	0
38	0	0

39	27	11
40	66	23
41	37	10
42	96	23
43	18	7
44	16	8
45	53	22
46	28	10
47	34	0
48	20	11
49	87	30
50	17	4
51	17	8
52	18	5
53	23	11
54	113	32
55	63	22
56	84	18
57	12	3
58	12	3
59	277	113
60	78	3
61	0	0
62	77	14
63	0	0
64	0	0
65	0	0
66	39	18
67	28	7
68	0	0
69	0	0
70	66	20
71	0	0
72	12	0
73	6	0
74	68	27
75	47	11
76	68	36
77	61	28
78	71	26
79	39	32
80	130	26
81	0	0

82	54	27
83	20	10
84	11	7
85	24	15
86	21	10
87	0	0
88	48	10
89	0	0
90	163	42
91	10	0
92	65	10
93	12	7
94	30	16
95	42	31
96	38	15
97	15	9
98	34	8
99	42	0
100	37	18
101	22	15
102	5	3
103	23	16
104	38	25
105	31	26
106	43	16
107	50	12
108	2	1
109	8	3
110	39	30
111	0	0
112	68	13
113	6	0
114	8	3
115	22	7
116	184	0
117	20	8
118	33	15

Table B.3: IEEE 118-bus system: Cost coefficients

S.No.	Bus No.	*a*	*b*	*c*
1.	1	0	20	0.0193648335
2.	4	0	40	0.01
3.	6	0	40	0.01
4.	8	0	40	0.01
5.	10	0	40	0.01
6.	12	0	20	0.0222222222
7.	15	0	20	0.117647059
8.	18	0	40	0.01
9.	19	0	40	0.01
10.	24	0	40	0.01
11.	25	0	40	0.01
12.	26	0	20	0.0454545455
13.	27	0	20	0.0318471338
14.	31	0	40	0.01
15.	32	0	20	1.42857143
16.	34	0	40	0.01
17.	36	0	40	0.01
18.	40	0	40	0.01
19.	42	0	40	0.01
20.	46	0	40	0.01
21.	49	0	20	0.526315789
22.	54	0	20	0.0490196078
23.	55	0	20	0.208333333
24.	56	0	40	0.01
25.	59	0	40	0.01
26.	61	0	20	0.064516129
27.	62	0	20	0.0625
28.	65	0	40	0.01
29.	66	0	20	0.0255754476
30.	69	0	20	0.0255102041
31.	70	0	40	0.01
32.	72	0	40	0.01
33.	73	0	40	0.01
34.	74	0	40	0.01
35.	76	0	40	0.01
36.	77	0	40	0.01
37.	80	0	20	0.0209643606

38.	85	0	40	0.01
39.	87	0	20	2.5
40.	89	0	20	0.0164744646
41.	90	0	40	0.01
42.	91	0	40	0.01
43.	92	0	40	0.01
44.	99	0	40	0.01
45.	100	0	20	0.0396825397
46.	103	0	20	0.25
47.	104	0	40	0.01
48.	105	0	40	0.01
49.	107	0	40	0.01
50.	110	0	40	0.01
51.	111	0	20	0.277777778
52.	112	0	40	0.01
53.	113	0	40	0.01
54.	116	0	40	0.01

Publications

Journals- SCIE/SCOPUS-Indexed:

1) **Ravi Kumar Avvari** and Vinod Kumar D.M. "A New Hybrid Evolutionary Algorithm for Multi-Objective Optimal Power Flow in an Integrated WE, PV, and PEV Power System." **Electric Power Systems Research**, Elsevier, Vol. 214, 108870, Jan 2023. **(SCIE, IF: 3.818).**

2) **Ravi Kumar Avvari** and Vinod Kumar D.M. "Multi-Objective Optimal Power Flow including Wind and Solar Generation Uncertainty Using New Hybrid Evolutionary Algorithm with Efficient Constraint Handling Method." **International Transactions on Electrical Energy Systems**, Wiley, Vol. 2022, 7091937, Jul 2022. **(SCIE, IF: 2.639).**

3) **Ravi Kumar Avvari** and Vinod Kumar D.M. "Multi-Objective Optimal Power Flow with efficient Constraint Handling using Hybrid Decomposition and Local Dominance Method." **Journal of The Institution of Engineers (India): Series B**, Springer, Vol. 103, No. 5, pp. 1643-1658, Oct 2022. **(Scopus).**

4) **Ravi Kumar Avvari** and Vinod Kumar D.M. "A Novel Hybrid Multi-Objective Evolutionary Algorithm for Optimal Power Flow in Wind, PV, and PEV Systems." **Journal of Operation and Automation in Power Engineering**, Vol. 11, No. 2, pp. 130-143, Aug 2023. **(Scopus).**

Curriculum-Vitae

Name:	Avvari Ravi Kumar
Date of Birth:	23 November, 1991
Gender:	Male
Contact Number:	+91-7382405100
Email Id:	avvari.ravi@gmail.com

Academic Qualifications:

Program	Specialization	University	Division	Year of Completion
M.Tech	Electrical Power Systems	JNTUH, Hyderabad	First Class with Distinction	2015
B.Tech.	Electrical and Electronics Engineering	Sri Venkateswara University, Tirupati	First Class with Distinction	2013